

AN INVESTIGATION OF THE
TOTAL REFLECTION OF SOFT X-RAYS.

by

JAMES HENRY UNDERWOOD

A thesis submitted to the University of
Leicester for the degree of Ph.D. in the
Faculty of Science.

1963

UMI Number: U280626

All rights reserved

INFORMATION TO ALL USERS

The quality of this reproduction is dependent upon the quality of the copy submitted.

In the unlikely event that the author did not send a complete manuscript and there are missing pages, these will be noted. Also, if material had to be removed, a note will indicate the deletion.



UMI U280626

Published by ProQuest LLC 2015. Copyright in the Dissertation held by the Author.
Microform Edition © ProQuest LLC.

All rights reserved. This work is protected against
unauthorized copying under Title 17, United States Code.



ProQuest LLC
789 East Eisenhower Parkway
P.O. Box 1346
Ann Arbor, MI 48106-1346

X75296 3405



THESIS
566129

ABSTRACT.

The design and construction of a vacuum reflectometer for the study of the total reflection of soft X-rays is described. The instrument, which uses a plane mica monochromator and a proportional counter detector, was used to obtain curves of reflecting power versus glancing angle for a number of characteristic wavelengths in a region previously neglected by experimenters. New data is given for reflection by optical flats of glass and stainless steel. These results are used to test (a) the Fresnel equations for reflection, modified to take account of absorption and (b) the theories of X-ray dispersion. From the discrepancies between theory and experiment, conclusions are drawn regarding the surface structure of the specimens.

Some results are also given for evaporated films of copper and ytterbium fluoride. From the latter, it would seem that the Drude-Lorentz dispersion theory holds near an X-ray absorption line.

ACKNOWLEDGMENTS

The author would like to thank Professor E.A. Stewardson for suggesting this topic, and for his constant interest and encouragement throughout the course of the work.

He wishes to thank Dr. P.C. Russell for his interest, and advice on X-ray techniques, and Dr. E. Mathieson, for suggesting the circuit of Figure 4.7.

Thanks are also due to the Workshop and Laboratory Staff of the Physics Department, for assistance in the following respects: Mr. R. Cox and Mr. G. Henderson for their help in the construction of the apparatus; Mr. E.B. Waterson for his general helpfulness; Mr. M.K. Hanson for the preparation of the photographs, and Miss H. Boyes for the reproduction of the text.

Finally, the author wishes to thank the Department of Scientific and Industrial Research for the award of a Research Studentship.

CONTENTS

ABSTRACT.

ACKNOWLEDGMENTS.

	Page
1. INTRODUCTION.	
(i) Early experiments on the reflection and refraction of X-rays.	1
(ii) The reflection equations for an absorbing medium.	3
(iii) Significance of the quantities of δ and β .	7
2. THEORIES OF THE ABSORPTION AND DISPERSION OF X-RAYS	
(i) The classical (Drude-Lorentz) theory.	10
(ii) 'Virtual oscillators' - The Kramers-Kallmann-Mark theory.	14
(iii) Dispersion relations.	16
(iv) Hönl's quantum mechanical theory.	17
3. REVIEW OF PREVIOUS WORK.	
(i) Experimental methods.	18
(ii) List of previous investigations.	20
(iii) Discussion of the published work.	27
(iv) Reasons for the present work.	30
4. THE APPARATUS.	
(i) Design criteria.	32
(ii) Construction of the instrument: Tank and Vacuum equipment.	35
(iii) The source.	42
(iv) The crystal and 2 : 1 linkage.	44
(v) The slits.	46
(vi) The specimen mount.	47
(vii) The counter and electronics.	48

CONTENTS (Cont.)

	Page
5. EXPERIMENTAL METHOD.	
(i) Preliminary alignment.	53
(ii) Calibration of monochromator and reflector.	57
(iii) Method of obtaining reflectance curves.	60
(iv) Reduction of data.	64
(v) Experimental error.	65
6. RESULTS AND DISCUSSION.	
(i) Pyrex glass.	68
(ii) Discussion of results for glass.	82
(iii) Stainless steel.	88
(iv) Discussion of results for stainless steel.	89
(v) Evaporated copper.	101
(vi) Ytterbium fluoride.	103
(vii) Conclusions.	104
APPENDIX A. THE 'CURRENT MODE' OF OPERATION OF A PROPORTIONAL COUNTER.	107
APPENDIX B. RESOLUTION OF PROPORTIONAL COUNTERS IN THE SOFT X-RAY REGION.	110
REFERENCES.	115

1.

CHAPTER 1

INTRODUCTION

1 (i). Early experiments on the reflection and refraction of X-rays.

In 1916 A. Köhler (1), a radiographer, noticed that a bright strip was often visible around the edges of radiographic images of objects, if a strongly over-exposed positive copy of the original radiograph was made. Two years later, Einstein (2) proposed an explanation of this effect in terms of the total reflection of X-rays. He suggested that the X-rays incident at glancing angles upon the edges of the body were being totally reflected, and were thereby increasing the intensity of the general background of radiation near the boundaries of the body, causing a greater blackening of the film in these regions. *

He pointed out that, from the Drude-Lorentz dispersion theory, one would expect the refractive index of materials for X-rays (henceforth denoted by μ) to be slightly different from unity in the X-ray region, so that in the case of $\mu < 1$ total external reflection at angles of incidence approaching 90° would be possible at the boundary between air and a denser medium. He suggested that an experimental determination of μ might be made by the method of total reflection.

* B. Walter (3) later suggested an alternative, and perhaps more likely explanation - that solarisation of the plates used by Köhler was occurring in the regions unshaded by the object being radiographed, thus the regions around the edges of the object, which would not receive quite so much radiation, would show a greater blackening.

2.

In the following year, W. Stenström (4) produced the first experimental evidence to show that μ was less than unity. He noticed that the Bragg law of crystal reflection, when used to predict the angles of reflection in different orders of X-rays of wavelengths greater than about 3\AA , gave results which differed by a small amount from those found experimentally. He attributed this small discrepancy to refraction in the crystal, and estimated the refractive index of a sugar crystal. He found it to be slightly less than unity, in accordance with the Drude-Lorentz theory. Experiments performed later by Duane (5) and by Siegbahn (6) on the reflection of X-rays of ordinary wavelengths from calcite confirmed Stenström's results. This effect had been predicted by C.G. Darwin (7) as early as 1914.

These early experiments provided the first evidence that X-rays could be reflected or refracted. The direct attempts which had been made by Roentgen and others to reflect or refract X-rays by means of mirrors, lenses and prisms had all been unsuccessful. It was not until 1922 that the reflection of X-rays was demonstrated directly. The experiment suggested by Einstein was performed by A.H. Compton (8) who reflected tungsten $L\beta$ radiation ($\lambda = 1.279\text{\AA}$) from polished sheets of glass, silver and copper, using angles of glancing incidence ($\theta = 90^\circ$ - optical angle of incidence) of a few minutes of arc. For glass, a sharp critical angle was found at $\theta = 11$ minutes, which gives a value for the decrement of the refractive index $\delta = 1 - \mu$ of 5×10^{-6} , in good agreement with the classical dispersion theory.

3.

In 1924, Siegbahn, Larson and Waller (9) succeeded in refracting X-rays with a prism. They arranged their apparatus so that the beam of X-rays struck a face of the prism at a small glancing angle, and were able to record the direct, reflected and refracted beam on a photographic plate, and to find a value for the dispersion of the prism.

Following these workers, a large number of experimenters have studied the reflection and refraction of X-rays. The work has moved gradually towards longer wavelengths, and reflection studies have now been carried out at wavelengths up to the beryllium K line at 113\AA (10). At long wavelengths there is no longer a sharp critical angle, but a more or less gradual decrease in reflectance towards larger values of θ . This effect is due to absorption, and can be described in the theory by the introduction of a complex index of refraction μ_c , as will be shown in the next section.

1 (ii). The reflection equations for an absorbing medium.

When a beam of electromagnetic radiation, or a train of any other form of waves, meets a surface at which there is a change in the value of the velocity of propagation of the waves in question then the wave will, in general, split into two - a reflected wave and a refracted one - at the surface. We need use Huyghens' construction only to obtain Snell's law and the law of reflection (angle of incidence = angle of reflection) and to show that if the velocity of propagation is greater in the second medium, then a

4.

refracted wave cannot exist for all angles of incidence, and total reflection occurs when the optical angle of incidence θ is greater than the critical value θ_c given by the relation:

$$\sin \phi_c = c_1/c_2 \quad . \quad . \quad . \quad . \quad . \quad (1.1)$$

where c_1 and c_2 are the values of the phase velocity in the first and second medium respectively. To obtain these results we need only make the assumption that c changes at the boundary. If, however, we wish to obtain the fractions of the incident intensity which are reflected and refracted, as a function of the angle of incidence, then we must specify the boundary conditions more exactly, and this involves making some assumptions about the properties of the particular kind of waves under consideration. In 1815 Fresnel derived equations for the coefficients of reflection and refraction of light, using an elastic-solid theory, but this involved his introducing some rather arbitrary boundary conditions. We may derive the same equations, which are usually known as Fresnel's equations, using the electromagnetic theory, and the only boundary conditions we need introduce are the ordinary electric and magnetic ones concerning the continuity of the components of E and H .

Consider X-rays incident upon medium 2 from medium 1, and let subscripts 1, 2, refer to these media. Let us consider the reflection of radiation which is polarised so that the electric vector lies perpendicular to the plane of incidence. We will denote this type of polarisation by the subscript s, using the subscript p for the

5.

type in which the E vector is in the plane of incidence. We may consider the amplitudes of the reflected and incident radiation to be complex quantities. Let E_s denote the complex amplitude of the electric component of the incident radiation, R_s the complex amplitude of the electric component of the reflected radiation. It may be shown without much difficulty, by using Maxwell's equations and the condition that the tangential component of E is continuous at the boundary, that:

$$\frac{R_s}{E_s} = \frac{\cos \phi_1 - \sqrt{\frac{K_2 \gamma_1}{K_1 \gamma_2}} \cos \phi_2}{\cos \phi_1 + \sqrt{\frac{K_2 \gamma_1}{K_1 \gamma_2}} \cos \phi_2} \dots \dots \dots (1.2)$$

where ϕ_1, ϕ_2 are the optical angles of incidence and refraction, K is the dielectric constant and γ the permeability of the medium. This equation is one of the Fresnel equations.

It may be shown (11) that for optical and higher frequencies γ is effectively equal to 1. If medium 1 is air or a vacuum, then $K = 1$, and (1.2) reduces to:

$$\frac{R_s}{E_s} = \frac{\cos \phi_1 - \sqrt{K_2} \cos \phi_2}{\cos \phi_1 + \sqrt{K_2} \cos \phi_2} \dots \dots \dots (1.3)$$

In the case of total reflection $\sin \phi_2$ is greater than unity and $\cos \phi_2$ is imaginary, so that by using Snell's law and the fact that $\mu^2 = K$, where μ is the refractive index, we obtain:

$$\cos \phi_2 = \sqrt{1 - \sin^2 \phi_1 / K_2} = \sqrt{1 - (1 - \sin^2 \theta) / K_2} \dots (1.4)$$

where θ = glancing angle of incidence = $90^\circ - \phi_1$

6.

Substituting in (1.3), and dropping the subscript on K , we obtain:

$$\frac{R_s}{E_s} = \frac{\sin \theta - (K - 1 + \sin^2 \theta)^{\frac{1}{2}}}{\sin \theta + (K - 1 + \sin^2 \theta)^{\frac{1}{2}}} \quad (1.5)$$

Let us now introduce a complex dielectric constant K_c , given by the equation:

$$K_c = (1 - 2\delta - 2i\beta)^2 = |\mu_c|^2 \quad (1.6)$$

where μ_c = complex index of refraction. The significance of the two quantities δ , β will be discussed later. We may, however, use here the experimental fact that they are small quantities, of the order 10^{-6} , so that we may neglect their squares and products compared with their first powers. Substituting in (1.5) and simplifying, we obtain:

$$\frac{R_s}{E_s} = \frac{\theta - (\theta^2 - 2\delta - 2i\beta)^{\frac{1}{2}}}{\theta + (\theta^2 - 2\delta - 2i\beta)^{\frac{1}{2}}} \quad (1.7)$$

This equation gives the ratio of the amplitudes of the incident and reflected radiation. In order to obtain the ratio of the intensities, we must multiply through by the complex conjugate.

Carrying out this process, we arrive at the following relation:

$$\frac{I}{I_0} = \left| \frac{R_s}{E_s} \right|^2 = \quad (1.8)$$

$$\frac{[\theta - \frac{1}{2}\sqrt{(\theta^2 - 2\delta)^2 + 4\beta^2 + \theta^2 - 2\delta}]^2 + \frac{1}{2}[\sqrt{(\theta^2 - 2\delta)^2 + 4\beta^2} - \theta^2 + 2\delta]}{[\theta + \frac{1}{2}\sqrt{(\theta^2 - 2\delta)^2 + 4\beta^2 + \theta^2 - 2\delta}]^2 + \frac{1}{2}[\sqrt{(\theta^2 - 2\delta)^2 + 4\beta^2} - \theta^2 + 2\delta]}$$

In the case of p polarisation, we obtain a different equation which reduces, however, to (1.8) at the small glancing angles necessary for the total reflection of X-rays.

7.

If we now make the change of variables $Y = \beta/\delta$, $X = \frac{\theta}{\theta_c}$, we obtain the reflection equation:

$$\frac{I}{I_0} = \frac{[2X - \sqrt{(X^2-1)^2 + Y^2} + (X^2-1)]^2 + \sqrt{(X^2-1)^2 + Y^2} - (X^2-1)}{[2X + \sqrt{(X^2-1)^2 + Y^2} + (X^2-1)]^2 + \sqrt{(X^2-1)^2 + Y^2} - (X^2-1)} \quad (1.9)$$

The reflection curves are plotted in Figure (1.1) as a series of curves of $\frac{I}{I_0}$ against X for different values of the parameter Y . The quantity $\frac{I}{I_0}$ will be referred to as the 'reflectance'.

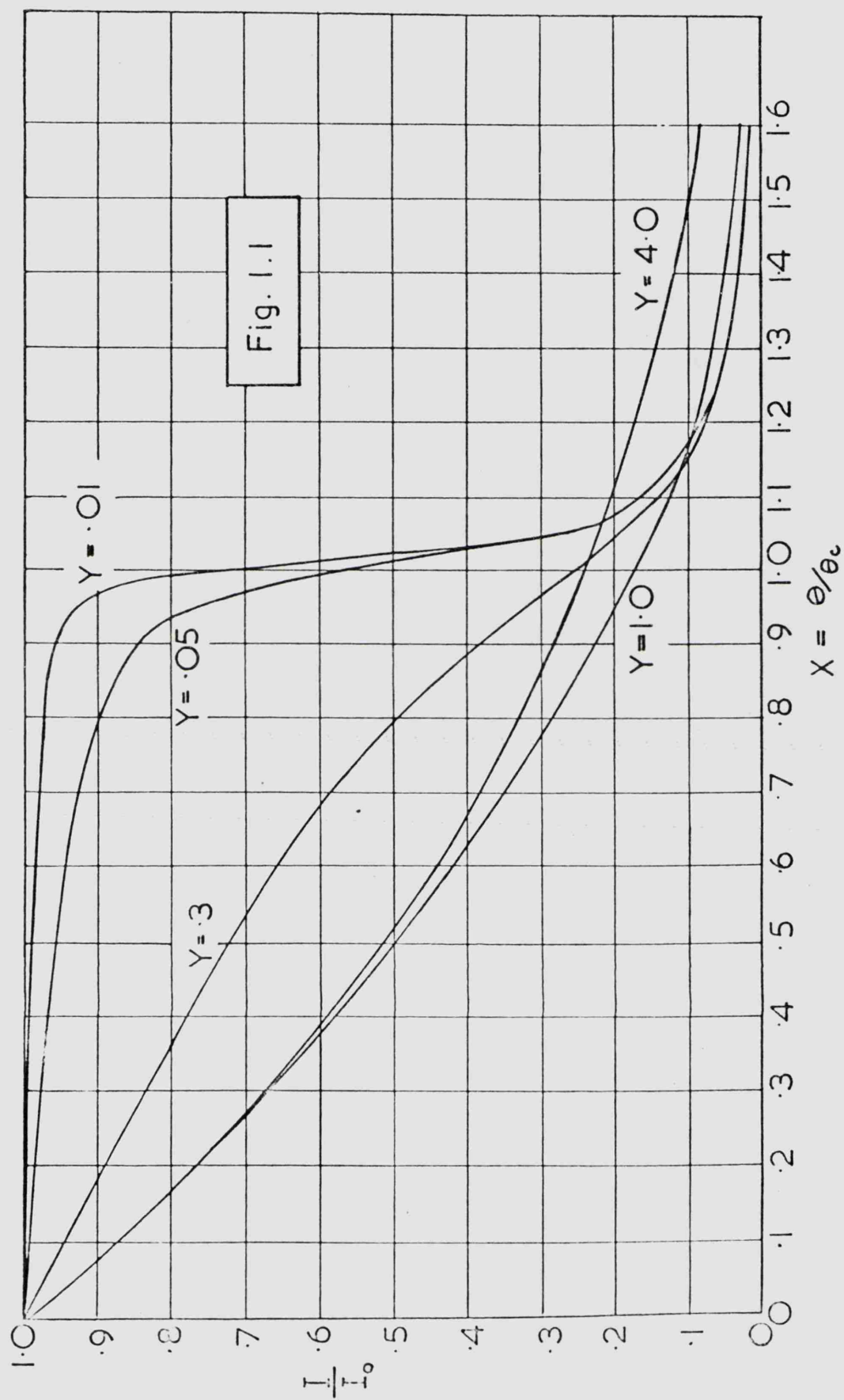
1 (iii). Significance of the quantities δ and β .

The derivation of equation (1.9) follows closely the treatment given by Compton and Allison (12) who also discuss the significance of the two parameters δ , β , which we have introduced into our reflection equations via the complex dielectric constant κ_c . It can easily be shown that the real part $(1 - \delta)$ of the dielectric constant is related to the phase velocity of the waves in the medium, and therefore determines the real index of refraction. δ and the critical glancing angle are related by the simple equation:

$$\delta = \frac{1}{2} \theta_c^2 \quad (1.10)$$

The imaginary part β is related to μ , the linear absorption coefficient of the material by:

$$\beta = \frac{\lambda}{4\pi} \mu_c \quad (1.11)$$



THEORETICAL REFLECTION CURVES

9.

We see, therefore, that the total reflection of X-rays is described by a family of curves containing two parameters, one of which depends on the real refractive index and which determines the critical angle, and the other, which is related to the absorption coefficient, determines the shape of the reflectance curve at the critical angle, i.e., the sharpness of the cut-off. It can be seen from the curves of Figure (1.1) that the transition becomes more and more gradual as the absorption increases. As was mentioned in section 1.1, experiments have confirmed that a sharp critical angle is lacking when soft X-rays are reflected. It has been found that equation (1.9) describes quite well the variation of reflectance with glancing angle in the soft X-ray region if suitable values of X and Y are chosen, although the results of some experimenters seem to show a disagreement with theory.*

We must now consider attempts to predict theoretical values of \hat{C} as a function of wavelength, that is to say, to construct a dispersion theory. We shall see that the development of a dispersion theory is connected with the theory of absorption that we choose to employ, for the two phenomena are inseparably linked through the complex index of refraction μ_c .

* See Chapter 3 for a fuller discussion of previous work.

THEORIES OF THE ABSORPTION AND DISPERSION OF X-RAYS.

2 (i). The classical (Drude-Lorentz) theory.

The classical electromagnetic theory of the absorption and dispersion of X-rays follows exactly the same lines as the theory of optical dispersion, and leads to results similar to those obtained by Lorentz and others for the optical region. It is assumed that an electron executes forced vibrations when an alternating electromagnetic field such as a light wave or an X-ray acts upon it, and that this vibrating electron radiates electromagnetic energy of the same frequency, the loss of this energy causing its vibrations to be damped. It is also assumed that the electrons in the atoms which constitute the dispersing medium possess one or more fixed natural frequencies of vibration, which lead to resonant effects when the frequency of the incident radiation is near to one of these.

In the optical region, these frequencies correspond to the frequencies of absorption lines or the edges of absorption bands. In the X-ray region, however, line absorption does not normally take place,* but we may arrive at a formula for the variation of σ with wavelength by taking as the 'critical frequencies' those frequencies f_q which correspond to the K, L, M,.....absorption limits of the atom.

* A few cases of line absorption are known in the X-ray spectra of the rare earth elements.

11.

Carrying out the calculation, we arrive at the following equations for δ_q and β_q , where q denotes the effect due to absorption by the q^{th} shell.

$$\delta_q = - \frac{2\pi n_q e^2 m c^2 (k_q - k^2)}{m^2 c^4 (k_q^2 - k^2) + \frac{4}{9} e^2 k^6} \quad \dots \quad (2.1)$$

$$\beta_q = \frac{4\pi n_q e^4 k^3}{3 \left\{ m^2 c^4 (k_q^2 - k^2) + \frac{4}{9} e^2 k^6 \right\}} \quad \dots \quad (2.2)$$

In these equations

n_q = number of electrons of type q per c.c.

e = charge on the electron (e.s.u.).

m = mass of the electron.

c = velocity of light.

k = $2\pi/\lambda$.

The term $\frac{4e^2 k^6}{9}$ in the denominator of these expressions is the classical damping term, and is very small compared with the first term unless k is exceedingly near to k_q , and may therefore be neglected. Equation 2.1 then simplifies to:

$$\delta_q = - \frac{2\pi n_q e^2}{m c^2 (k_q^2 - k^2)} = \frac{n_q e^2 \lambda^2}{2\pi m c^2 \left(\frac{\lambda_q^2}{\lambda^2} - 1 \right)} \quad \dots \quad (2.3)$$

12.

Figure 2.1 (solid curve) shows δ versus λ for a material with a 'critical absorption frequency' at 8\AA and $n_q = 3 \times 10^{22}/\text{c.c.}$ It will be seen that δ is positive at wavelengths less than λ_q , therefore the refractive index is less than unity, and total reflection can take place. δ , and therefore the critical angle $\theta_c = \sqrt{2\delta}$, rise to a high value near λ_q .

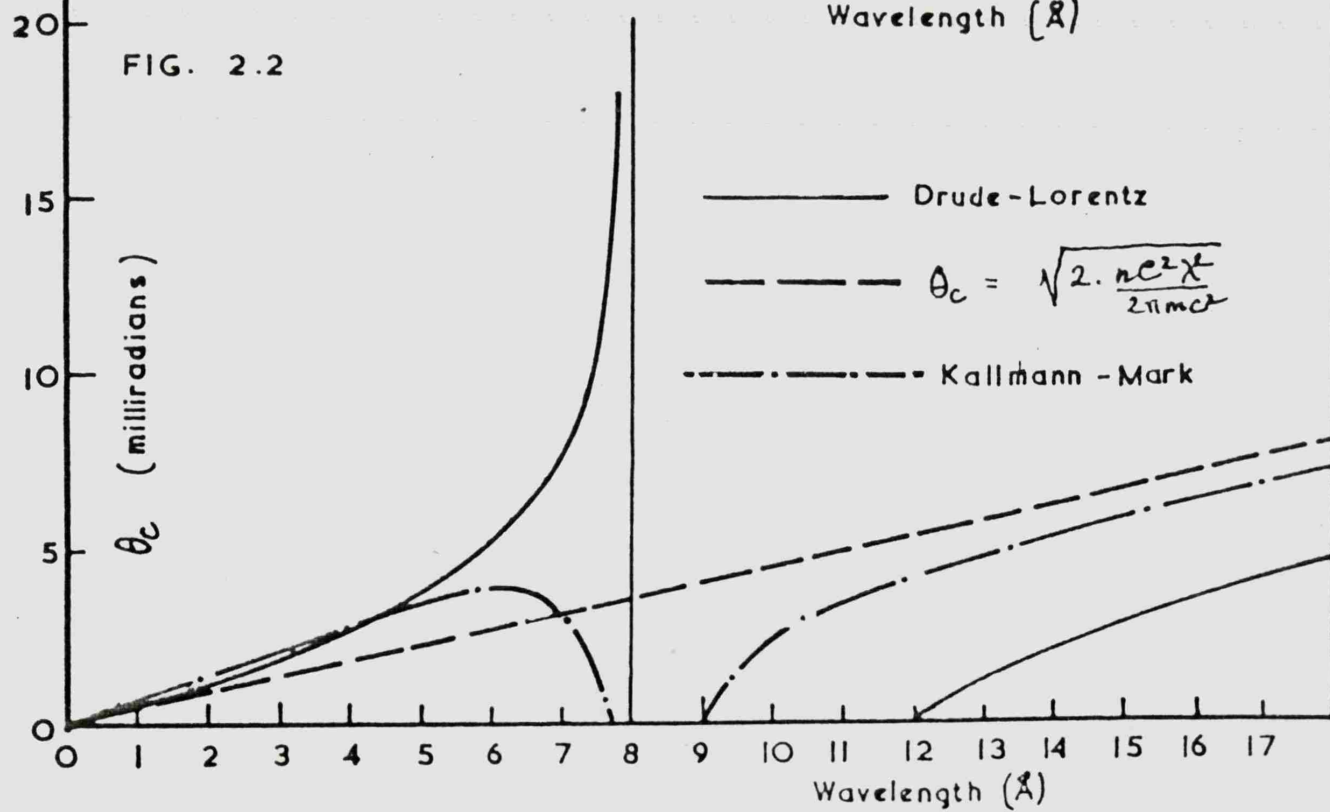
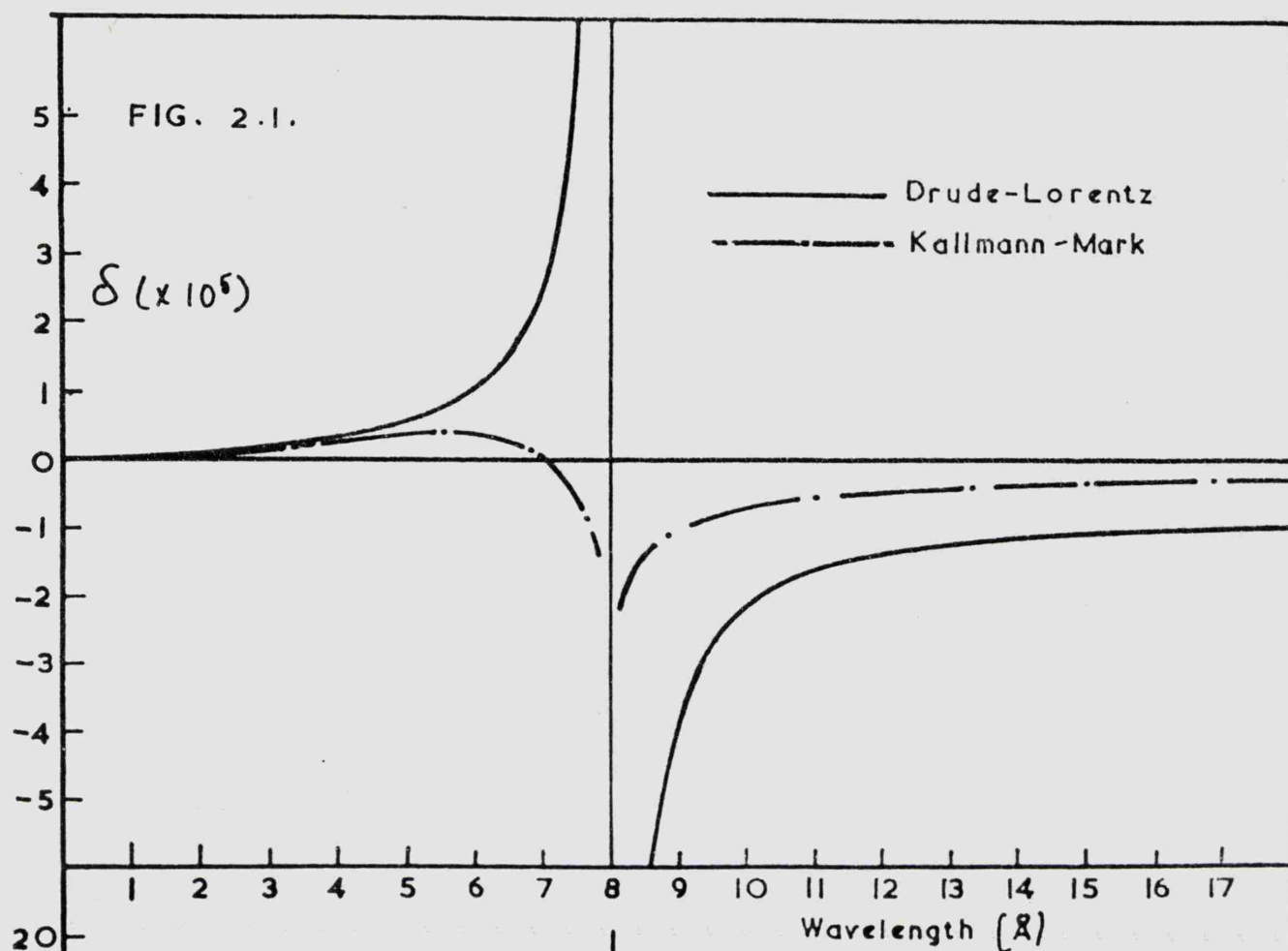
It would seem from this curve that no reflection can take place at values of λ greater than λ_q , as $\delta < 0$, but if we take into account the higher shells of the atom, δ becomes positive again, except for values of λ just greater than λ_q .

Figure 2.2 (solid curve) shows the variation of θ_c with λ , when higher shells are taken into account. The values of δ for the higher shells are calculated from the formula

$$\delta = \frac{n_q e^2 \lambda^2}{2\pi m c^2} \quad (2.4)$$

which is a simplification of 2.3 for the case when $\lambda \ll \lambda_q$.

Most workers on X-ray reflection have found that the rough formula 2.4 predicts quite well the value of δ in regions well away from an absorption edge (see Chapter 3). However, most of the reflection experiments performed to test equation 2.3, as well as experiments on the variation of δ with λ made by other methods, such as the measurement of the deviation from the Bragg law, have shown that 2.3 does not even predict qualitatively the right sort of variation near an edge. It is found that the value of δ ~~decreases~~, instead of rising, in the region just below the edge. In addition, equation 2.2 predicts Lorentz line absorption of the X-rays centred about the wavelength λ_q , which is not in agreement with the well-known λ^3 law of absorption.



It is necessary, therefore, to seek a more adequate dispersion theory for the X-ray region.

2 (ii). 'Virtual Oscillators' - The Kramers-Kallmann-Mark theory.

In order to explain the observed law of X-ray absorption, Kramers suggested that there exist in the atom, instead of a single oscillator corresponding to the critical frequency f_q , a whole series of 'virtual' oscillators which have a continuous distribution of frequencies from $f = f_q$ to $f = \infty$, i.e., on the high-energy side of the absorption edge. Oscillators which have frequencies which lie near that of the incident radiation will contribute strongly to the absorption of this radiation, while those further away will not contribute quite so much. The total number of these oscillators corresponding to the q th absorption limit must equal the total number of electrons associated with this limit, i.e., the electron population Z_q of the level, as given by the Pauli exclusion principle.

$$Z_q = \int_{f_q}^{\infty} F(f) df \quad \dots \dots \dots (2.5)$$

Where $F(f)$ is the distribution function of the virtual oscillators.

The method of deriving a dispersion formula using these assumptions as a basis may now be briefly outlined. Equations 2.1 and 2.2 were obtained by writing down an expression for the complex refractive index (μ_c) (which is equal to $1 - \delta_q - i\beta_q$) in terms of ω ($=2\pi f$) and ω_q , and separating the real and imaginary parts, which we then equate

with $1 - \delta_q$ and with β_q respectively. If, in our initial expression for $(\mu_c)_q$, we replace ω_q by $F'(\omega)d\omega$ (where $F'(\omega)$ is now the distribution-in- ω of the oscillators) and integrate from ω_q to infinity, we obtain new formulae for $(\mu_c)_q$, and its real and imaginary components δ_q and β_q .

Kallmann and Mark (13) introduced empirically the λ^3 law of absorption, which leads to the following expression for $F'(\omega)$:

$$F'(\omega) = \frac{2 \omega_q^2 z_q}{\omega^2} \quad (2.6)$$

This theory leads to expressions for δ and β which contain damping terms (see reference 12). Neglecting these terms, we obtain the following expressions for δ_q , which are valid in regions not too near an absorption edge:

(a) for $\lambda < \lambda_q$

$$\delta_q = \frac{n_q e^2 \lambda^2}{2 \pi m c^2} \left\{ 1 + \frac{\log \left(\frac{\lambda_q^2}{\lambda^2} - 1 \right)}{\lambda_q^2 / \lambda^2} \right\} \quad (2.7)$$

(b) for $\lambda > \lambda_q$

$$\delta_q = \frac{n_q e^2 \lambda^2}{2 \pi m c^2} \left\{ 1 + \frac{\log \left(1 - \frac{\lambda_q^2}{\lambda^2} \right)}{\lambda_q^2 / \lambda^2} \right\} \quad (2.8)$$

These equations are plotted in Figure 2.1 (dashed line).

Although the curves plotted in Figures 2.1, 2.2 neglect damping, they enable us to compare the predictions of the two dispersion theories qualitatively. It will be seen that equation 2.7 predicts a maximum in the curve of δ versus λ below the edge. Larsson (14) claims

to have found evidence of the existence of this maximum, which gives qualitative support to the Kramers-Kallmann-Mark theory.

2 (iii). Dispersion Relations.

In the two treatments of dispersion given above, a law of absorption was assumed in both instances. In the case of the Drude-Lorentz theory we effectively assumed a line absorption, in the case of the Kallmann-Mark theory, the λ^3 law. In general, it is always possible to deduce the variation of δ as a function of ω if the law of absorption is known, as the real and imaginary parts $1 + \delta(\omega)$ and $i\beta(\omega)$ of the complex refractive index form a function $\mu_c(\omega)$ of a complex variable and must, therefore, be interdependent. If the real part is known as a function of ω we may deduce the complex part, and vice versa. This process is carried out by the use of the dispersion relations (see reference 15 for a discussion of this subject) which have recently found important applications in quite different branches of Physics, although they were first used by Krönig (16) to investigate dispersion in the X-ray region.

The law of absorption which we use may be an experimentally derived absorption curve, or an empirical law fitted to the experimental data. The λ^3 law is only an approximation, and the exponent varies for absorption by different shells of the atom. Parratt and Hempstead (17) have treated the cases where the exponent is 2, $\frac{7}{3}$, $\frac{5}{2}$, $\frac{11}{4}$, 3 and 4.

2 (iv). Hönl's Quantum-mechanical theory.

So far the discussion of dispersion has taken place entirely along classical lines, based on the concepts of oscillators and resonance. H. Hönl (18) has derived expressions for δ and β using an entirely wave-mechanical theory. His calculations are based on computations by Y. Sugiyama (19) of the oscillator strengths corresponding to transitions from quantized configurations in the hydrogen atom to configurations of positive energy belonging to the continuous spectrum. His predictions differ from those of the Kramers-Kallmann-Mark theory ~~mainly~~ in that the number of electrons to be assigned to a particular level in the atom is smaller than the population of that level as given by the Pauli exclusion principle. Krönig and Kramers (19a) have given a theoretical discussion of this effect, and it has been investigated experimentally by J.A. Prins (24) and others. Prins found that the effective number of electrons to be assigned to the K-shell of iron was 1.3, in good agreement with Hönl's theory, which predicts 1.32.

We must now examine the previous work on reflection and dispersion more closely, to see how well the results fit in with the predictions of the various theories.

CHAPTER 3

REVIEW OF PREVIOUS WORK.

3 (i). Experimental methods.

If we wish to study experimentally the reflection of soft X-rays by a solid specimen, there are a number of methods by which we may proceed. For instance, to obtain monochromatic radiation, we may filter characteristic X-rays, or we may use a crystal or grating monochromator to pick out a wavelength from a continuous or characteristic spectrum. There exist quite a number of soft X-ray detectors which can be used, and among those which have been employed for this purpose are the photographic plate, the ionization chamber, and the various types of photon counter - Geiger, proportional and scintillation counters. If a photographic plate is used as the detector, then we may either allow a converging beam of the radiation to fall upon a stationary specimen and record the reflected beam over a large range of angles simultaneously, or we may allow a fine pencil of rays to fall upon the specimen, and vary the glancing angle by rotating the reflector. In another method a diffraction grating of the material under investigation is used, and the intensity of reflection of a spectrum line in different orders is measured.

Figure 3.1. shows diagrammatically a number of the experimental methods that have been described in the literature. Obviously a large number of variations on these methods is possible.

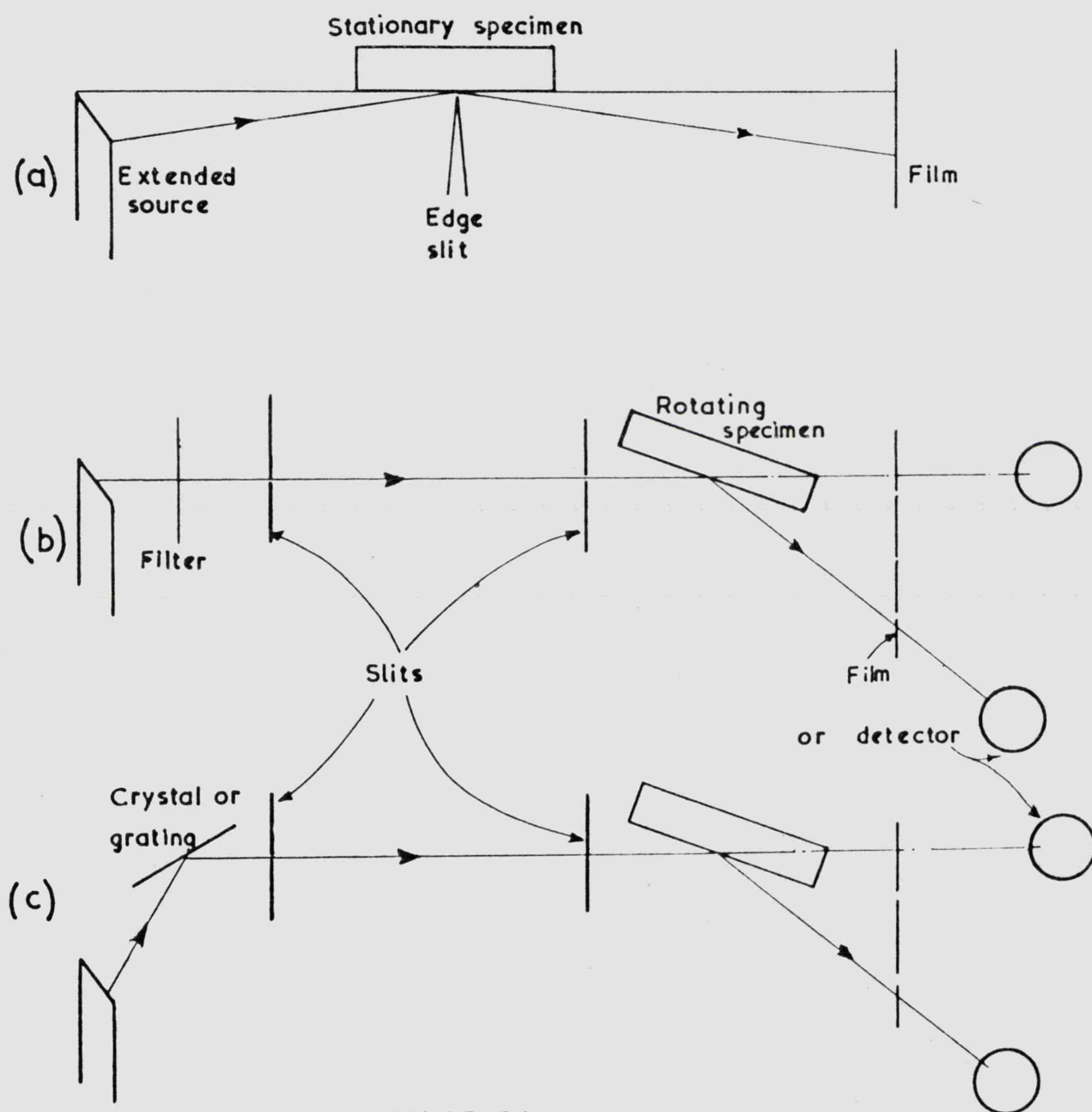


FIGURE 3.1.

3 (ii). List of previous investigations.

The following is a chronological list of published work on the reflection of X-rays with some notes on the methods used and the results obtained in each case. As the literature on the subject is fairly extensive, the list is confined to those investigators which deal with the reflection of X-rays of wavelength above 5\AA ('soft' X-rays) and those which describe important effects due to absorption, dispersion, thickness of films, interference, etc.

1923

A.H. Compton (8) First published account of the reflection of X-rays. Calcite crystal monochromator and ionisation chamber used. X-rays ($1-2\text{\AA}$) reflected from polished sheets of glass and copper, and values of θ_c and \mathcal{S} were obtained which agree roughly with equation (2.4).

F. Holweck (20) Investigated reflection from polished metal surfaces of continuum X-rays produced at low tube voltages ($V < 265$ Volts). Showed that reflecting power decreased as wavelength decreased. Reflections were obtained at angles up to 16.2° .

1927

R. Forster (21) Investigated the variation of \mathcal{S} with λ in the region of the K-edge of copper. Concluded that both the Drude-Lorentz and the Kallmann-Mark theories give the right order of magnitude in regions far from an edge, but his experimental results show a variation

of \mathcal{S} near the edge which is unlike that predicted by either of the two theories.

1928

T.H. Laby, R. Bingham and J. Shearer. (22) Reflected soft X-rays (mostly carbon K radiation) from flats and from gratings and observed reflections up to quite large angles (Reflectivity was 20% at 20° glancing angle for one glass specimen). They concluded that the Fresnel equations in the form given in Chapter 1 are not applicable in this region, and give alternative formulae for the variation of I/I_0 with θ .

J. Thibaud. (23) Measured θ_c for reflection from glass of X-rays of wavelengths 1.5, 20, 44.9, 54.9 and 65 Ångström units, and found a roughly linear relation between θ_c and λ . His method of recording photographically and estimating the critical angle by eye is not capable of a high degree of accuracy, and his results differ considerably from those of other experimenters.

J.A. Prins. (24) Measured \mathcal{S} for a stainless steel mirror by the method of total reflection for a number of wavelengths around the K-edge of iron. He concluded that his results support the Kallmann-Mark theory, if the effective number of electrons in the K-shell of the iron atom is taken as 1.3 instead of 2. This is in agreement with the predictions of Hönl, whose theory appeared in 1933.

H.E. Stauss. (25) In his two papers, Stauss described the results of investigations on reflection from sputtered films nickel, platinum and silver. He found that thin films of nickel and platinum gave lower values of θ_c than those obtained for thicker films. He suggested that this was because the density of the thin films was below the density of the bulk material. Sputtered silver films did not, however, behave in this fashion but gave a value of θ_c of the same order as that predicted from the density of the bulk metal.

1929

M. Schön. (26) Obtained curves of reflectance versus glancing angle for glass, diamond, quartz and aluminium (evaporated) in the wavelength range between 3 and 13\AA , by a photographic method. He investigated the dispersion of quartz near the Si K edge and aluminium near the Al K edge and his results show qualitative agreement with the Kallmann-Mark theory.

M.A. Valouch. (27) Investigated the reflection from glass and aluminium mirrors of radiation consisting mainly of the carbon K line at 44.5\AA . His paper contains a curve of I/I_0 versus θ for flint glass, in which $\theta_c = 7^\circ 45'$.

1921

E. Dershem. (28) 1931. E. Dershem and M. Schein. (29) These papers contain descriptions of very thorough investigations of the reflection of carbon K radiation from glass and quartz. The line was isolated by

a grating and allowed to fall on a mirror of the material under investigation. Experimental curves of I/I_0 versus θ are given, and Fresnel curves fitted to these. It was found that the equations fitted the experimental data extremely well, but a value for the absorptive parameter (β in equation 1.8) had to be assumed which was higher than that calculated from the experimentally measured values of the mass absorption coefficient. This effect has been found by some other experimenters (31), (38) and it has been suggested that some modification of the Fresnel theory is required to account for the small discrepancy.

Another paper by Dershem describes the results of an investigation of the dispersion of certain materials (platinum, silver, calcite and glass) in the wavelength range 0.80 to 9.15 Å. The type of variation found consist of a drop in the value of δ on both sides of an absorption edge, in agreement with the Kallmann-Mark theory. No attempt was made to plot curves of I/I_0 versus θ , the critical angle being estimated by a photographic method.

1929

S.D. Gehman. (30) Measured the reflecting power of aluminium, copper and platinum mirrors for non-characteristic soft X-rays as a function of voltage. The method he used was similar to Holweck's (20) and he found peaks in the curves of percentage reflection (at a fixed glancing angle) versus tube voltage, which he was not able to interpret. The angles used were quite large, typically 10° - 20° .

H.W. Edwards. (31) Investigated the reflection from films of nickel sputtered on glass and nickel sputtered on platinum sputtered on glass. He found that the critical angle of the former films (for X-rays of $\lambda = 0.707 \text{ \AA}$) increased with the thickness of the film, whereas the critical angle for the films on platinum decreased with the film thickness. He interpreted this effect as an indication that 'total reflection is not merely a surface effect, as the radiation penetrates some distance into the material, so that reflection from the substrate becomes important in the case of very thin films.

1930

E. Nähring. (32a, b) In (a), Nähring gives a review of the field of X-ray dispersion (theoretical and experimental) up to 1930. In (b) he gives some experimental results of his own on the reflection of hard X-rays. He also points out in this paper that there is a rather flat minimum in the curve of percentage reflection at the critical angle versus the absorption parameter β which extends over a rather large range of β (from about $\beta = 0.4$ to $\beta = 3.0$). It is possible to estimate the critical angle for a strongly absorbing medium by finding the value of θ for which the reflectance equals the value at this minimum, which is 18%.

J.E. Henderson and E.R. Laird. (33). J.E. Henderson and

E.B. Jordan.(34). The former paper describes a study of the reflection

25.

by glass of continuum radiation with tube voltages of 100-4000 volts and a nickel target. Reflection was found to be appreciable up to 20° glancing angle. The second paper deals with the reflection of 'molybdenum radiation' by sputtered gold and silver films. The authors found a thickness effect (cf. 25, 31).

1931

C.B.O. Mohr. (35) Investigated the reflection of mirrors of quartz, calcite, steel, gold and silver at 8.3 \AA , and quartz, glass and steel at 13.3 \AA . He found disagreement between the values of θ_c predicted from the Drude-Lorentz theory, and those found experimentally, for the heavier materials.

H. Kiessig. (36) Made a careful determination of I/I_0 versus θ curves in the $1-2 \text{ \AA}$ region for mirrors of glass and nickel. The anomalous dispersion is investigated in the region of the Ni K edge, and the results are in fairly good agreement with the Kallmann-Mark theory.

1949

W. Ehrenberg. (37) Studied the effect of surface imperfections on the reflection of X-rays of wavelength about 1.5 \AA . He came to the conclusion that most of the blurring of the astigmatic image formed by a bent optical flat is due to light scattered into the focal region by surface imperfections which may be described by taking the Fourier components of a periodic surface structure with a period of about $.1 \text{ cm}$.

26.

and a height of the order of 10 \AA . Gold, evaporated in strips across the surface of the flat, gave a similar effect.

1954

L.G. Parratt. (38a) Parratt was interested in using X-ray reflection as a tool for the investigation of the surface structure of solids. Differences between the experimental and theoretical Fresnel curves were explained in terms of various surface models. Some of his conclusions are discussed in Chapter 6, with reference to the present experiments.

R.W. Hendrick. (38) A very useful study of the reflection of a number of materials for filtered Al K radiation. Hendrick was one of the first to make use of photon counting techniques for making reflection measurements (scintillation counter). He gives I/I_0 versus θ curves for glass and evaporated films of a number of metals and draws the conclusion that the Fresnel equations fit the experimental data well if values of the β -parameter are chosen which are lower than those calculated from experimental values of X-ray absorption coefficients.

1957

L.M. Rieser. (39) Measured I/I_0 versus θ for a number of metal films evaporated on glass, at wavelengths of 1.54 and 2.28 \AA , and compared his results with Fresnel curves calculated using theoretical values of

27.

the parameters. Most of his results show fairly good agreement with theory, but nearly all the curves approach a value of I/I_0 which is smaller than unity, as θ tends towards zero.

1959

R. Groth. (40) Made a number of measurements of I/I_0 versus θ curves for glass and evaporated gold and silver at a wavelength around 9 \AA (filtered WM radiation) by a photographic method. Discussed also the effect of microcrystalline surface structure on the quality of the reflection.

1962

R.F. Wuerker. ¹⁰~~(4)~~ Dr. Wuerker has kindly made available to me a large amount of experimental data from his thesis on the reflection of Carbon K radiation. The curves show the variation of reflectance with glancing angle for many materials including glass, quartz and evaporated layers. In contrast with the results of Laby, Bingham and Shearer, these curves seem to be in good agreement with the Fresnel equations, except in the case of thin evaporated layers, when interference effects occur.

3 (iii). Discussion of the published work.

The following conclusions may be drawn from the work quoted above:

a) Fresnel's equations, when modified to take account of absorption,

describe the variation of reflecting power with glancing incidence extremely well throughout the wavelength range 0.8 to 45 Å. The anomalous effect found by Laby, Bingham and Shearer at 44.6 Å has not been found by other experimenters (28, 41), and it would seem that the effect was due, not to any fault in the Fresnel theory, but to some experimental cause such as poor monochromation of the incident beam. The values of the two parameters β and δ , which must be put into the Fresnel equation to describe the reflection by a particular medium do not, however, always correspond with the values calculated for the medium or, in the case of the absorption parameter, inferred from measurements of the absorption coefficient of the medium. In the case of reflection by evaporated or sputtered layers, it appears that the reflecting properties of the layer may be very different from those of the bulk material. In the case of the discrepancy found by Hendrick between the values of the absorption parameter inferred from reflection experiments and those calculated from tables of experimentally determined absorption coefficients, it may be mentioned that some of the values given in the tables available to Hendrick (S.J.M. Allen in reference 12) have recently been shown to be in error by quite large amounts (41). The β values calculated from the latest results agree closely with those found by Hendrick.

b) The simple equation 2.4 predicts quite well the value of δ for a material in regions well away from an absorption edge. For

regions near an edge, the Drude-Lorentz theory fails to predict, even qualitatively, the correct variation. It seems, however, that measurements of δ involving the estimation of the critical angle of total reflection by photographic methods, especially that in which the position of the 'cut-off' on the photographic film is estimated by eye, do not yield accurate results and do not, therefore, provide sensitive tests of the dispersion theories.

c) When X-rays are reflected from evaporated or sputtered films anomalous results are sometimes obtained, possible reasons being:

1) The density of the film may be different from that of the bulk material, leading to values of δ and/or β different from that calculated using the bulk density.

2) Radiation may penetrate the deposited layer and be reflected from the substrate, causing an apparent change in the critical angle, and sometimes interference effect.

3) The micro-crystalline structure and surface irregularities of the evaporated layer may lead to a change in its reflecting properties.

The last effect tends to make the quality of the reflected image from an evaporated layer poorer than that from a surface polished by the usual optical techniques and it is better, therefore, to use the latter for practical purposes such as X-ray microscopes and telescopes.

3 (iv). Reasons for the present work.

The investigations described in this thesis were undertaken for the following reasons:

a) Because accurate data on the reflecting power of substances, as a function of glancing angle and of wavelength, was completely lacking in the wavelength region between Al $K\alpha$ and C K radiation, i.e. between 8.3 and 44 Å. This region is most important for X-ray microscopy of biological specimens, as it contains the absorption edges of oxygen and introgen. It is also important from the point of view of solar and stellar X-ray studies, and reflection data was required for a number of projects being undertaken jointly by the Space Research Groups of the University of Leicester and University College, London, in particular an X-ray spectroheliograph for the 8-20 Å region.

b) For the project mentioned above, a method had to be found for producing a grazing incidence paraboloidal mirror with good reflecting properties in the 8-20 Å region. Information was therefore required on the suitability of mirrors produced by different processes such as polishing, electroforming, evaporation, and so on.

c) A study of total reflection in this region is of interest from the point of view of testing the Fresnel equations for soft X-rays. This can be done by fitting a curve of the type given by equation 1.9 to an experimentally determined curve of I/I_0 versus θ , and comparing

the values of the X and Y parameters thus obtained with those calculated theoretically. The variation of these parameters with wavelength also gives a test of the various dispersion theories. A case of particular interest is the dispersion near the M-absorption region of Ytterbium compounds containing the Yb^{+++} ion, since these give, not an absorption edge, but an absorption line, due to the incomplete filling of the 4f shell. It was expected that a compound such as ytterbium fluoride would give results which agreed qualitatively with the simple Drude-Lorentz theory.

CHAPTER 4

THE APPARATUS

4 (i). Design criteria.

a) The monochromator.

In much of the previous published work on the reflection of soft X-rays, the spectral region of interest was selected by means of filters. Although the method is capable of giving good results, it is never perfectly satisfactory as the filters always transmit a rather wide band of wavelengths, and so a filtered characteristic line is always flanked by part of the continuum, and usually by other components and satellite lines as well. It was decided, therefore, at the beginning of this investigation, that a crystal monochromator would be used wherever possible. This method also offers the possibility of isolating a narrow band of wavelengths in the continuous spectrum, which is an advantage if one wishes to examine the reflecting properties of a material in a wavelength region in which there are no characteristic lines.

With a crystal monochromating system, one is faced with the choice of a number of geometries. One may use the simple plane crystal geometry, or a focussing spectrometer system, such as the Johansson may be considered. It may easily be seen, however, by reference to Figure 4.1, that any attempt to increase the X-ray intensity available for measurements by focussing the radiation by bending the crystal

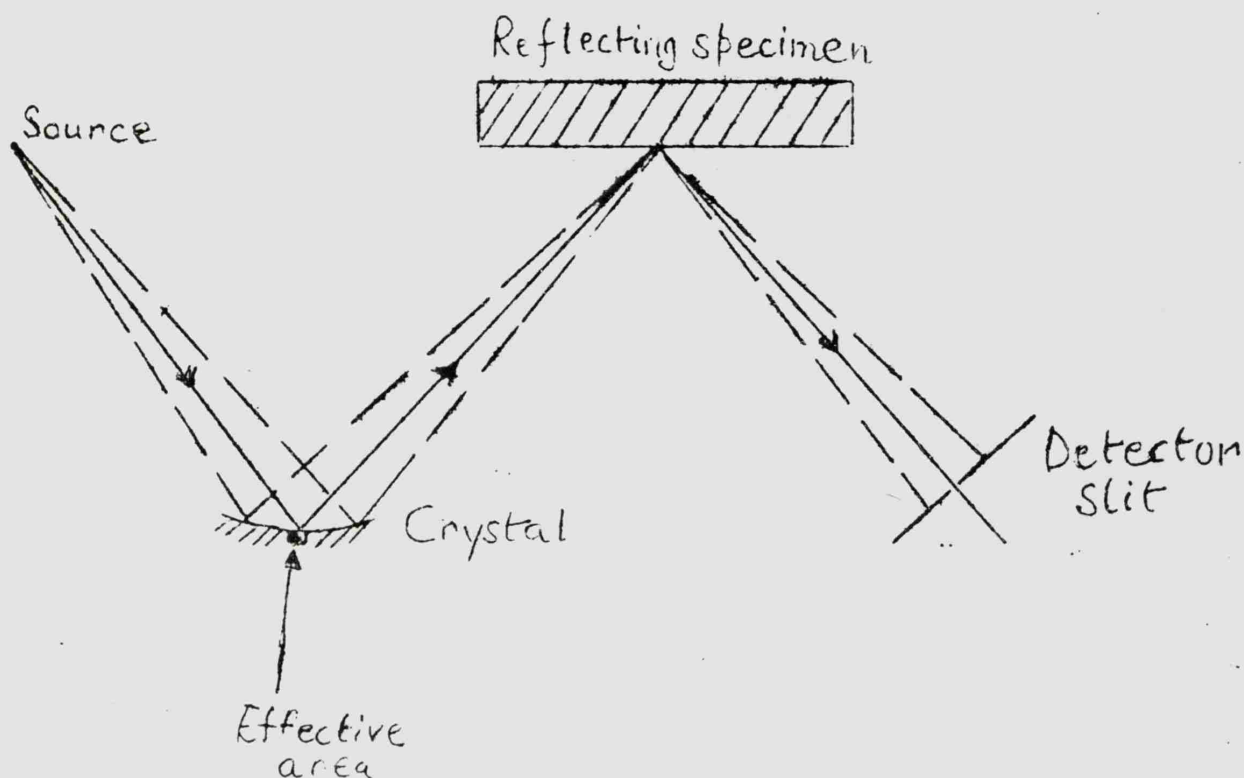


Figure 4.1

about an axis at right angles to the plane in which dispersion takes place leads to the radiation's being incident on the specimen over a range of angles, and as the angles of reflection and incidence must be precisely defined (e.g., by the detector slit) radiation is received from a small area of the crystal only, and the other focussing elements are wasted. Focussing by bending about an axis which is in the plane of dispersion is not feasible, for similar reasons. The simplest arrangement, the plane crystal monochromator, was therefore chosen. This is essentially the same arrangement as was used by A.H. Compton in

his original experiments. The wavelength region of interest extended from 6-20 Å, so a mica crystal was chosen.

b) The detector.

For this item, the proportional counter was the obvious choice, as it combined the advantages of high efficiency, simplicity, and ability to count at a high rate, which made it superior to the other possible alternatives of Geiger counter, scintillation counter and ionization chamber. In addition, by using a single channel pulse height analyser one may discriminate against very soft radiation ($\lambda > 44$ Å) totally reflected from the analysing crystal, and higher orders of Bragg reflected radiation, and so one is able to run the X-ray source at a voltage several times that necessary to excite the required line, thereby obtaining a higher intensity.

c) The reflector mounting.

In the only other investigation of total reflection of soft ($5 < \lambda < 20$ Å) X-rays carried out using pulse-counting techniques, that of Hendrick (38), the reflectances I/I_0 which were measured were not absolute, but were measured with respect to the reflected intensity at a fixed angle, and normalised by assuming that the curves of I/I_0 versus θ approached unity as the glancing angle approached zero. This procedure seemed undesirable, as other workers (39) (40) had found that some surfaces yielded curves which tended to a value considerably less than 1. In view of this, it was decided that, in the present investigations, all

measurements of reflectance would be made with respect to the direct beam. In order to do this, some means of retracting the specimen from the beam had to be provided, so that the incident intensity I_0 could be measured directly.

The most important design criteria for the reflectometer may now be summarised:

- a) Plane mica crystal monochromator.
- b) Proportional counter as detector, in conjunction with pulse-analysing electronics.
- c) Provision for withdrawing the specimen from the beam, and accurate re-positioning.

In addition, it was necessary to enclose the whole instrument in a vacuum tank for operation in the soft X-ray region, and it was desirable to have the facility to carry out as many operations as possible without breaking the vacuum.

The general layout of the apparatus corresponds to that shown diagrammatically in Figure 3.1 (c). A plan of the apparatus is given in Figure 4.2, and photographs of it in Figures 4.4 and 4.5, and 4.6.

4 (ii). Construction of the instrument: Tank and vacuum equipment.

The reflectometer was enclosed in a circular tank approximately two feet in diameter with a base of $1\frac{1}{2}$ inch thick cast and machined aluminium alloy. The wall was a ring of the same material one inch

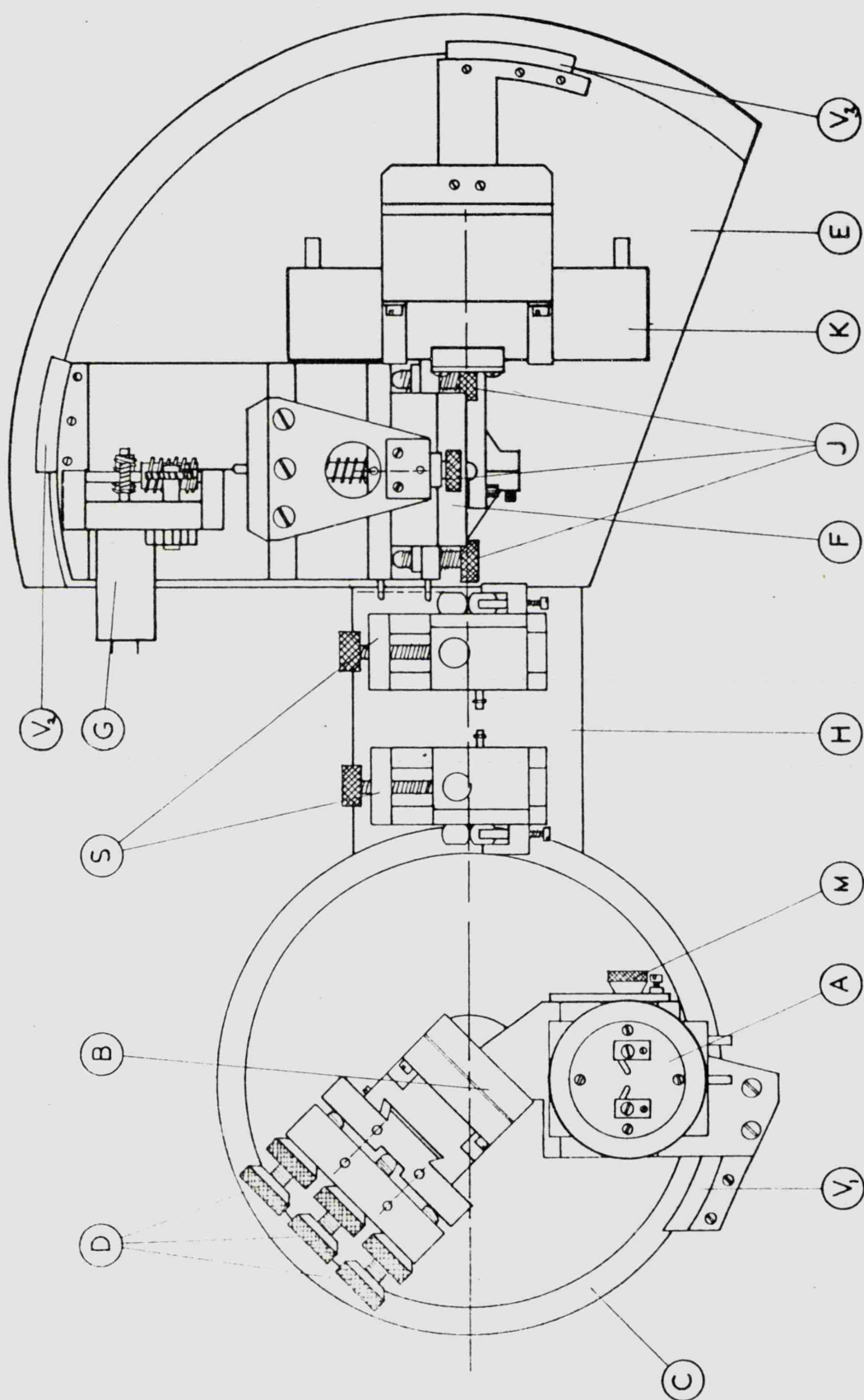


FIG. 4.2. PLAN VIEW OF REFLECTOMETER

KEY TO FIGURE 4.2.

- A X-ray source.
- B Crystal block.
- C Wavelength scale.
- D Crystal adjusting screws.
- E Glancing angle scale.
- F Reflecting specimen.
- G Specimen retracting motor.
- H Base plate ($\frac{3}{8}$ " steel gauge plate).
- J Adjusting screws for specimen.
- K Proportional counter.
- S Slits.
- V₁ Wavelength vernier.
- V₂ Counter vernier.
- V₃ Glancing angle vernier.
- M Source adjusting screw.

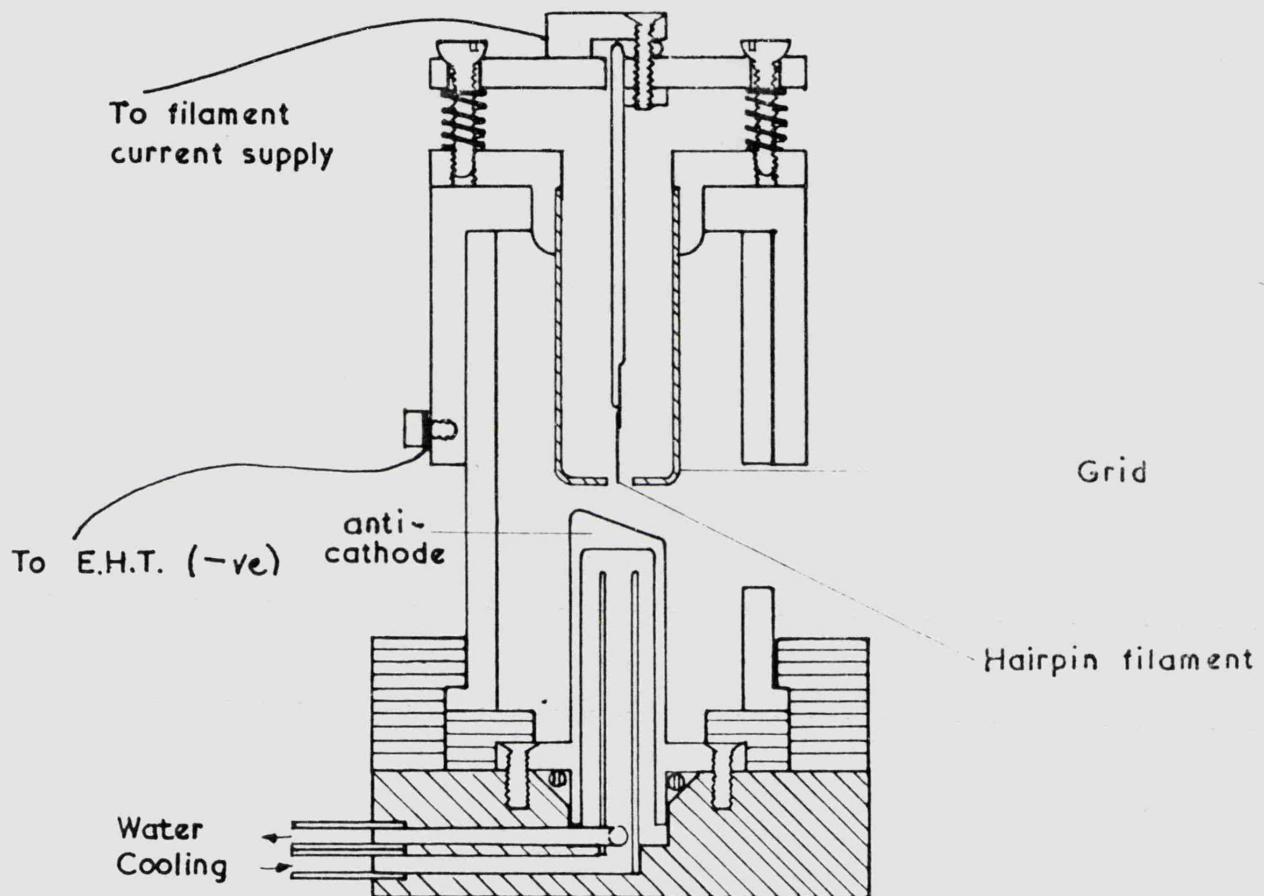
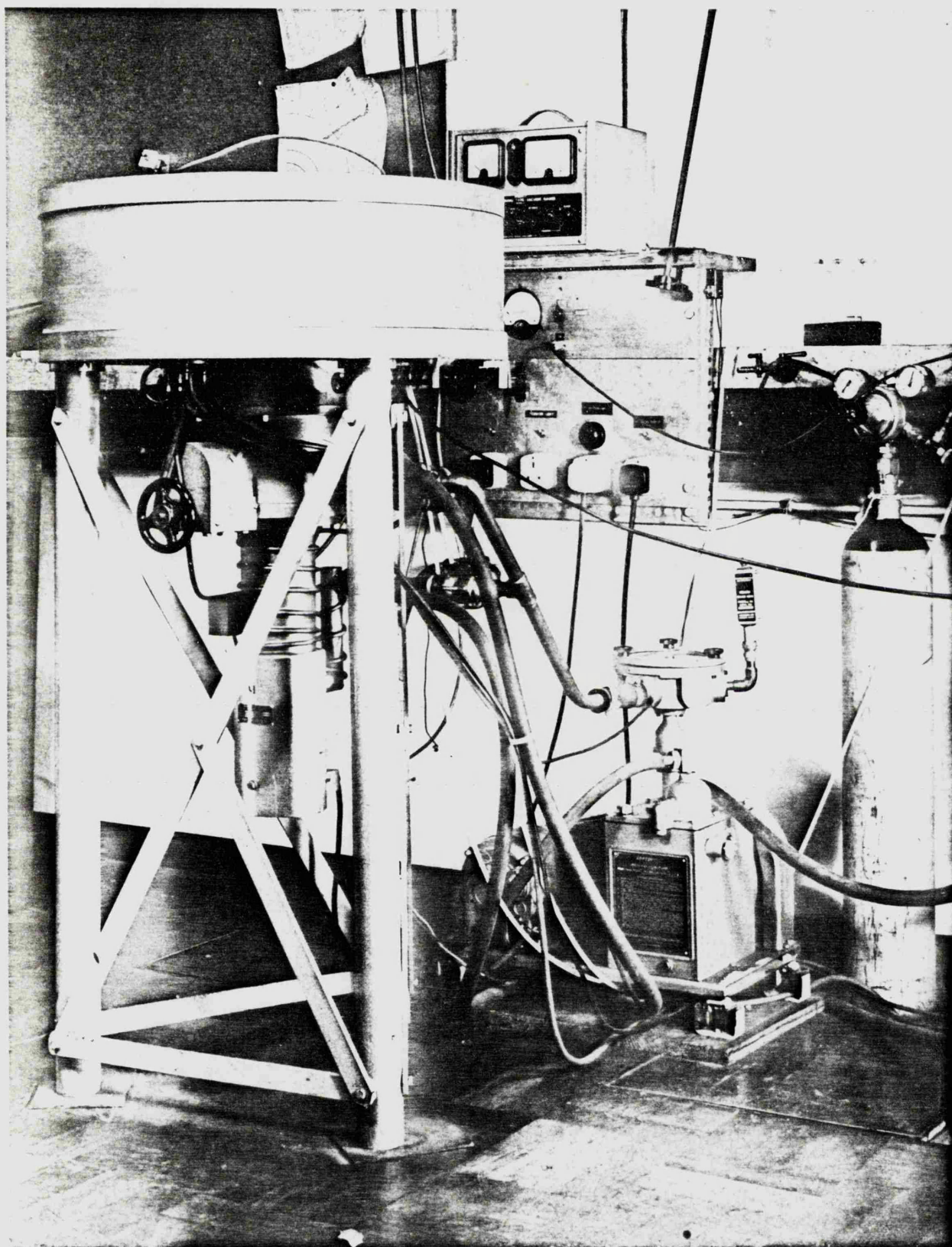
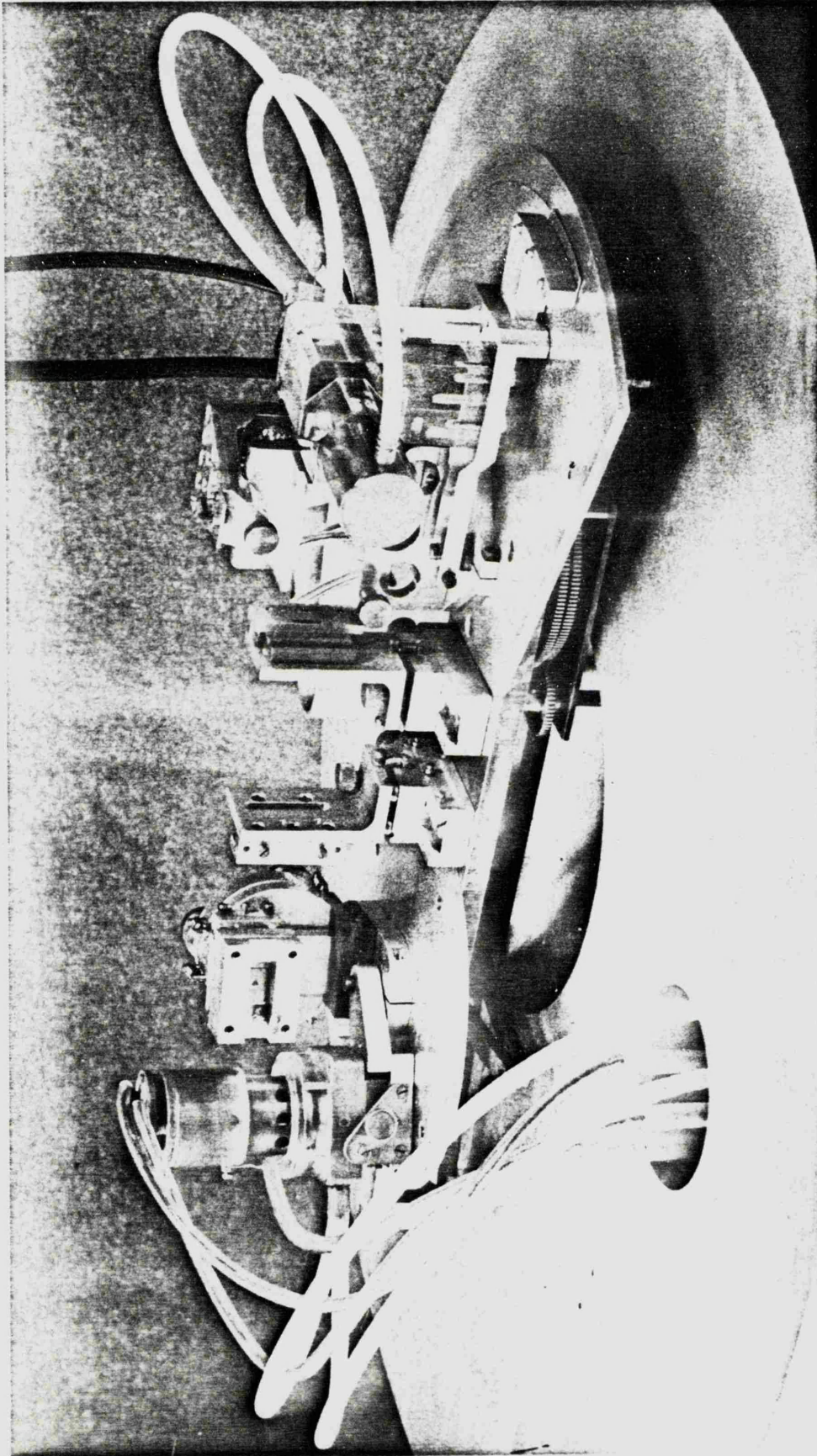


FIG. 4.3. CROSS-SECTION OF X-RAY SOURCE.

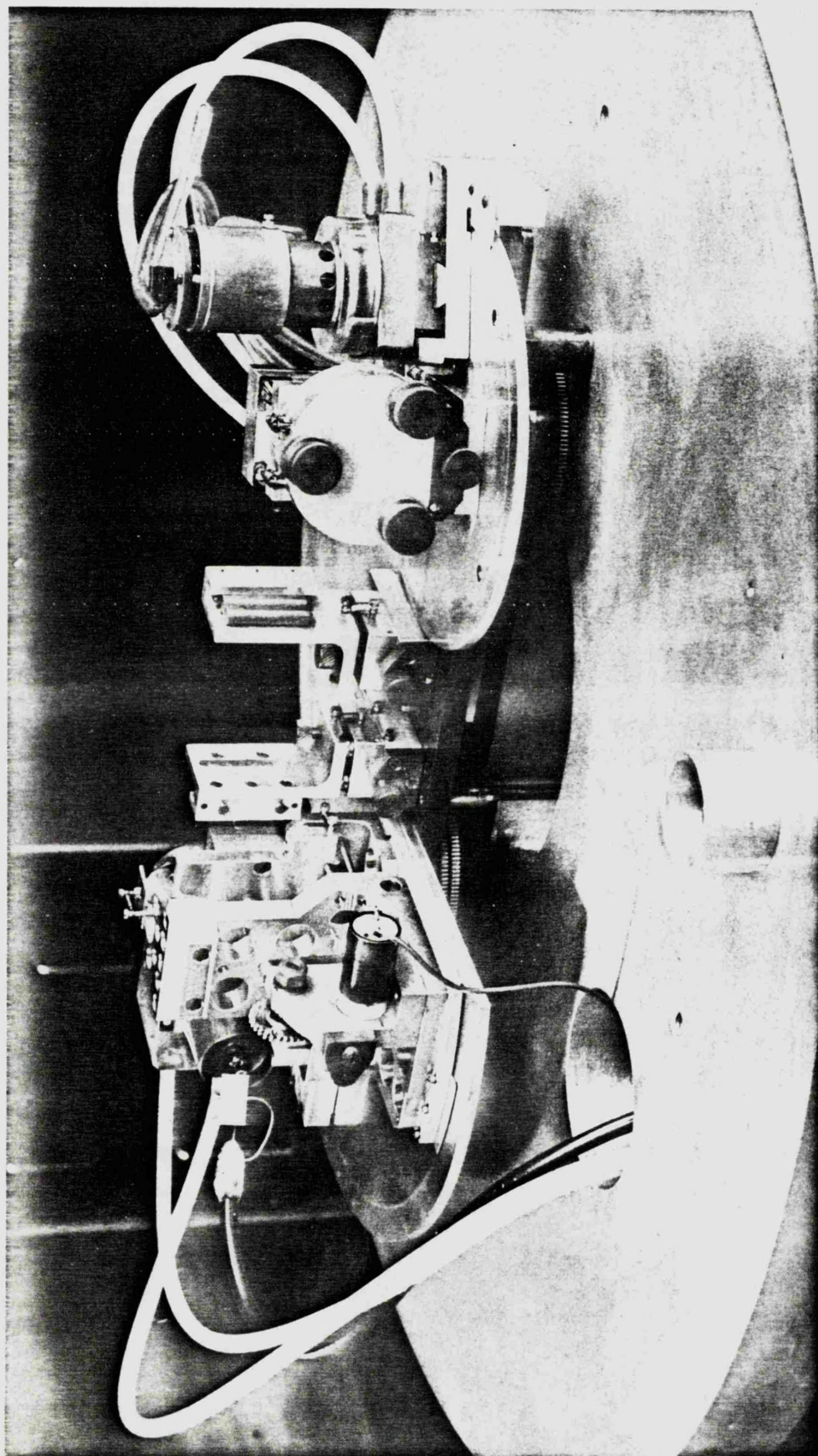


4.4 General view of apparatus.



4.5 Tank interior.

41.



4.5 Tank interior - rear view.

thick and six inches high. The lid, again a machined aluminium casting, had two $\frac{3}{4}$ " thick 'Perspex' windows, sealed by 'O' rings, let into it. The joints between the lid, wall and base were also sealed by 'O' rings.

A hole was cut in the centre of the baseplate and the diffusion pump and baffle valve connected to the tank via the hole and an 'O' ringed circular flange about $1\frac{1}{2}$ " deep. The moving parts inside the tank were driven by steel rods which passed through rotary vacuum seals in the wall of this flange.

The diffusion pump was backed by a rotary pump and the tank and backing pressures were measured by a Penning gauge and a Pirani gauge respectively. The tank was evacuated to a pressure of about 2×10^{-5} torr when the source was running.

4 (iii). The source.

Owing to the geometry of the system, it was not expected that the intensity of the Bragg reflected beam would be very high and it was therefore necessary to use an X-ray source with as fine a focal spot or line as could be obtained, in order to obtain a useful count rate. Several types of source were tried, including a wire anode source as used by Hendrick (38) and an electrostatic fine-focussing source of the Ehrenberg-Spear variety (44). It was found that the latter could not be made to operate satisfactorily at the low voltages required (0-5 kV),

whereas the beam current obtainable from the wire anode source was limited by heating of the wire to a few milliamps. The source which was eventually built and used is shown in Figure 4.3.

The anticathode of this source was demountable, so that targets of different materials could be used. Targets sloping at angles of 20° and 30° were tried in order to investigate whether the slope of the target made any difference to the X-ray output. One would expect that the more steeply sloping target would give the ~~largest~~ output, as the X-rays have less material to penetrate in escaping from the point inside the target where they are produced. In fact, no conclusions could be drawn on this point as the intensity of emission from a single target underwent considerable fluctuations. These fluctuations frequently made reflection measurements very difficult, as will be described later.

The source high voltage and filament current were supplied by a regulated high voltage unit and stabilised filament supply manufactured by A.P.T. Electronic Industries Ltd. By means of an H.T. battery and a potentiometer, a negative voltage could be applied to the grid with respect to the filament. This voltage had little effect in focussing the electron beam, but was very effective in reducing stray radiation produced by electrons from the filament reaching earthed parts of the apparatus other than the target. This effect often causes trouble when the filament is run at a high negative

potential with respect to an earthed target, as it was in the present apparatus, for simplicity of target cooling.

The source was mounted on a dove-tail cross-slide and its position could be finely controlled by means of the fine-pitch screw M_2 , so that the maximum intensity could be obtained in the Bragg reflected beam. The cooling water was supplied by a constant head device through thick polythene tubes.

4 (iv). Crystal and 2 : 1 linkage.

Although a plane crystal geometry was decided upon, it is not easy to obtain a perfectly flat specimen of mica. Most cleaved natural specimens have a slightly wavy surface which makes them unsuitable for X-ray spectroscopic work. It is not easy to straighten such a crystal so as to obtain a sufficiently plane surface, but the waviness may be 'ironed out' by bending the crystal to a large radius of curvature between cylindrical blocks. The radius of curvature of a crystal bent in such a fashion may be altered slightly, within limits, and the crystal may be tested in a simple manner for perfection, as will be described later. For these reasons, a crystal bent to 2 metres radius was used. As the area of crystal in use is very small (see Figure 4.1) the crystal may be considered effectively plane over this area.

The crystal was bent between two matching aluminium blocks

machined and lapped together to the required radius of curvature (B in Figure 4.2). A hole 1 cm. x 1.5 cm. was cut in the front (convex) block to allow the radiation to reach the crystal. The blocks were held together by four finger screws at the corners which allowed the crystal to be adjusted so as to be perfectly cylindrical. This adjustment was carried out in the following manner:

The crystal block was placed on an optical bench with an illuminated pinhole at the centre of curvature. The front surface of the mica, acting as a cylindrical mirror, formed an astigmatic image of the pinhole, which appeared as a line in an eyepiece placed alongside the pinhole position. A poor piece of mica, or a good piece which was out of adjustment, gave an image which was distorted, multiple and blurred, but by adjusting the four screws at the back of the crystal block, a good specimen could be made to yield a single straight sharp line. When these adjustments had been made, the screws were painted with shellac to prevent their loosening. The piece of mica eventually selected was exceptionally good, as no reduction of the crystal aperture was needed to produce a good image.

The crystal block was mounted on a dovetail slide, so that it could be adjusted in the vertical direction. This in turn was mounted on an adjustable 3-point kinematic assembly, on another dovetail slide driven by a micrometer screw. These adjustments allowed the crystal face to be brought coincident with, and parallel to, the axis of rotation.

The source and crystal arms were driven by concentric shafts protruding through the steel supporting plate and the engraved scale C. A linkage of the type described by Hendrick (38) ensured that the source always moved through twice the angle that the crystal moved through, so that the Bragg reflected beam always travelled in the direction of the slits. This linkage was made from machined brass strips, the holes being drilled on a milling machine with a spacing tolerance of $\pm \frac{1}{2}$ thou.

The source-crystal angle was read off on the scale C by means of the vernier V_1 attached to the source arm. This scale could be read to ± 2 minutes of arc.

4 (v). The Slits.

Each of the 2 slits was made of 2 pieces of $\frac{5}{16}$ " silver steel rod held in a frame, and kept apart by small compression springs let into holes drilled in the ends of the rods. One rod was fixed to the frame and the other could be pressed against it by two small screws bearing on the top and bottom. The width of the slits could be adjusted in this way, by means of a feeler gauge. The frame holding the rods was fixed to an adjustable 3-point kinematic assembly attached to a dovetail slide, which was driven by a micrometer screw. These adjustments allowed the slits to be brought onto the axis of the instrument (the line joining the axes of rotation of the crystal and

and reflecting specimen), and parallel to the face of the specimen.

At the beginning of the investigation, it was found that the polished surface of the silver steel rods reflected X-rays quite well, and this effect was causing erratic results. The trouble was cured by etching the rods in nitric acid to give them a matt surface.

In addition to the two fine slits, an additional rough screening slit cut from a sheet of aluminium was interposed between them to reduce the stray scattered radiation reaching the detector.

4 (vi). The specimen mount.

The specimens were all in the form of rectangular flats 2" x 1" x $\frac{3}{8}$ " thick. These were fixed to mounting blocks which could be screwed to a flat aluminium plate $\frac{3}{8}$ " thick. This plate was spring loaded against three fine-pitch screws which could be adjusted to bring the face of the specimen parallel to, and coincident with, its own axis of rotation.

Retraction of the specimen was performed by means of a small d.c. motor, geared down by a series of worms, which drove a rod attached to the back of the aluminium plate by a ball and socket joint. The latter allowed the plate to pivot freely and be firmly relocated against the three adjusting screws when the specimen was brought back into the beam. The whole assembly was mounted on a rotating table, to which was attached a vernier reading to one minute of arc on the

engraved scale. This scale had an arbitrary zero, and had to be calibrated to find the glancing angle (see next chapter).

The reflector and detector were again driven by concentric shafts, connected through gear trains to knobs outside the vacuum tank.

4 (vii). Counter and electronics.

The detector was a flow proportional counter made by 20th Century Electronics Ltd to the author's design. The stainless steel cathode was $1\frac{1}{4}$ " in diameter and carried a small saddle to which the windows could be attached. A slit 1 cm. long and 1 mm. wide was cut in the saddle and the counter wall, perpendicular to the length of the counter, to allow the radiation to enter. The window was a piece of 'Melinex' stretched under gentle heat until it showed interference colours, and estimated to be less than one micron thick. The central wire was one thou tungsten, and the flow gas a mixture of 90% argon, 10% methane. The gas was supplied to the counter through polythene tubes. P.V.C. tubes were found to give off vapours which impaired the resolution.

The counter was mounted in a horizontal position on a rotating arm which allowed it to be moved back and forth from the reflected to the direct beam.

In the usual mode of operation, the voltage pulse from a proportional counter is fed into a cathode follower or head amplifier

mounted close to the counter, and from thence into the main amplifier, via a fairly long cable. This arrangement may cause some difficulties when the counter is in a vacuum system, as extra lead-through terminals must be provided for the cathode follower/head amplifier H.T. and filament supplies. The amplifier must be switched off when the tank is pumping down, to prevent discharges, and there is also the possibility that valve electronics working in vacuum may become overheated.

It is possible to avoid these difficulties by operating the counter in the so-called 'current mode' (45, 46). In this mode of operation the current pulse from the counter is fed down a long cable into an amplifier of low input impedance. This low input impedance is easy to achieve with transistors, as the input impedance of transistor circuits is inherently low, but a valve amplifier of low input impedance can be made by using a 'virtual earth' circuit. This method of approach was used in the present investigation, and the circuit of the amplifier is given in Figure 4.7. A discussion of the 'current mode' and of this circuit is given in Appendix A.

With this circuit, a cable up to 20 feet long could be used with only a 30% reduction in pulse height, and no loss of proportionality. A six-foot cable was used in the actual apparatus.

A block diagram of the electronics is shown in Figure 4.8. The main amplifier also supplied the H.T. and filament supplies for the current amplifier. The scaler and timer were claimed by the makers

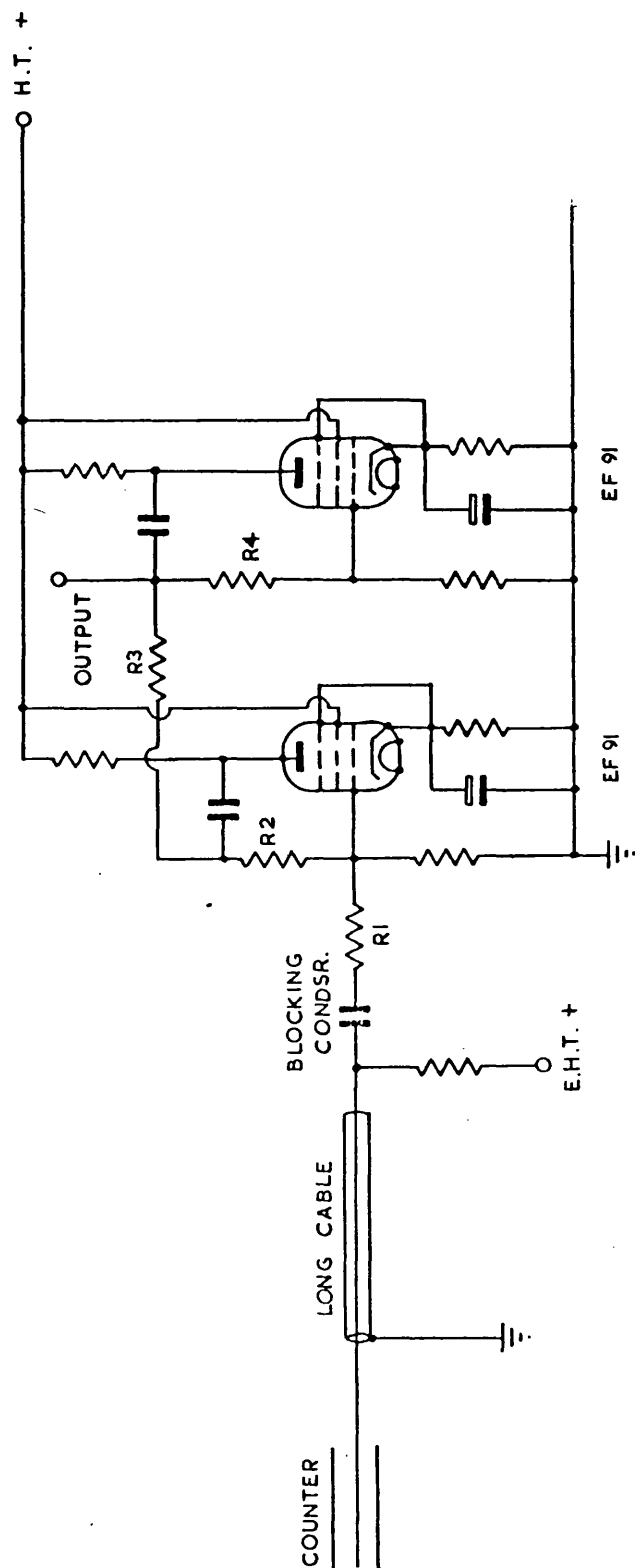
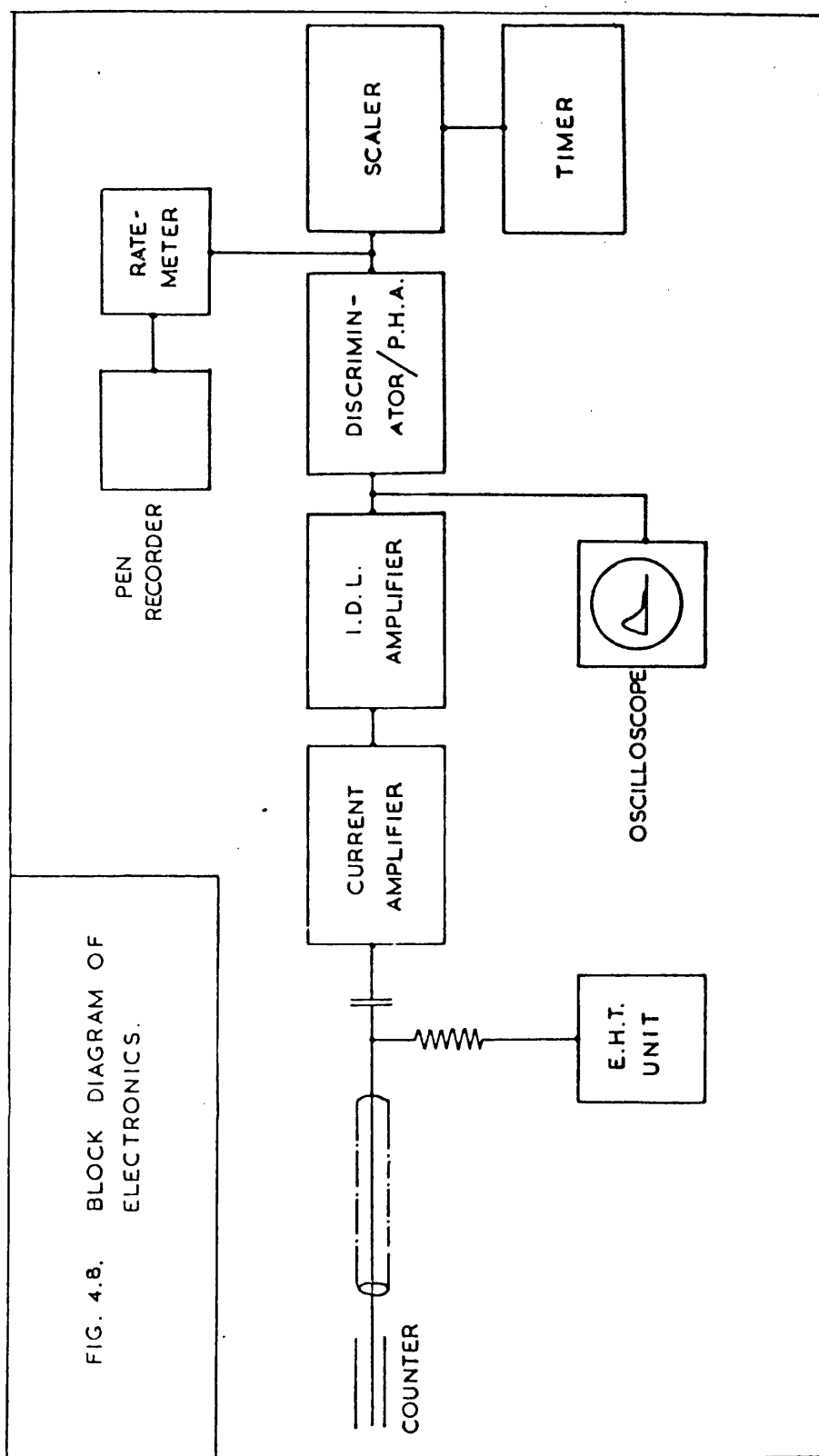


FIG. 4.7 CURRENT AMPLIFIER CIRCUIT.



(Labgear Limited) to operate at speeds of up to 20,000 counts per second. This was verified by means of a double pulse generator.

When the apparatus had been set up and was working well, the resolution of the proportional counter was measured using various characteristic radiations. As these tests yielded interesting results, they have been made the subject of a separate appendix (Appendix B). It is sufficient to note here that the resolution was quite adequate to discriminate against higher orders of Bragg reflected radiation.

CHAPTER 5

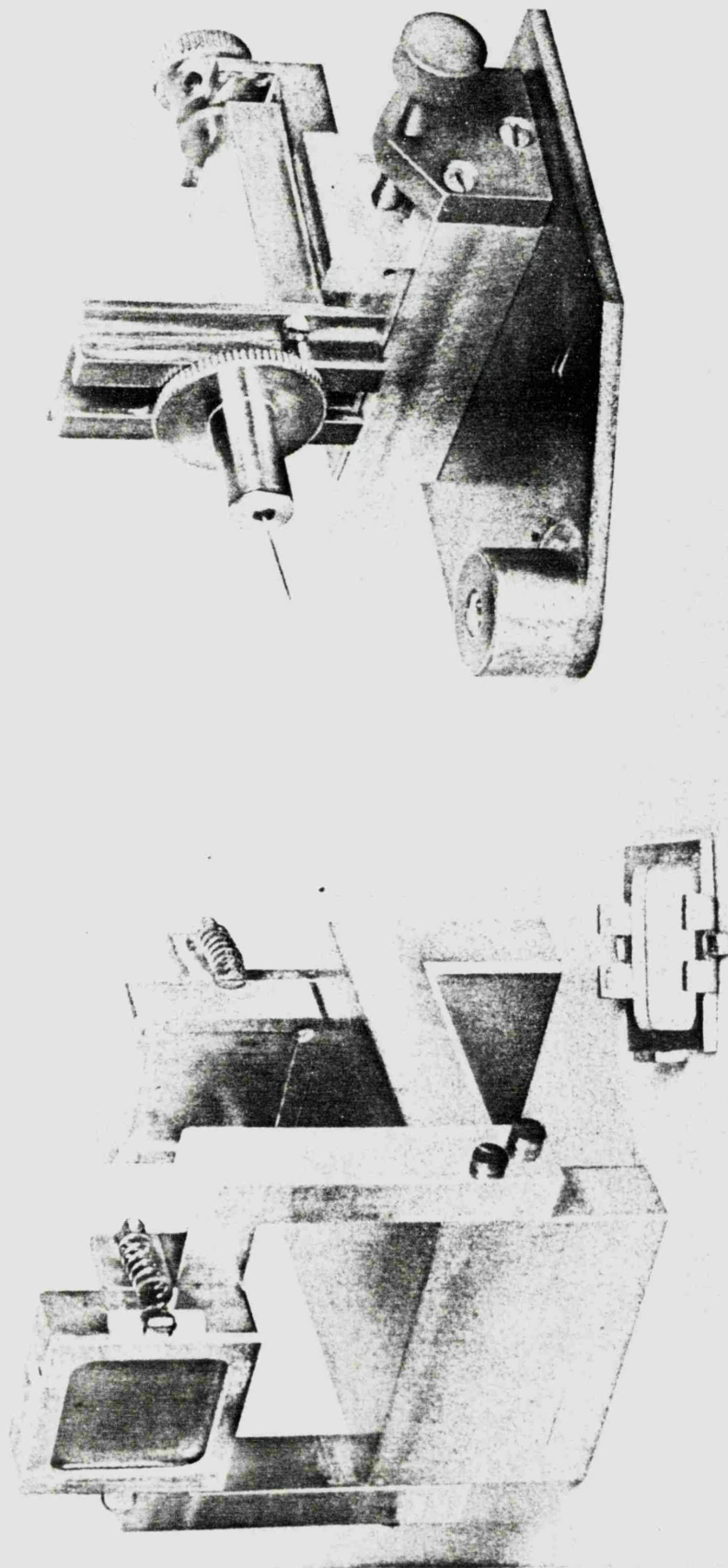
EXPERIMENTAL METHOD

5 (i). Preliminary alignment.

Before the completed apparatus could be used for reflection measurements, the following preliminary adjustments had to be made:

- a) The surface of the mica crystal had to be brought parallel to, and coincident with, its own axis of rotation.
- b) The same adjustment had to be made for the reflecting specimen.
- c) The slits had to be brought onto the axis defined by these two axes of rotation.
- d) The slits also had to be adjusted so as to be vertical, i.e., parallel to the axes of rotation of crystal and specimen.
- e) The position of the X-ray source had to be adjusted for maximum intensity in the Bragg reflected beam.

The first two adjustments were made by a method due to Siegbahn (see Handbuch der Physik, Volume XXX, page 103). A fine needle was mounted on two crossed dovetail slides so that it could be moved in two mutually perpendicular directions in a horizontal plane by means of micrometer screws. The assembly, shown in Figure 5.1, could be attached to the inner of either set of concentric shafts and rotated in a circle. The point of the needle was observed through a microscope, and could be seen describing a small circle when the system was rotated. By means of the adjusting screws, the point could be made to coincide with the



5.1 Auxiliary apparatus.

Left: double film holder.

Right: Crystal aligning device.

axis of rotation. The crystal could then be brought on to the axis by observing, through a microscope, the image of the needle point formed by reflection in the point surface of the crystal. The three screws at the back of the crystal mount, and the screw controlling the slide on which the crystal assembly moved, were adjusted until the point of the needle appeared to coincide with its own image. When this occurred, the point of contact of the needle point and its image was on the axis of rotation. In order to bring the crystal surface parallel to the axis, the height of the needle was changed, and the process repeated.

As the adjustments were not independent, they were repeated alternatively several times. The adjustment of the reflecting specimen was carried out in exactly the same manner.

Adjustment (c) was performed using a travelling microscope supported over the apparatus. The slide of the instrument was brought parallel to the line joining the axes of rotation of crystal and reflector by focussing on the needle point of the device previously described with it first on the crystal axis, then on the reflector axis. When the microscope could be moved from one axis to the other, the needle point still remaining at the centre of the cross-wires, its direction of travel was coincident with the line joining the rotation axes. The slits were then brought on to this line with the aid of the microscope.

When this adjustment had been performed, a beam of light was directed down the slits, and the tilt of the slits adjusted until the line of light emerging from the second slit, observed on a screen, was straight and intense, indicating that the slits were parallel to each other. By reflecting the beam from the specimen at a small angle, so that part of the direct beam spilled past the specimen, it was possible to observe the direct and reflected beams on the screen simultaneously, and to adjust the slits until the two lines were parallel, indicating that the slits were parallel to the specimen. The accuracy with which this adjustment could be carried out by this method was limited by diffraction, and so the adjustment was later repeated using X-rays and a photographic plate, once the alignment had been carried out roughly.

Adjustments c and d are interdependent, and had to be repeated alternatively several times.

Adjustment e was performed by shining the beam of light through the slits in the reverse direction, so that the beam was reflected off the front surface of the mica crystal and on to the target. The source on its cross-slide was adjusted by means of the micrometer screw until this reflected beam fell on the centre of the target, where there was most discolouration due to electron impact. When the adjustment was made in this way the count rate from a strong characteristic line such as Al K was between 1000 and 7000 counts per second, with 3 kV

excitation voltage and a few mA tube current. If the source was moved away slightly from this optimum position the available count rate fell considerably.

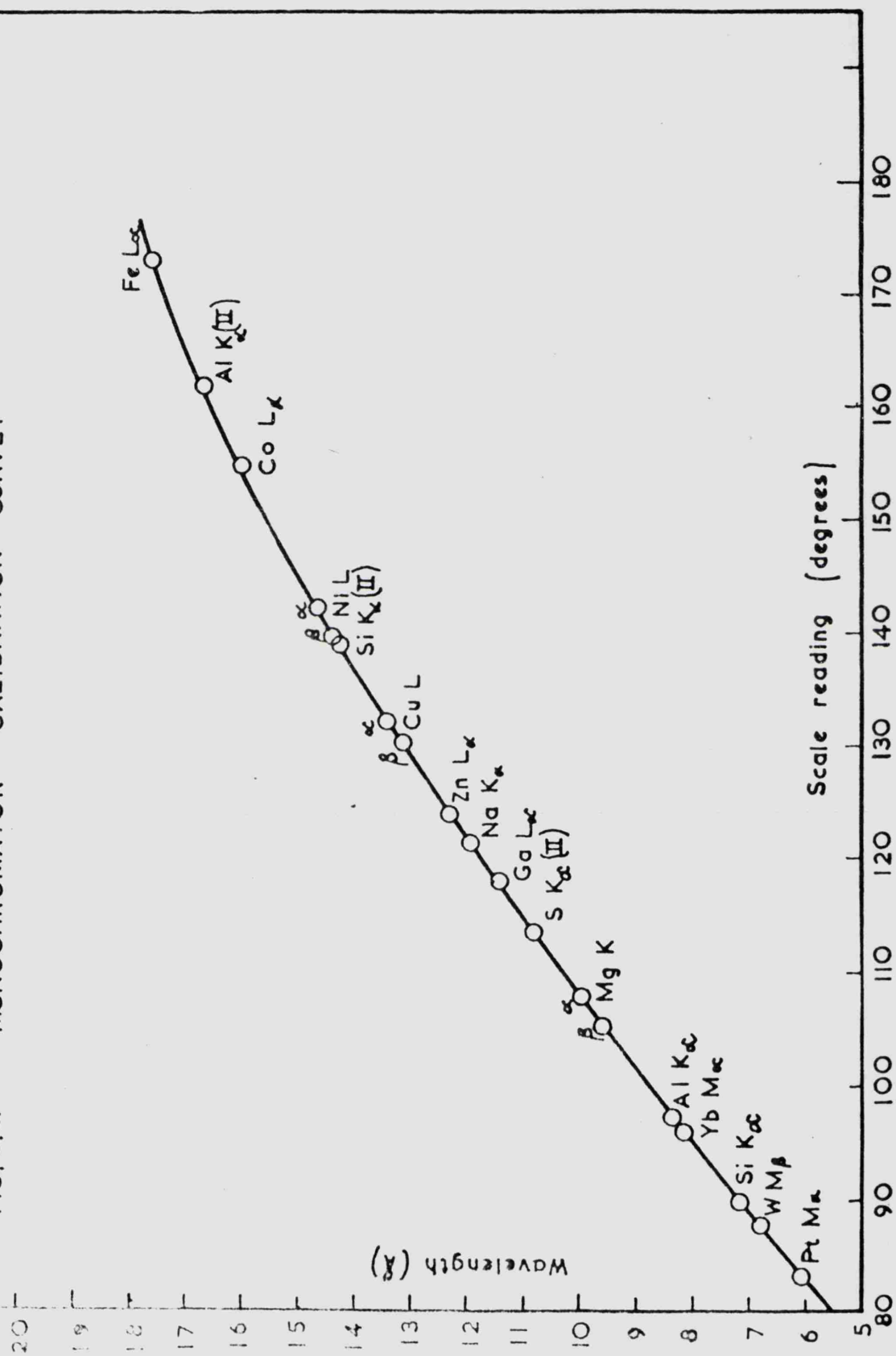
5 (ii). Calibration of monochromator and reflector.

The wavelength calibration of the monochromator was carried out using targets of different materials, or targets coated with a compound (usually the oxide) to give a characteristic line of an element. The source - crystal assembly was rotated until the line was picked up, and then adjusted until maximum count rate was registered. The angular position of the source arm was then read off. The curve of source position versus wavelength is given in Figure 5.2.

As was mentioned in Section 4 (vi), the reading of the vernier attached to the reflector mount gave the angular position of the specimen with respect to an arbitrary zero. In order to convert this to glancing angle θ , the true zero of the scale, i.e., the vernier reading with the reflector in the position corresponding to $\theta = 0$ had to be found.

In principle, this could be done by placing a position so far as to record the direct beam and the beam reflected at a given vernier setting. Knowing the distance D from the film to the specimen, and the distance d separating the two blackened strips on the film, one may calculate the value of θ corresponding to that vernier setting

FIG. 5.2. MONOCHROMATOR CALIBRATION CURVE.



($\tan 2\theta = \frac{d}{D}$) and thus find the true zero.

In practice, however, the distance D is difficult to determine, since at small angles the point at which the X-ray beam strikes the flat is uncertain, in fact different parts of the beam strike the specimen in different places. If, however, the single film is replaced by two plates separated by a precisely known distance, arranged in such a way that each intercepts half the X-ray beam, then this problem can be avoided.

Figure 5.3 shows the principle of the measurement when made in this manner.

A special double film holder was made for the purposes of this calibration and is shown in Figure 5.1. Pieces of X-ray film were clamped into the recessed holders by the spring loaded frames. The films were covered with 7 micron aluminium foil to exclude visible light. The prepared film holder was positioned in the tank, which was then pumped down. The films were then exposed to the direct beam. After this the reflector was carefully set to a known scale angle and the films exposed to the reflected beam. After development the separations of the blackened strips on the films were measured by means of a travelling microscope. This procedure was repeated a number of times, and the scale reading corresponding to $\theta = 0$ calculated.

A test was made on a piece of the film used to see if any shrinkage occurred during the development process, which might affect the accuracy of the calibration. This was done by shielding part of

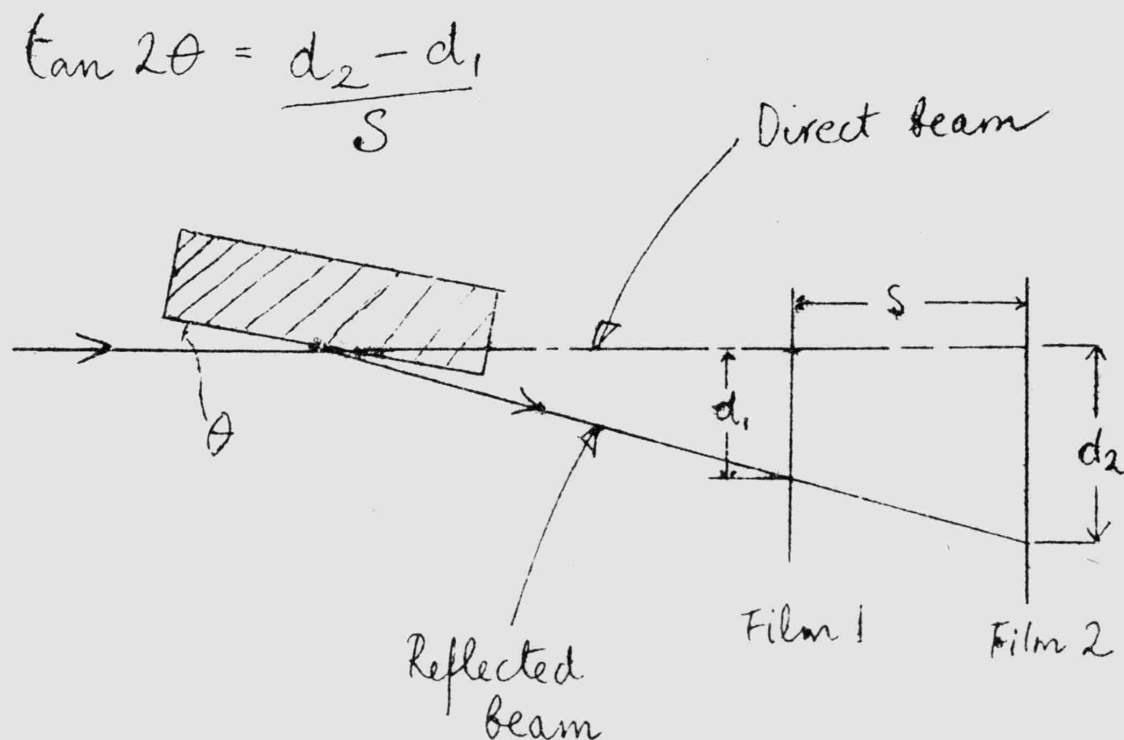


Figure 5.3.

the test piece with a metal strip of accurately known width while the rest of the film was momentarily exposed to light. Measurement of the width of the unblackened strip on the film after it had been processed showed that no detectable shrinkage had taken place.

When these calibrations were finished, the apparatus was ready for the measurement of reflection.

5 (iii). Method of obtaining reflectance curves.

The apparatus was used to obtain the variation of 'reflectance' I/I_0 with glancing angle θ for various materials, at a number of characteristic wavelengths in the range 5-16 Å. It was not possible to

make measurements right up to the wavelength limit at which the mica crystal could be used (19.8 \AA), owing to the low efficiency of production of X-rays in this region, and the rapidly increasing absorption of the counter window, which together resulted in a count rate too low for accurate intensity measurements to be made.

The curves of I/I_0 versus θ were obtained in the following manner:

First of all, a target was prepared which would give the chosen characteristic line. The target was either made from the element itself or coated with a compound (usually the oxide). Targets were coated by applying a paste of the compound made by grinding it up with water or some other vehicle in which it did not dissolve. The target was then re-assembled in the tank, which was then pumped down to a pressure of about 2×10^{-5} torr, and left for some time so that the target material could degas thoroughly. The X-ray tube was switched on and the tube current adjusted to a few milliamps. The specimen was retracted and the detector window brought into line with the direct beam. The pulses from the main amplifier were observed on the oscilloscope, and the discriminator level or pulse height analyser level were set so that unwanted radiation was not counted. Pulse height analysis was necessary only for the softest radiations ($\lambda > 14 \text{ \AA}$), as a high voltage had to be used to excite these in sufficient intensity, so that the Bragg reflected beam contained some higher order radiations from the continuum. The

harder radiations were produced using only twice the excitation voltage.

The tube current was set so as to obtain a convenient count rate (usually between 2000 and 4000 counts per second), and then the count rate was followed for a period of up to an hour. Usually, it fell steadily for the first ten minutes or quarter of an hour, and then remained steady, or sometimes began to rise again slowly. This effect was presumably due to this build-up of contamination such as carbon from the pump oil on the target. Most of the reflection runs were taken when the emission had reached a steady value. In some cases, however, the emission could not be held constant, but fell off rather rapidly to a low value. In these cases, measurements were still taken, by the method to be described, but the results are of course not as accurate (see Section 6.). Sometimes the run had to be stopped and the target cleaned before a complete set of readings could be taken.

In order to offset the effect of any drifts in emission, small or large, all the readings were taken by an interpolation method due to B. Nordfors (47). First, the specimen was set to a known glancing angle using the circular scale. With the counter in the direct beam, pulses were counted for a predetermined period (usually ten seconds). Let the number of counts accumulated in this period be N_1 . The specimen was then brought into the direct beam by actuating the driving motor, and the counter was moved round until the reflected beam was picked up. The number of counts accumulated in a further ten-second period was then

recorded. Without moving the specimen, another ten-second count was then made. Let these numbers be N_2, N_3 . The specimen was then retracted and the counter moved back into the direct beam. Two more readings N_4, N_5 were then taken. The process was repeated, taking the readings in pairs alternately until enough had been obtained to give a good average.

I/I_0 was then taken as the average of $\frac{N_2}{N_1}, \frac{N_3}{N_4}, \frac{N_6}{N_5} \dots \dots \dots$ etc. (after

background had been subtracted). It can be seen that this method compensates to some degree for a uniform drift, whereas if the readings had been taken singly and alternately, a greater error would have arisen.

Readings were taken with increasing values of θ until the value of I/I_0 had dropped to about 1%. As the beam was of finite width, and also diverging a small amount, it spilled past the reflector when set at small glancing angles. The smallest glancing angle at which measurements could be made was about $30'$.

When θ was large, and the number of counts in the reflected beam was small, a background count was subtracted from the reflected beam counts, but this was entirely negligible compared with the direct beam counts, and the reflected beam counts for smaller θ . The background count was taken as the number of counts measured in the 'reflected beam' position, but with the specimen withdrawn. At the count rates used, no correction for 'lost counts' was required.

5 (iv). Reduction of data.

In order to test the validity of the Fresnel equations, modified for absorption, it was necessary to compare the curves given by equation 1.9 with the experimental data. This was done by finding the values of Y and θ_c which, when substituted in equation 1.9 gave a curve which most nearly fitted the experimental points. This fitting was done with the aid of a computer (Elliott 803) programme which calculated the best value of the two parameters in the following manner:

The values of θ at which the reflectance was measured, and the corresponding values of I/I_0 , were fed into the computer, together with guessed starting values and maximum and minimum values for the parameters θ_c and Y . Using these starting values, the computer calculated the theoretical values of I/I_0 from equation 1.9 at each value of θ given, and subtracted these from the corresponding experimental values. These differences were squared and summed, resulting in a quantity S .

The values of the parameters were then changed by a predetermined amount (a 'step length' previously fed in with the other data) and the process repeated to give a new value of S . The parameters were changed again, a new value of S calculated, and so on until a minimum value of S was arrived at, using the step lengths originally given. This minimum was then printed out, together with the corresponding values of θ_c and Y , as the result of 'ITERATION 1'. The step lengths were then reduced by the computer, and the process repeated until a new minimum, and new values

of θ_c and Y were found and printed out as the result of 'ITERATION 2'. The programme was allowed to run until the results of successive iterations agreed to the sixth significant figure. This usually occurred around the seventh or eighth iteration.

The values of θ_c resulting from the curve fitting were compared with those predicted from the various dispersion theories. From the resulting Y values, values of the mass absorption coefficient of the medium were calculated, using the relation

$$\frac{\mu}{\rho} = \frac{4\pi Y \theta_c^2}{2\lambda \rho} \quad (5.1)$$

These mass absorption coefficients were compared with those obtained by other methods.

5 (v). Experimental Error.

The experimental curves of I/I_0 versus θ may be in error in the glancing angle determination and in the intensity measurements.

Considering the former, the vernier indicating the angular position of the reflector could be read to ± 1 minute. The photographic method of finding the true zero of the scale introduced an error of approximately one minute, arising from the measurement of the films, but as the calibration process involved taking a vernier reading, we must add a further one minute error, making the zero of the glancing angle scale

uncertain by about ± 2 minutes.

The intensity errors may be estimated using the rule that the probable error is equal to the square root of the number of counts taken. Except for the softest radiations used (Ni L_{α} at 14.6 \AA and Co L_{α} at 16.0 \AA) the number of counts from the direct beam was always well above 10,000, usually in the range 20,000-30,000, so that the error in measuring the incident intensity was below 1%. The number of counts in the reflected beam, however, varied from 0.9 to 0.01 times the number in the direct beam, so that the probable error varied from less than 1% to about 10%. This figure is, of course, reduced because a number of readings of I/I_0 were taken and averaged. This number was usually between 10 and 30. Taking account of these factors, and of drifts in intensity, it is considered that the values of I/I_0 are accurate to $\pm 3\%$ for wavelengths less than 14 \AA and values of I/I_0 greater than about 0.07, while for values of I/I_0 less than this, the error may be as much as 10%.

As a check on the error in intensity, 50 measurements of I/I_0 were made at a fixed angle on a Pyrex specimen at the wavelength of Al K_{α} radiation, and the standard deviation of the results was calculated. It was found that $I/I_0 = 0.582 \pm 0.0055$, an error of less than a percent. The emission was fairly steady during these measurements.

Owing to the lower intensity of the direct beam in the Ni L_{α} and Co L_{α} runs, and the greater drift, the estimated error in I/I_0 for these runs is approximately twice the corresponding error for the

harder radiations.

The curves could be repeated very well. Figure 5 in the next chapter shows the results of two separate runs on Pyrex at the wavelength of $\text{Al } K_{\alpha}$. The values of θ_c and of Y calculated from the two sets of points differ by less than one percent.

As a crystal monochromator was used, the results do not suffer from errors due to non-homogeneity of the incident radiation. Although the resolution was not great, the α and β components of a line could easily be separated. The band of wavelengths used for a particular measurement is, therefore, represented by the width of the spectral line + nearer components and satellites (those not more than 100 x. units away from the main line). Some of the flanking continuum is also present, but owing to the high line/continuum ratio in this region, the effect of this is negligible.

CHAPTER 6

RESULTS AND DISCUSSION

6 (i). Pyrex Glass.

The glass specimen was a 2" x 1" optical flat of borosilicate ('Pyrex' brand) glass. It was polished by conventional optical methods to a flatness tolerance of $\frac{1}{10}$ wavelength of visible (green) light. X-ray measurements were made on the specimen at the following wavelengths: P K_{α} (6.16 Å), Sr L_{β} (6.62 Å), W M_{β} (6.76 Å), Sr L_{α} (6.86 Å), Al K_{α} (8.34 Å), Mg K_{α} (9.89 Å), Ga L_{α} (11.31 Å), Zn L_{α} (12.28 Å), Cu L_{α} (13.36 Å), Ni L_{α} (14.60 Å), Co L_{α} (16.00 Å). The results are presented in Figures 6.1 to 6.11, together with the best fitting Fresnel curves, and are tabulated for convenience in table 6.1.

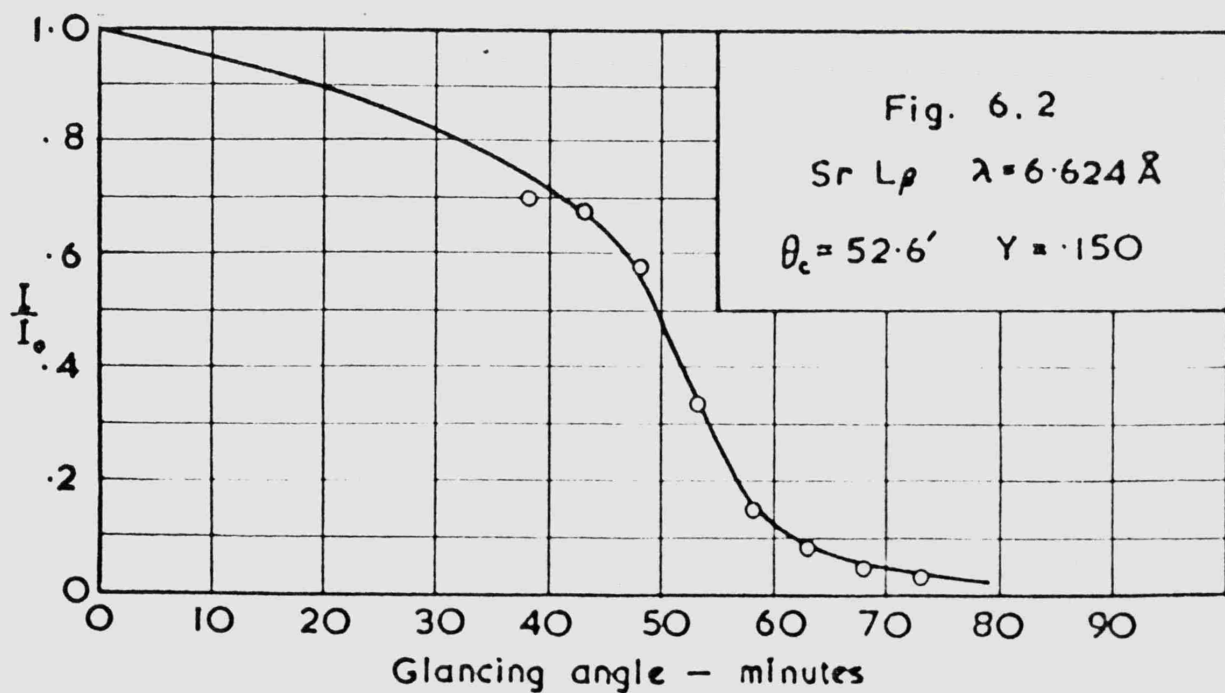
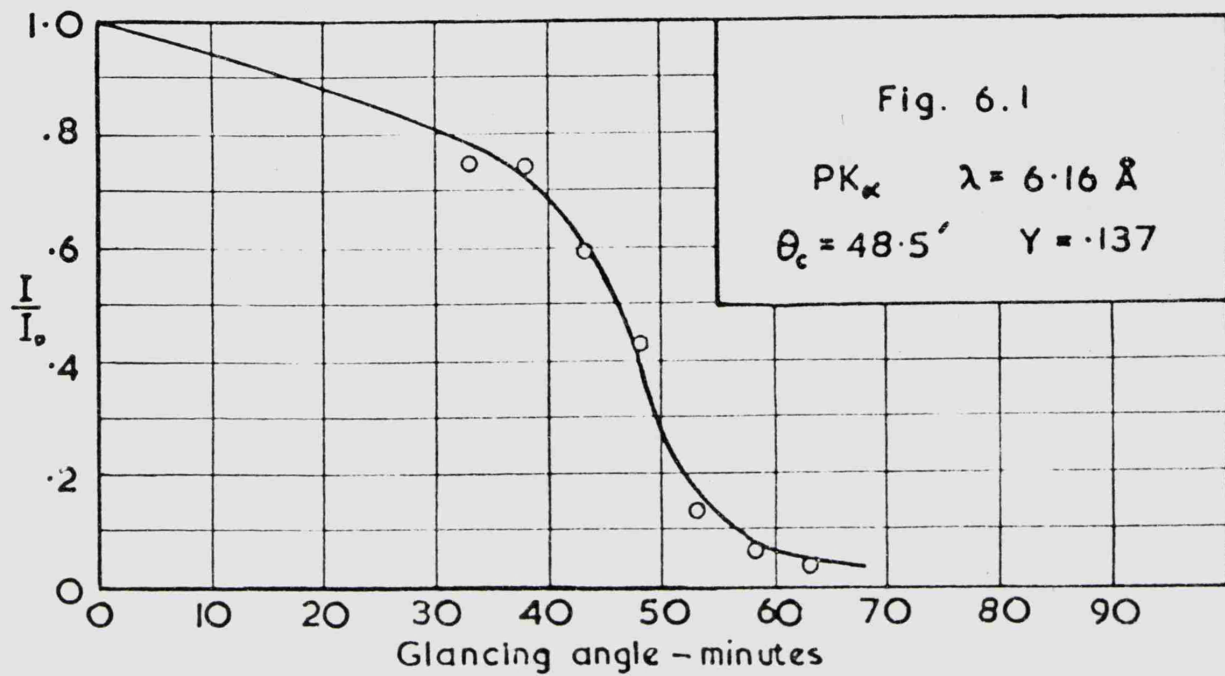
The values of θ_c and S derived from the curve fitting process are plotted as a function of wavelength in Figure 6.14. Shown also in this figure is the dispersion curve predicted from the Kallmann-Mark theory. In computing this curve, the glass was assumed to have the composition 80.7% Si O₂, 12.9% B₂ O₃, 3.8% Na₂ O, 0.4% K₂ O and 2.2% Al₂ O₃.

In Figure 6.13, the variation of $\frac{\mu}{\rho}$ with wavelength is shown, the $\frac{\mu}{\rho}$ values being calculated from the θ_c and Y values using equation (5.1). There exist no experimental values of $\frac{\mu}{\rho}$ for oxygen and silicon in this wavelength region, so that comparison with directly obtained experimental results is not possible. There are, however, 'semi-empirical'

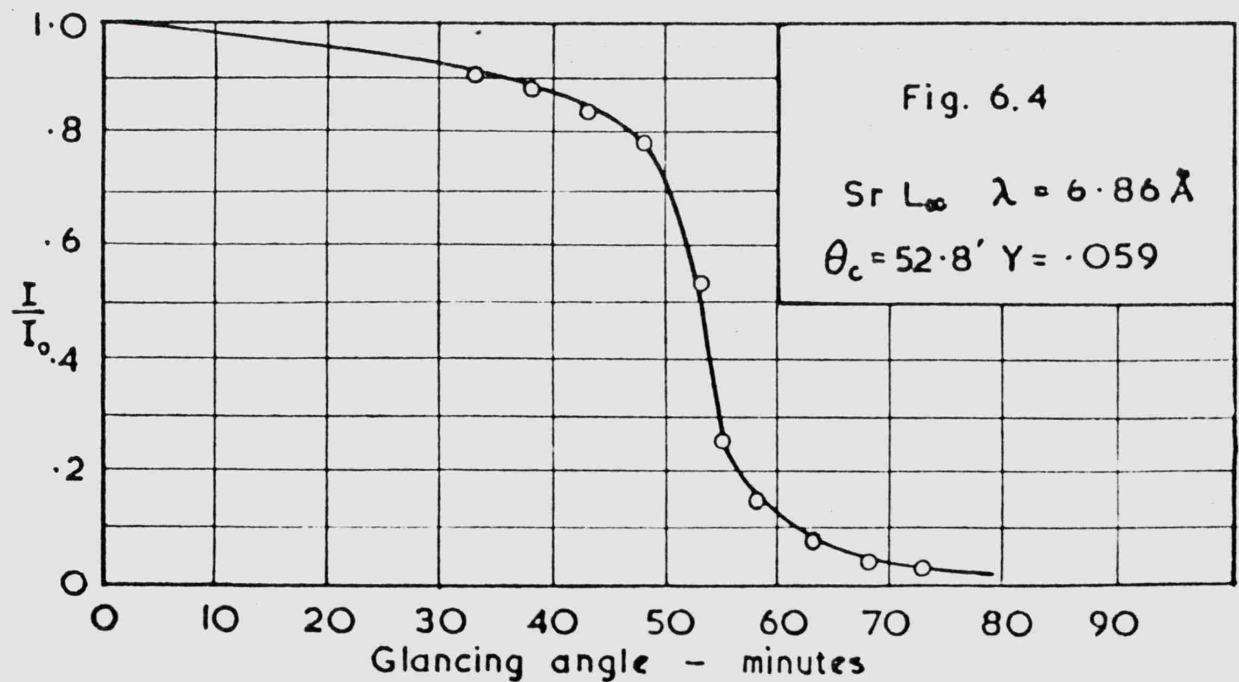
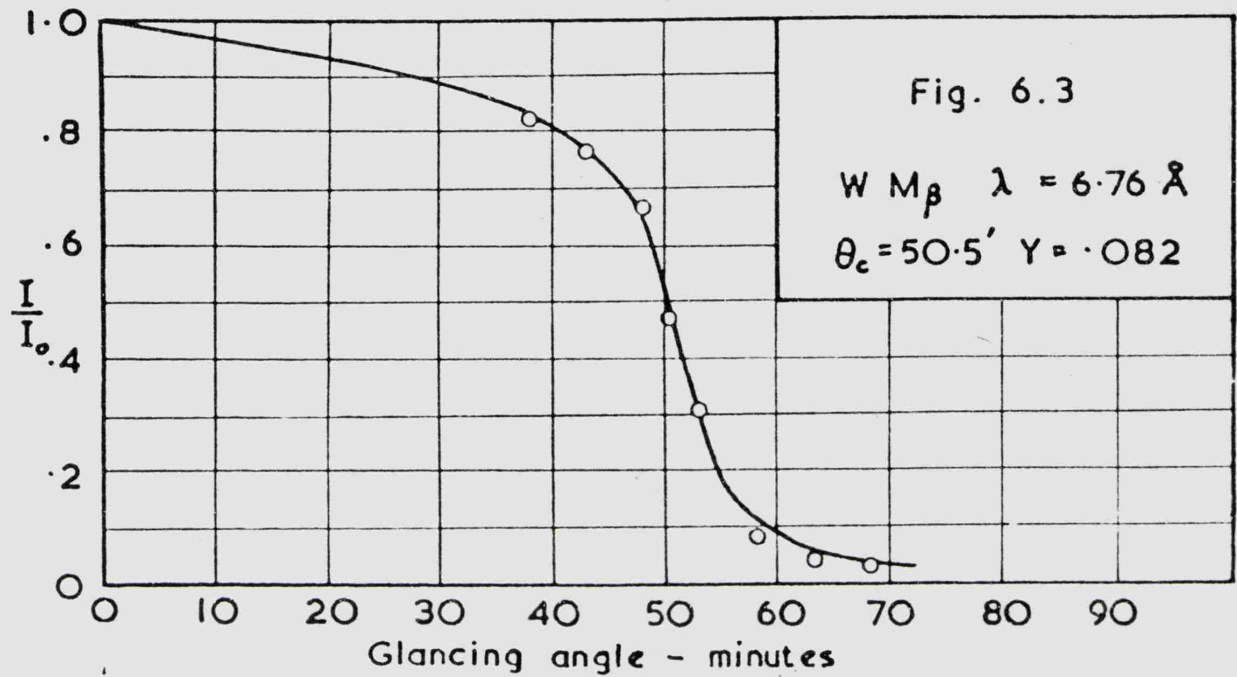
TABLE 6.1

Reflections of various radiations by 'Pyrex' glass.

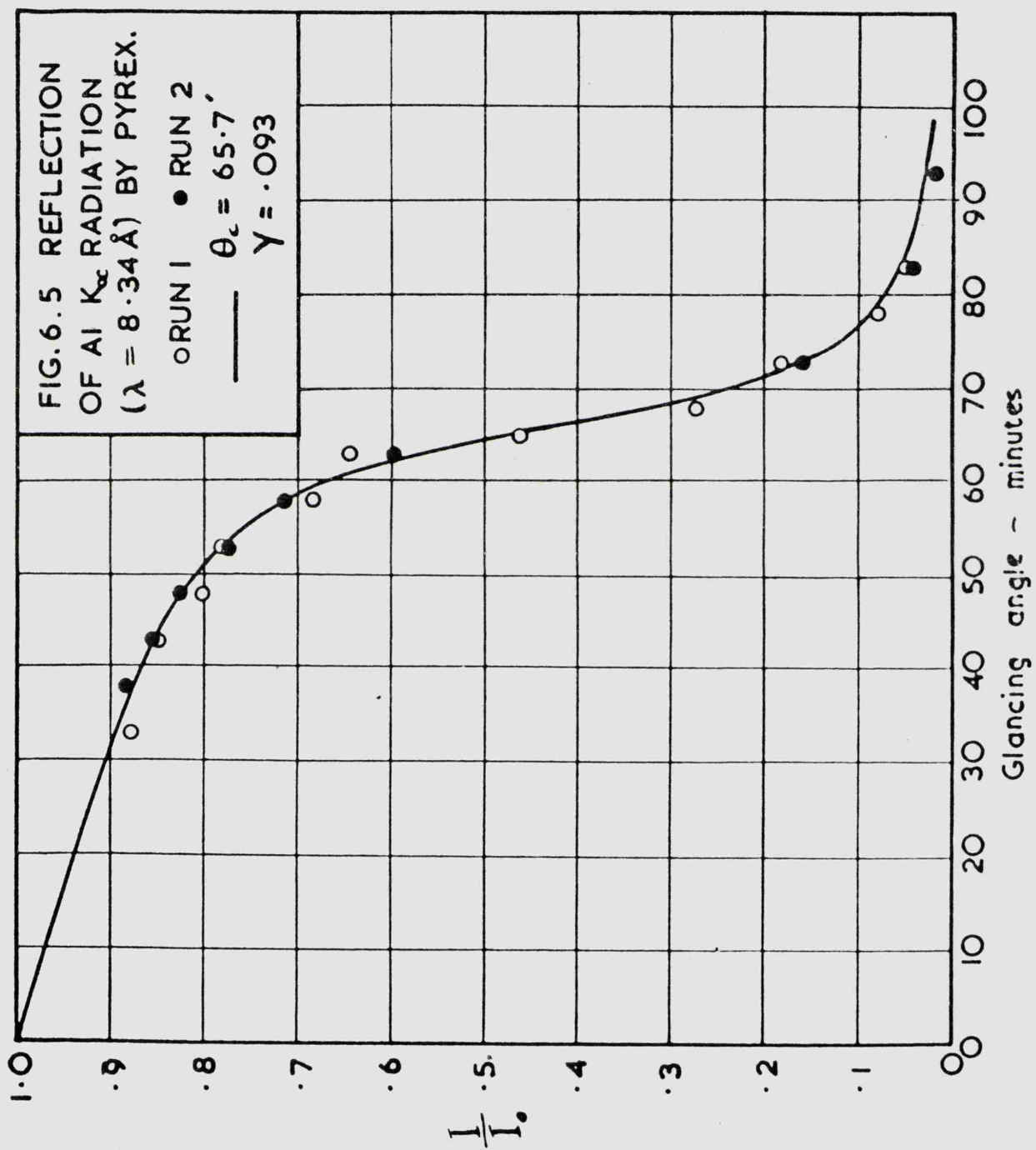
[illegible]

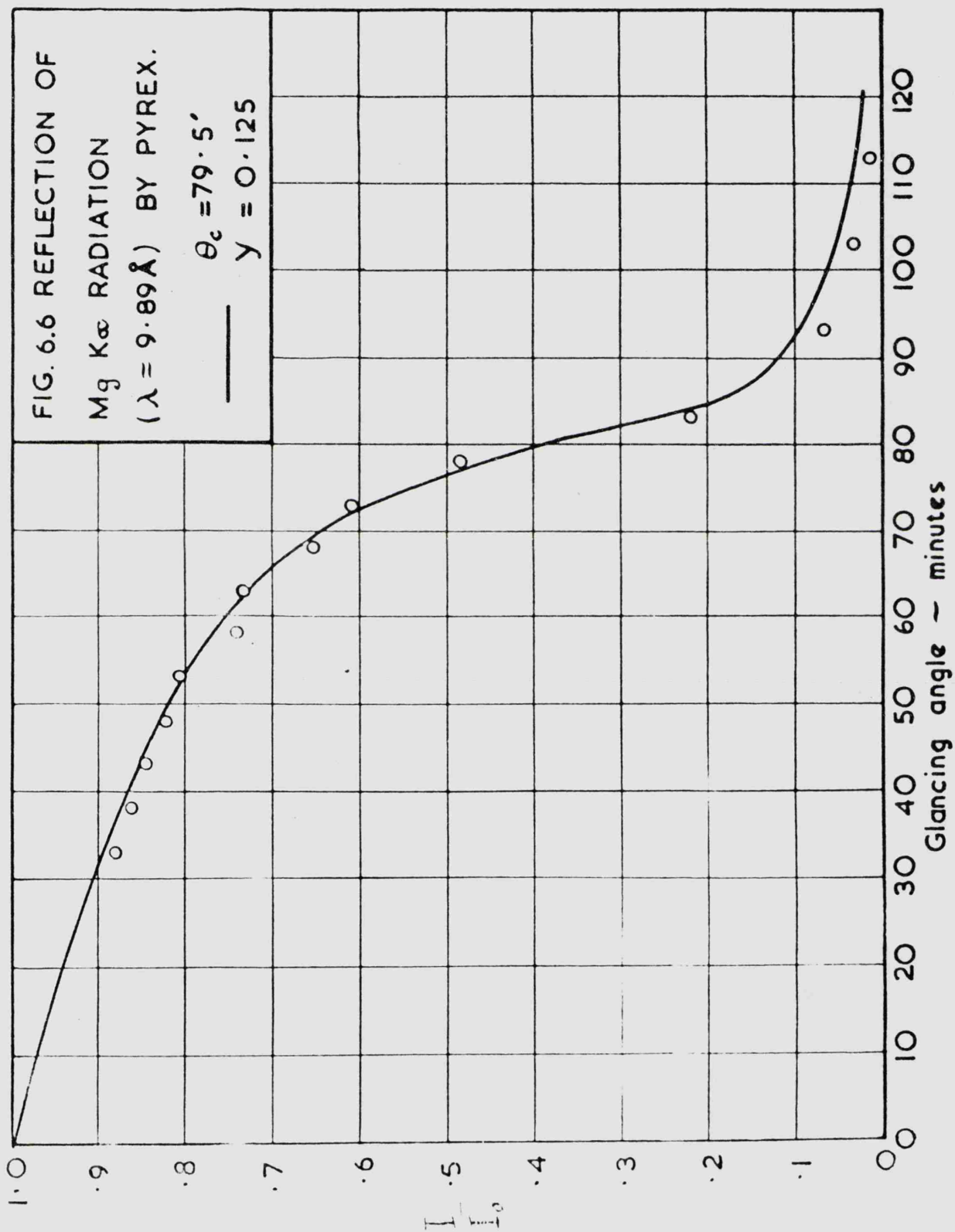


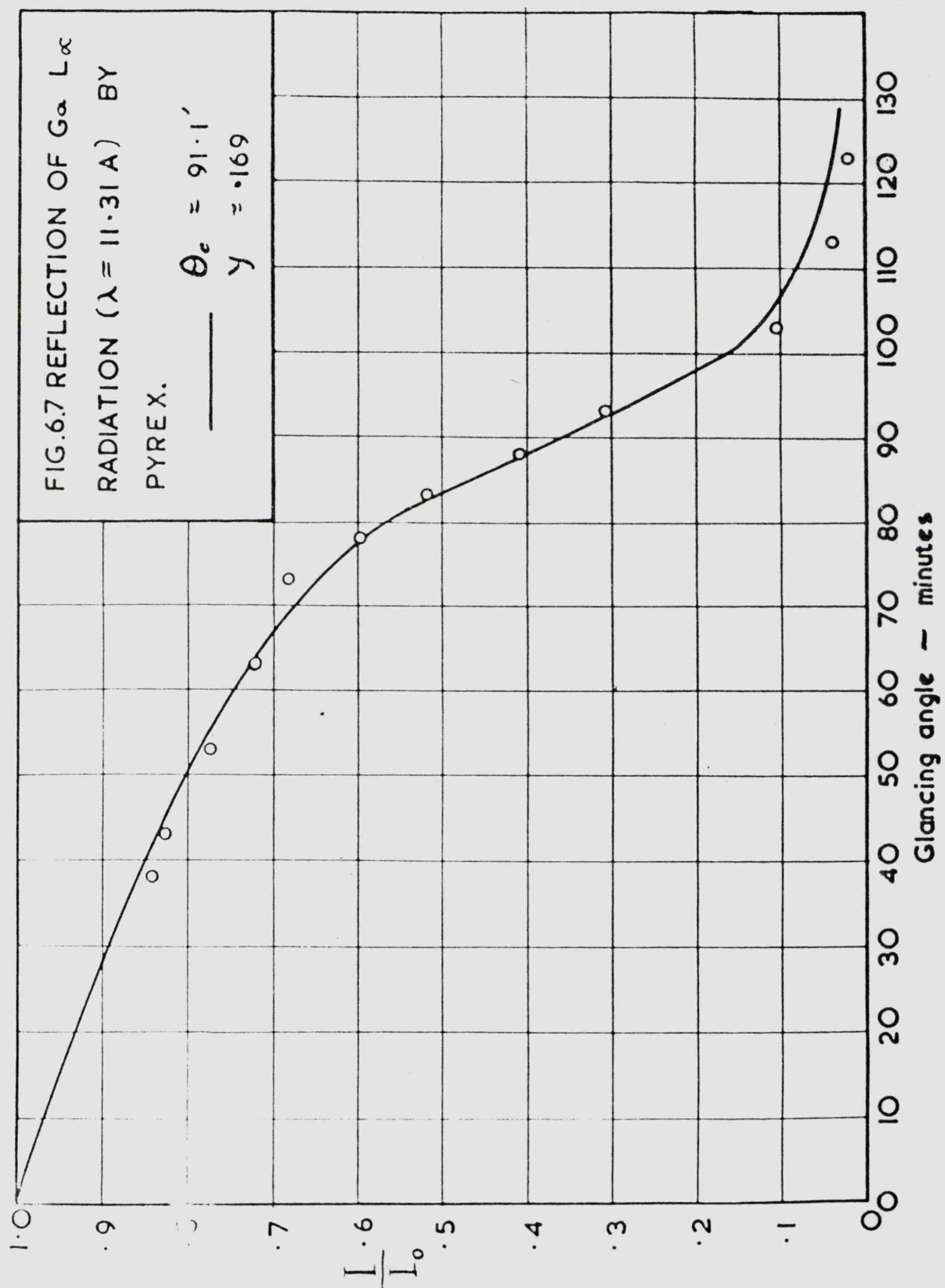
REFLECTION CURVES FOR PYREX

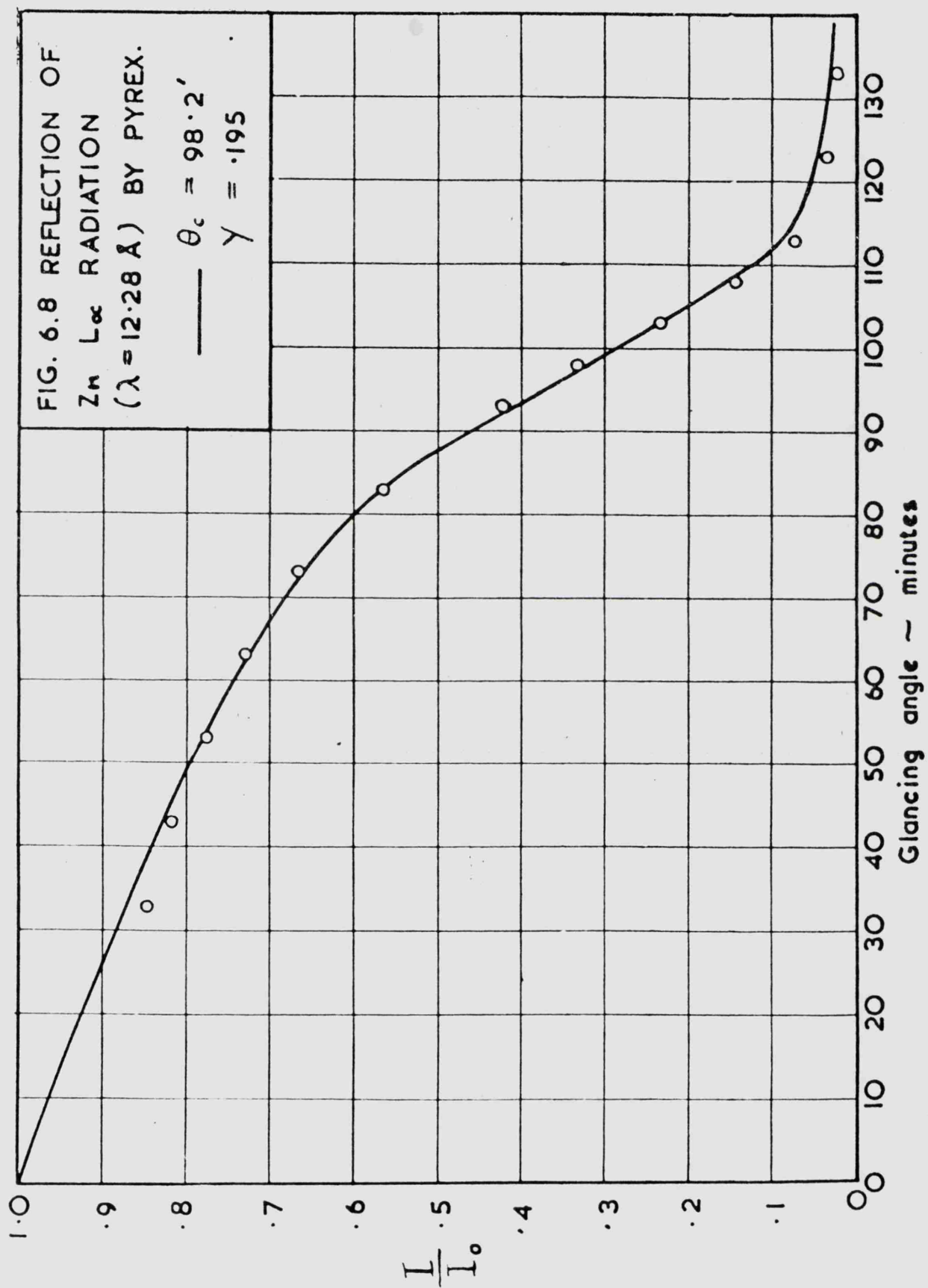


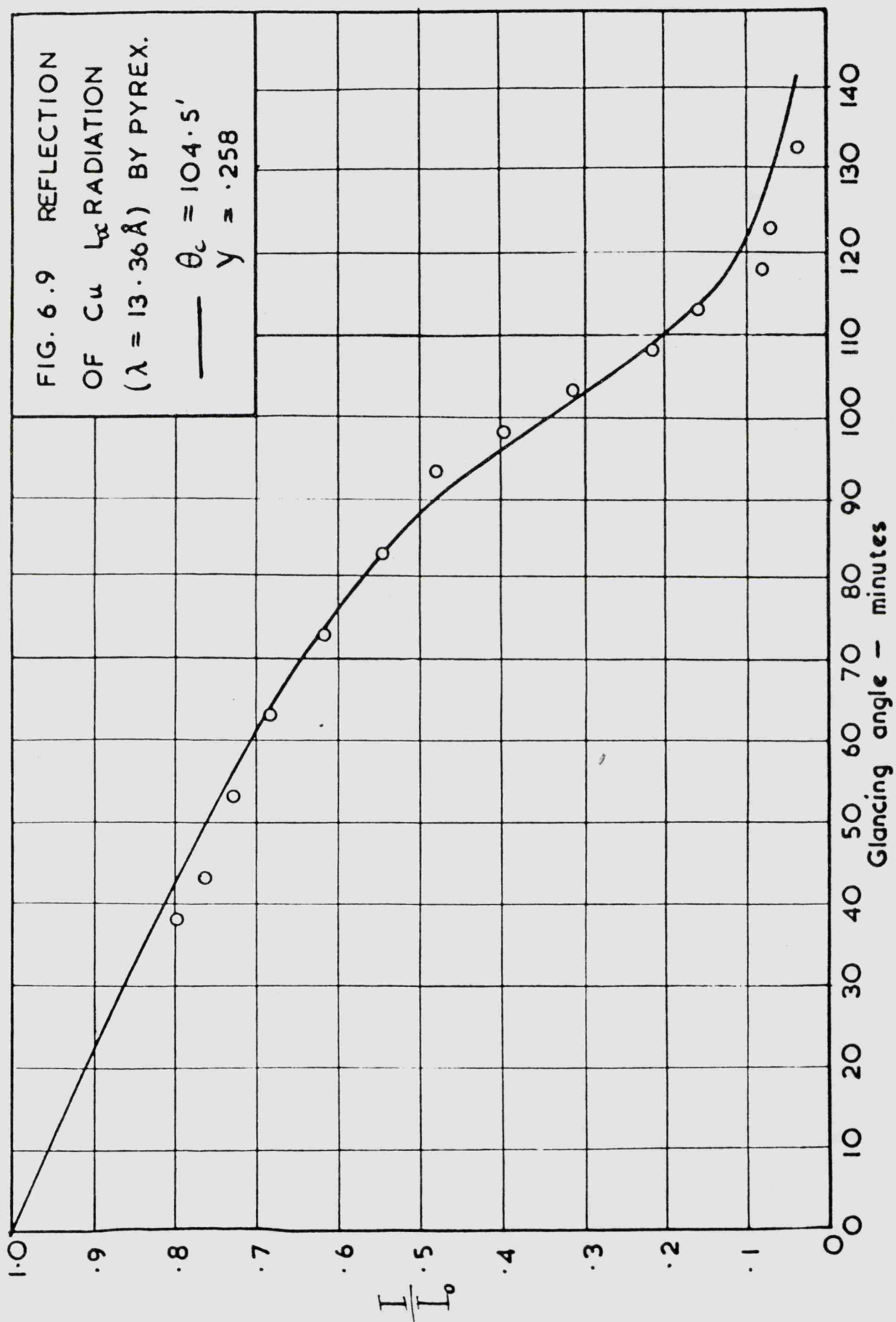
REFLECTION CURVES FOR PYREX

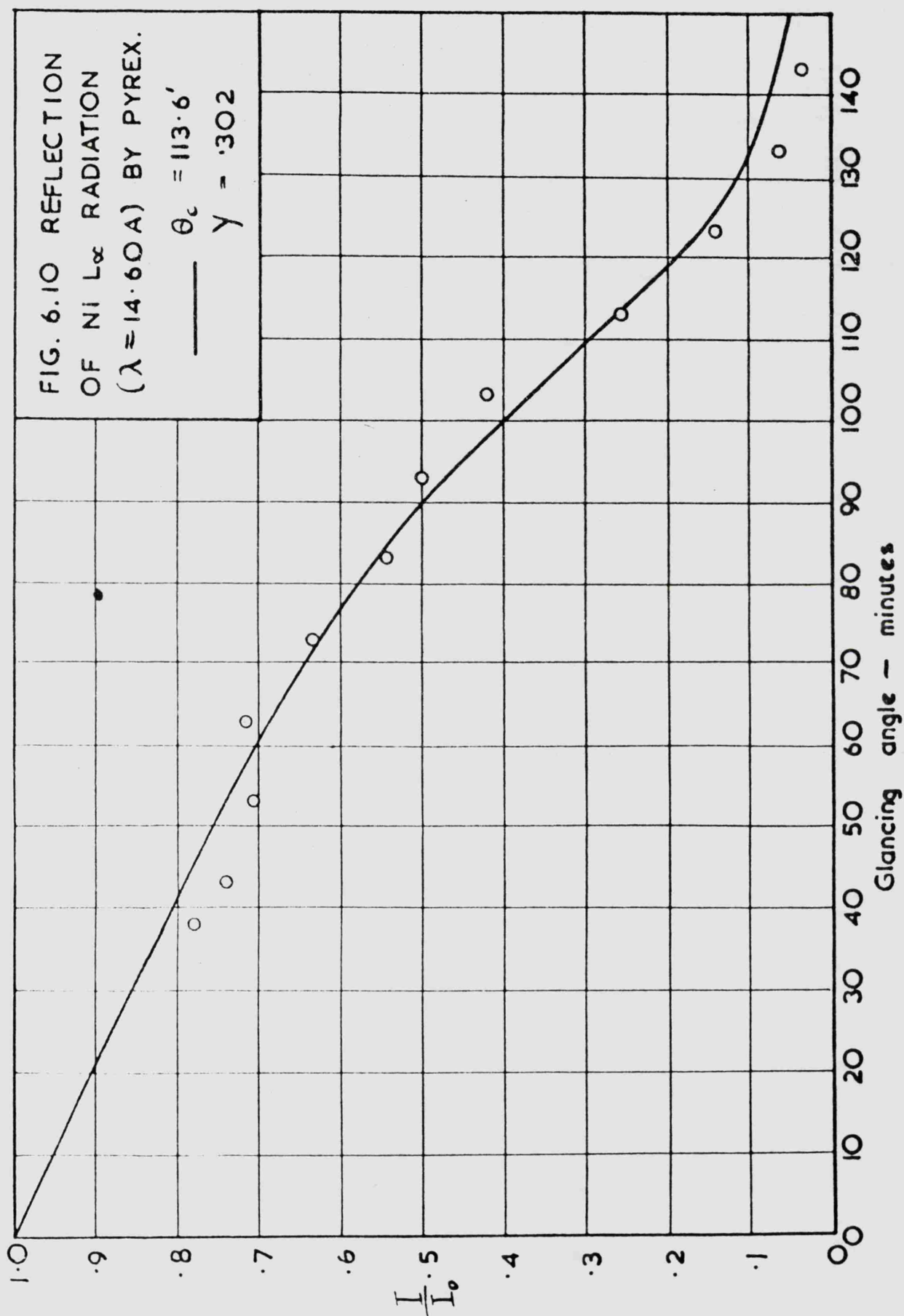


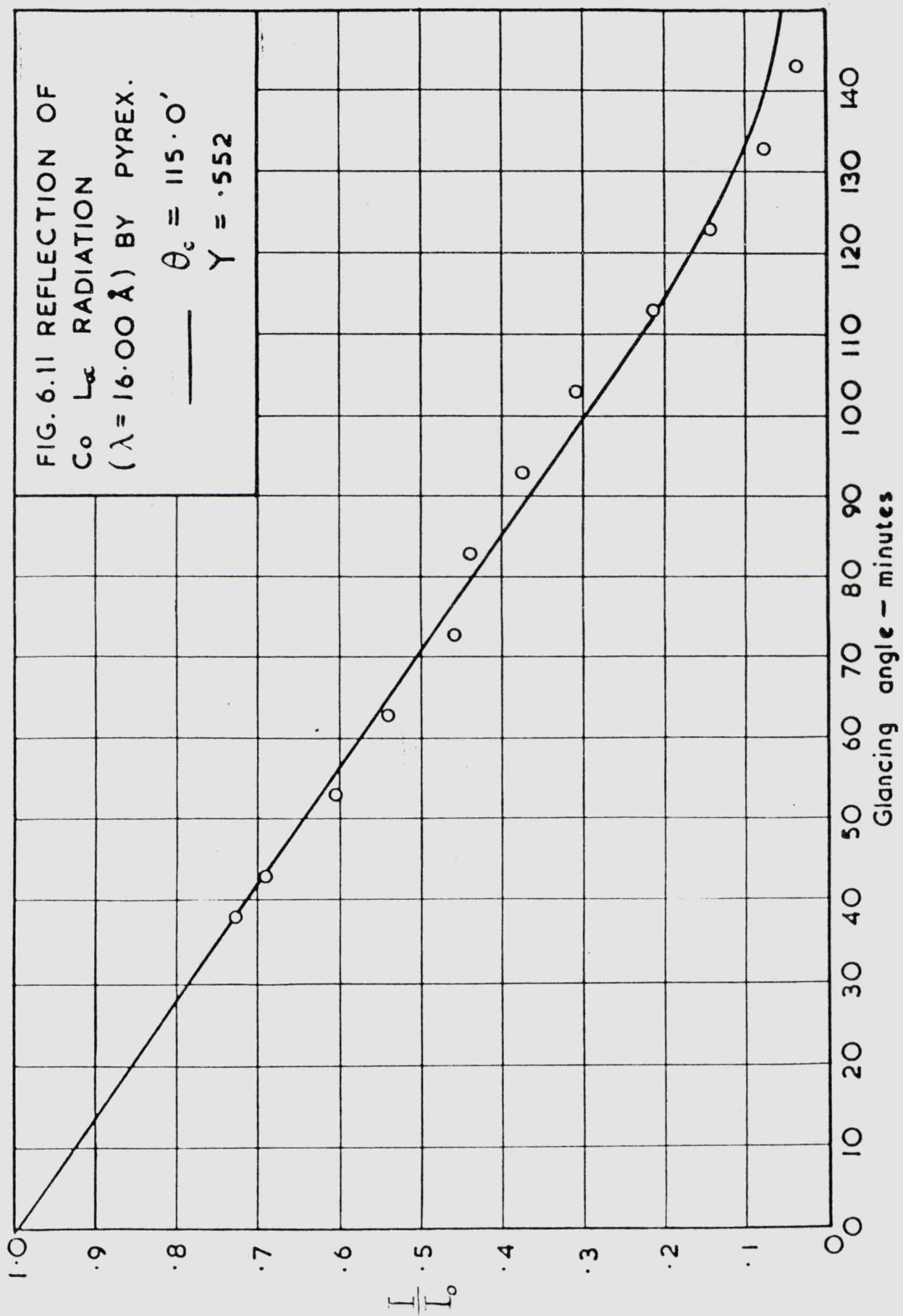












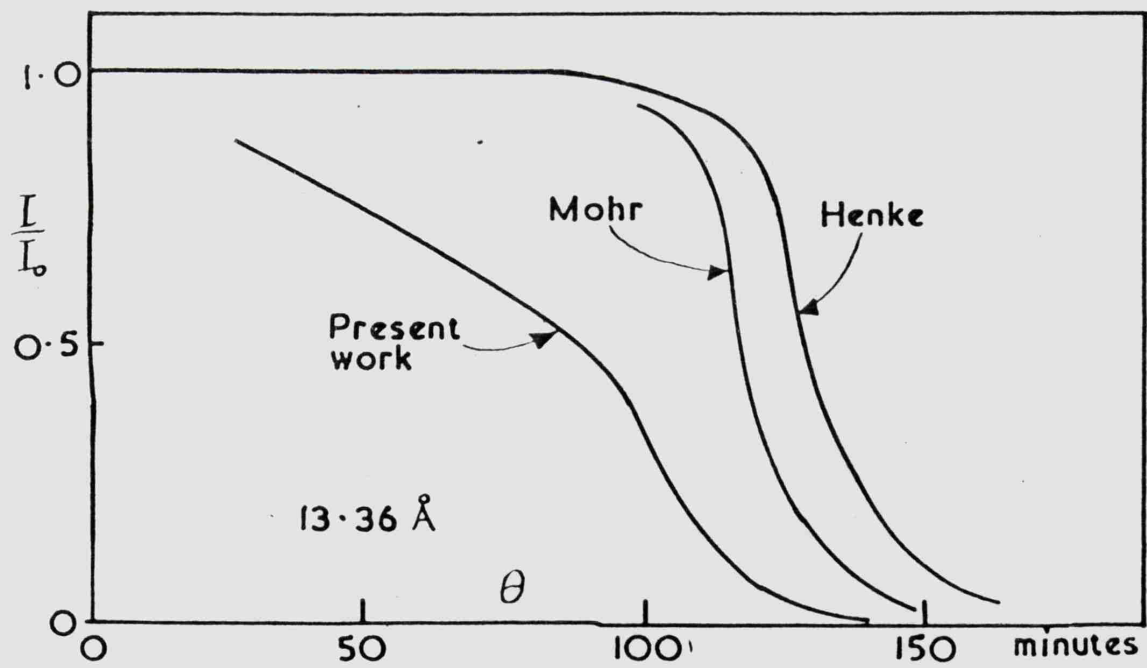
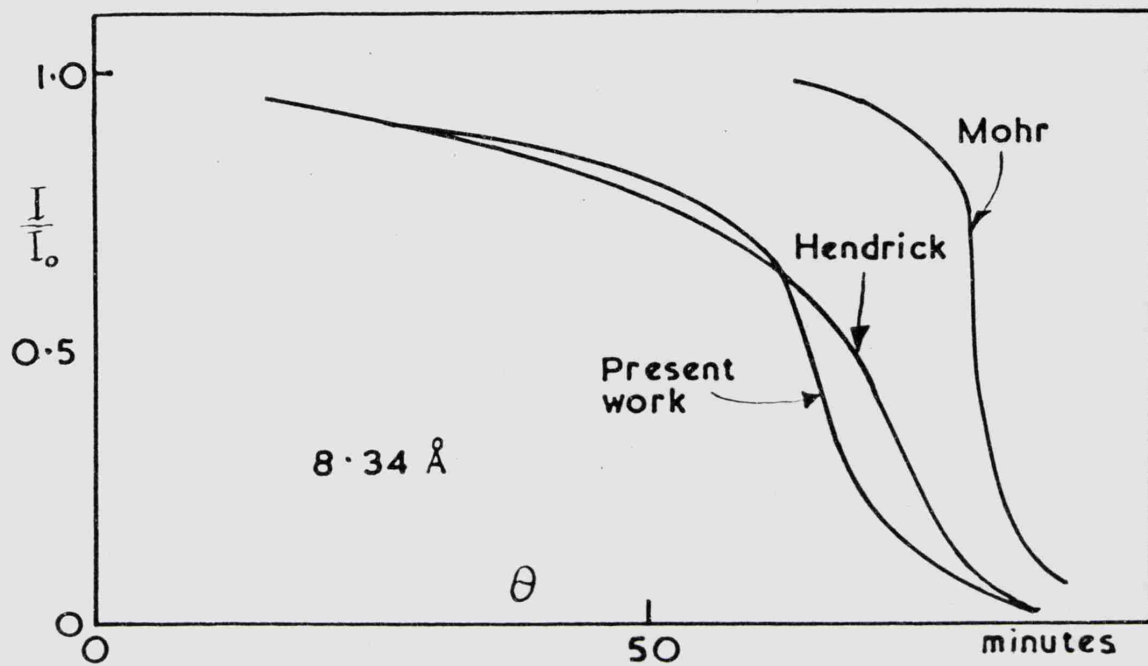
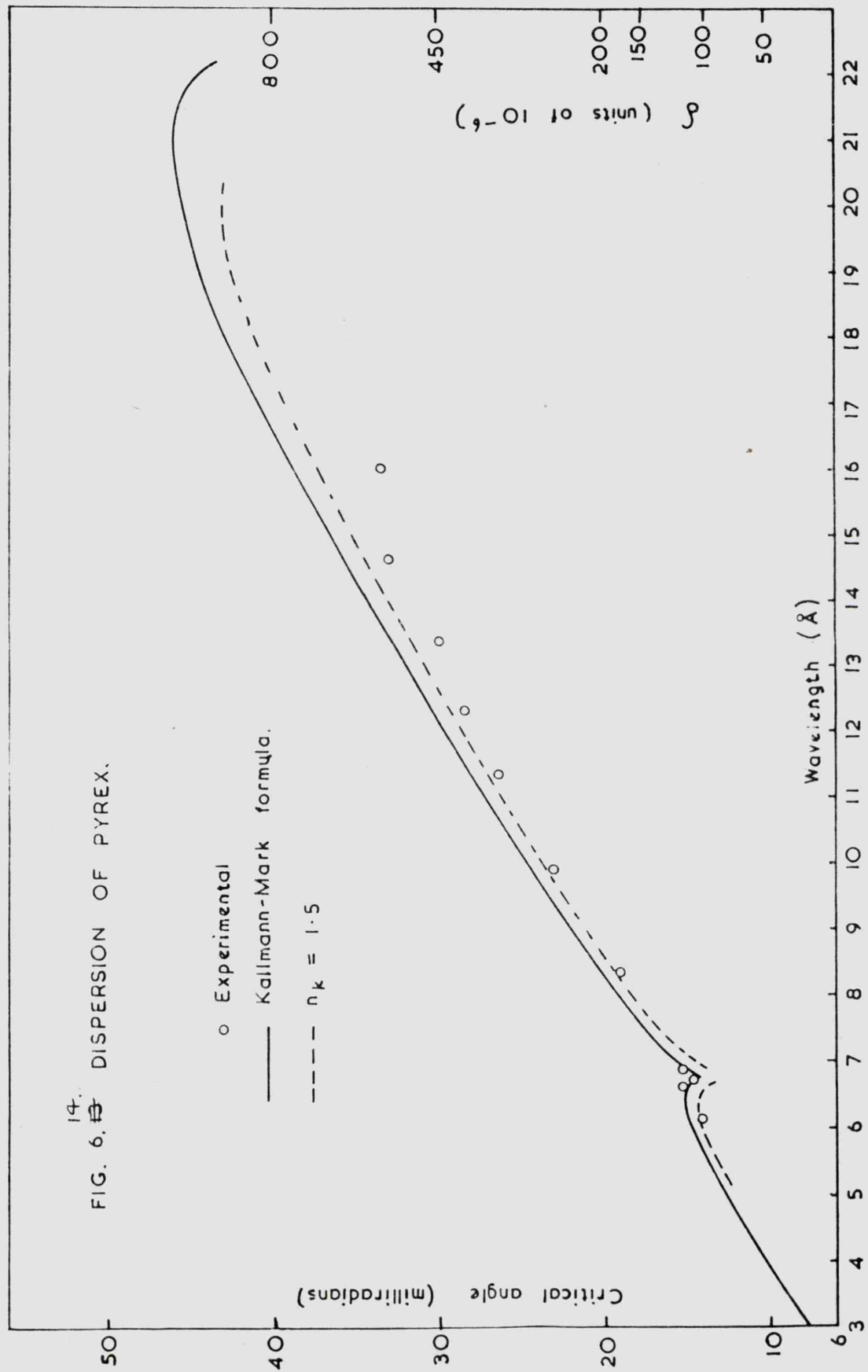
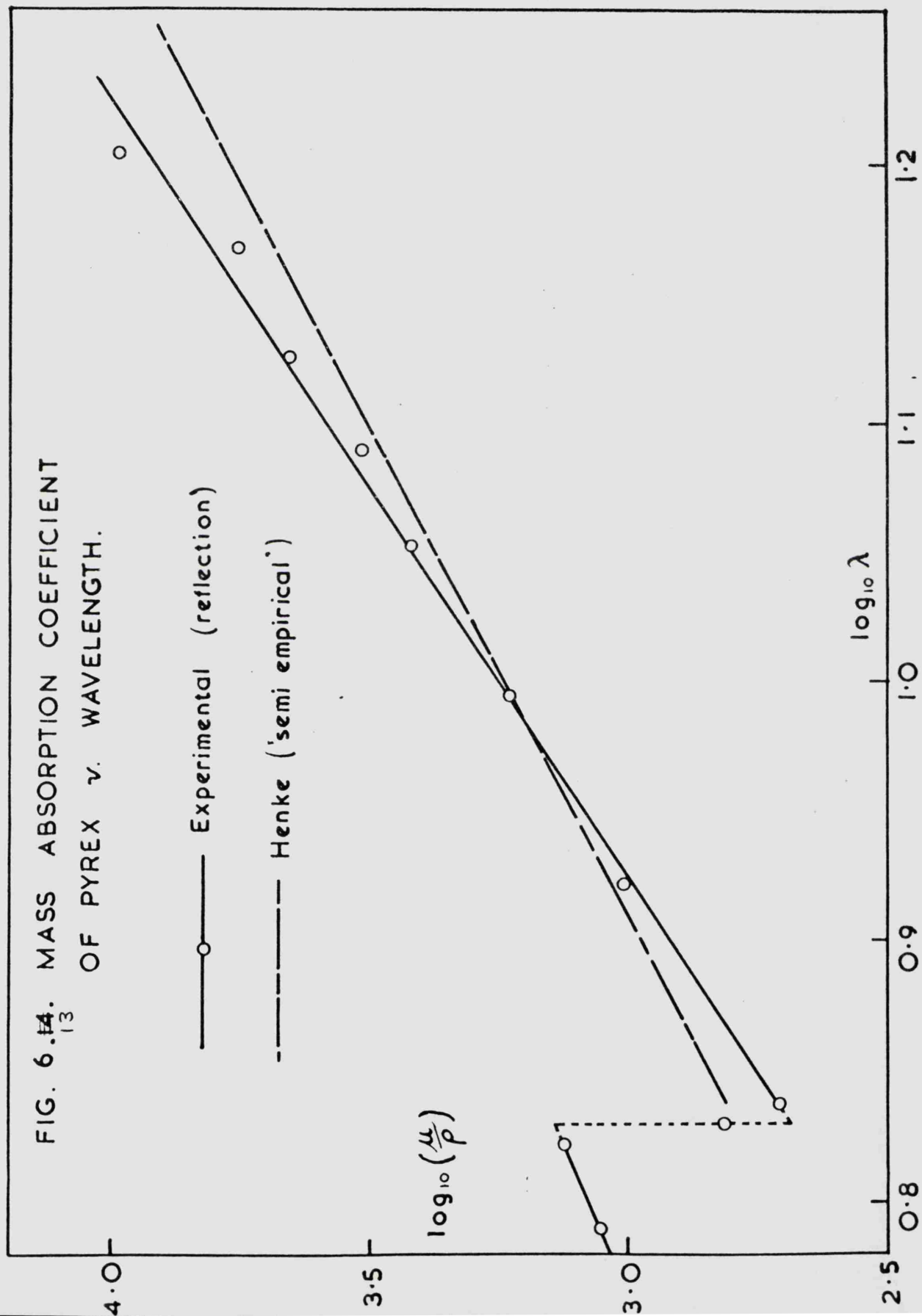


FIG. 6.12 COMPARISON WITH OTHER RESULTS.

14.
FIG. 6. $\frac{1}{2}$ DISPERSION OF PYREX.





values of $\frac{\mu}{\rho}$ calculated by B.L. Henke and co-workers (48), with which such a comparison may be made. These values are derived from existing experimental values of S.J.M. Allen (49) by a process of extrapolation and curve fitting. A mass absorption curve for Pyrex, calculated using Henke's tables of $\frac{\mu}{\rho}$ and the Pyrex composition already given, is plotted in Figure 6.13.

6 (ii). Discussion of results for glass.

The results given in the table and in the graphs were taken in a wavelength region which has remained largely uninvestigated. Comparison with other experimenters' results is possible, however, at 8.34 \AA (Hendrick, loc. cit., Mohr, loc. cit) and at 13.36 \AA (Mohr, Henke (50)). The comparisons are made in Figure 6.12. The curves drawn in these graphs are the lines through the experimental points, not the 'best Fresnel curves' as drawn in Figures 6.1 to 6.11.

It can be seen that Hendrick's curve at 8.34 \AA agrees reasonably well with the author's. Better agreement than this is not to be expected, as the composition of the glass used by Hendrick is not given, and it probably differs from that used in the present investigation. In addition, Hendrick used fitters to isolate the Al K line, a procedure which is bound to lead to some error due to non-homogeneity of the radiation. The curves of Mohr at 8.3 \AA , and of Henke and Mohr at 13.3 \AA , all given for Pyrex glass, are, however, considerably different from the present author's, in that they predict both a larger critical angle, and a larger

value for the reflection coefficient at all angles. Both these workers used a photographic method for their intensity measurements, and it seems that this has led to error. In the soft X-ray region the radiation is unable to penetrate far into a photographic emulsion, and so all the blackening is produced in a thin surface layer, which therefore becomes saturated very quickly. It is known that the density versus exposure curve is non-linear in this wavelength region (Hirsch, 51), but accurate data is lacking, especially in the region above 10 \AA . An early saturation of the film would lead to just the effects found by Henke and by Mohr - high values of I/I_0 and θ_c . Further confirmation of this hypothesis is given by the flat top on Henke's curve for $\text{Cu } L_\alpha$ radiation. This kind of reflection curve is, from the theory of reflection outlined in Chapter 1, clearly impossible, as some absorption must always take place. The curve indicates that the film has been saturated by both the direct and the reflected beam, up to a certain glancing angle, giving the appearance of equal intensities.

All the experimental results fit very well to curves of the modified Fresnel type (equation 1.9), and no drastic modification of the theory is required to account for high values of I/I_0 at angles greater than critical, as was suggested by Laby, Bingham and Shearer. On the contrary, the values of I/I_0 at such angles usually seem to lie below those predicted by the reflection equation. This effect is noticeable in the results of a number of other workers. It is extensively discussed

by Parratt (loc. cit.) who found it in experiments on the reflection of fairly hard X-rays from polished glass, and evaporated copper surfaces in different degrees of oxidation. He discounted instrumental effects and surface roughness as a cause of the effect, but looked for it in a variation in electron density in the surface layers. He proposed three types of variation to account for the phenomenon:

- 1) A general reduction of electron density throughout the whole surface region in which X-ray reflection takes place.
- 2) A layer of limited depth and varying density.
- 3) A 'reflection trap'.

Parratt showed that the observed discrepancies could not be completely explained on the basis of the first two assumptions. The 'reflection trap' mechanism was more promising. In this case, the composition and structure of the surface is supposed to lead to an electron density minimum a depth of a few tens of angstroms below the surface. The depth of penetration of X-rays into the medium varies with the glancing angle. At low glancing angles, this depth is small, being of the order of 50 angstroms for low absorption. As the glancing angle increases to θ_c and beyond, however, the depth of penetration increases until at near normal incidence it is given by the ordinary exponential absorption law. Thus, at small angles of incidence, the radiation does not penetrate far enough into the medium to be affected by the electron density minimum. At angles past critical, however, the radiation can

penetrate to a point past the minimum and, in trying to 'break out' from underneath, some of it is reflected back into the bulk of the mirror, where it is absorbed.

Parratt explained the electron density minimum, in the case of copper, by a process of oxidation of the surface crystallites which leads to an oxygen-impervious 'seal' at a certain depth below the surface. In the case of glass, an oxidation process cannot account for the reflection trap. Parratt suggested that it may be caused by close packing of crystallites whose size increases gradually with depth. On the extreme surface of optically polished glass the crystallites may be as small as the individual molecules, so that there would be virtually no intercrystalline space. Deeper down, where the crystallites are supposed larger, one would expect relatively large gaps between them. Another mechanism proposed by Parratt was the limited-depth absorption of oils or other materials from the laboratory air. "For copper, oxidation is probably the principal effect; for glass, we cannot distinguish without better controlled conditions between the two effects".

Another result of the 'reflection trap', or any other variation of electron density near the surface of the medium, would be that the value of \int obtained experimentally would differ from that calculated for the bulk material. As the penetration decreases with increasing wavelength, one would expect the reflection trap to become less and less effective as λ increased, and the experimental values of \int to approach

the theoretical ones. Parratt found this to be the case in two measurements on oxidised copper at 1.39 and 1.54 Å.

The values of δ obtained from the present experiments are compared with those predicted from the Kallmann-Mark theory in Figure 6.14. It can be seen that the curves are in fairly good agreement at the short wavelength end of the scale, but the experimental values fall below the theoretical ones at higher wavelengths to an extent which cannot be due to experimental error. This shift is not in agreement with the hypothesis of a reflection trap, but would appear to indicate a monotonic decrease in electron density from the interior of the material to the extreme surface. Experiments on stainless steel (Section 6 (iv)) led to a similar conclusion.

Figure 6.14 shows a slight dip in the curve of $\theta_c(\delta)$ versus λ at the Si K edge, which gives support to the Kallmann-Mark theory of dispersion. However, in view of the discussion given above, it cannot be claimed that the method of total reflection provides an accurate measurement of the refractive index, and a sensitive test of the dispersion theories. Matters would be somewhat improved if the relation between the shape of the reflection curves and the surface structure were better understood, and further work is obviously needed in this direction.

Reduction of the effective number of electrons in the K shells of silicon and oxygen improves slightly the agreement between theory and experiment. In plotting the dashed line in Figure 6.14 this number has

been taken as 1.5. There is still a large discrepancy at the longer wavelengths, however. In the present experiments, surface roughness cannot be discounted as a cause for the distortion of the Fresnel curves and the discrepancy between the experimental and theoretical values of

§ . A test of surface roughness was made by registering the direct and reflected beams ($\text{Al K}\alpha$ radiation) on a photographic plate and comparing them. For short exposures, both the blackened strips were sharp, but with longer exposures, the image of the reflected beam was bordered by a faint diffuseness. Under these conditions, the central part of the image was overexposed, so that no quantitative measurements could be made. The tests showed, however, that small regions of the surface were oriented at an angle to the 'mean surface' and were reflecting some of the radiation out of the direct beam. A possible model of such a surface would be one in which the elements of surface were distributed in angle about the mean surface and also had a size distribution, so that the small-scale appearance of the surface would be something like badly laid crazy paving. Such a model would be difficult to treat theoretically, but would obviously lead to conclusions different from those obtained from a model of perfect smoothness.

Any distortion of the curves by a mechanism such as we have been discussing would also lead to a discrepancy between the experimental and theoretical values of the mass absorption coefficient, so that

values of $\frac{\mu}{\rho}$ obtained in this way cannot be considered reliable. It was considered worth while, however, to make the comparison with Henke, White and Lundberg's semi-empirical values. This is done in Figure 6.13. The experimental values of $\frac{\mu}{\rho}$ lie on a straight line with slope 3.28 above the silicon K edge. (The region around this edge is shown dotted, as its shape cannot be found accurately from these rather coarse experiments). Above the edge, the values agree moderately well with the semi-empirical ones, although the latter are also somewhat doubtful, as Cooke et. al. (loc. cit.) showed that some of the original experimental values from which these are derived differ considerably from the latest experimental results. It is difficult, therefore, to draw any meaningful conclusions from Figure 6.13. The experiments have, however, yielded approximate values for the mass absorption coefficient of Pyrex in a region in which few values of $\frac{\mu}{\rho}$ are available, and further knowledge of the relation between the surface structure and the reflection curves may enable the method to be improved so as to be useful in cases where the ordinary methods for the measurement of X-ray absorption cannot be employed, e.g. for the absorption of very soft X-rays by the heavier elements.

6 (iii). Stainless steel.

The stainless specimen was a 2" x 1" flat polished to $\frac{1}{10}$ wavelength of green light. This flat was supplied by Taylor, Taylor and Hobson Ltd. of Leicester. Measurements were made on the flat at the wavelengths of Nb L_{α} (5.73 Å), Si K_{α} (7.15 Å), Al K_{α} , Mg K_{α} ,

Zn $L\alpha$, Cu $L\alpha$, Ni $L\alpha$ and Co $L\alpha$.

The results are tabulated in table 6.2 and are plotted, together with the best fitting Fresnel curves, in Figures 6.15 to 6.22. The mass absorption coefficient is plotted in 6.23 and the dispersion in 6.24.

6 (iv). Discussion of results for stainless steel.

Again, it may be said that the reflection curves fit the experimental data reasonably well, but the discrepancy at values of θ greater than θ_c is more pronounced in these curves than in those for glass. This is not surprising, whichever mechanism we choose to explain the effect. The surface of the steel would be expected to have a complex structure, perhaps consisting of a number of layers of different oxides, and also one would expect the surface to be less smooth than on a microscopic scale, as the metal is softer and less easy to polish. The photographic tests of surface smoothness, performed as described in Section 6 (ii) gave much the same result as for glass, but again no quantitative comparison was possible, owing to film saturation. It would appear that optically polished stainless steel is not much worse than optically polished glass for producing X-ray images. Indeed, there would be some advantage in using steel, as it can be used at a larger glancing angle, giving a gain in effective area.

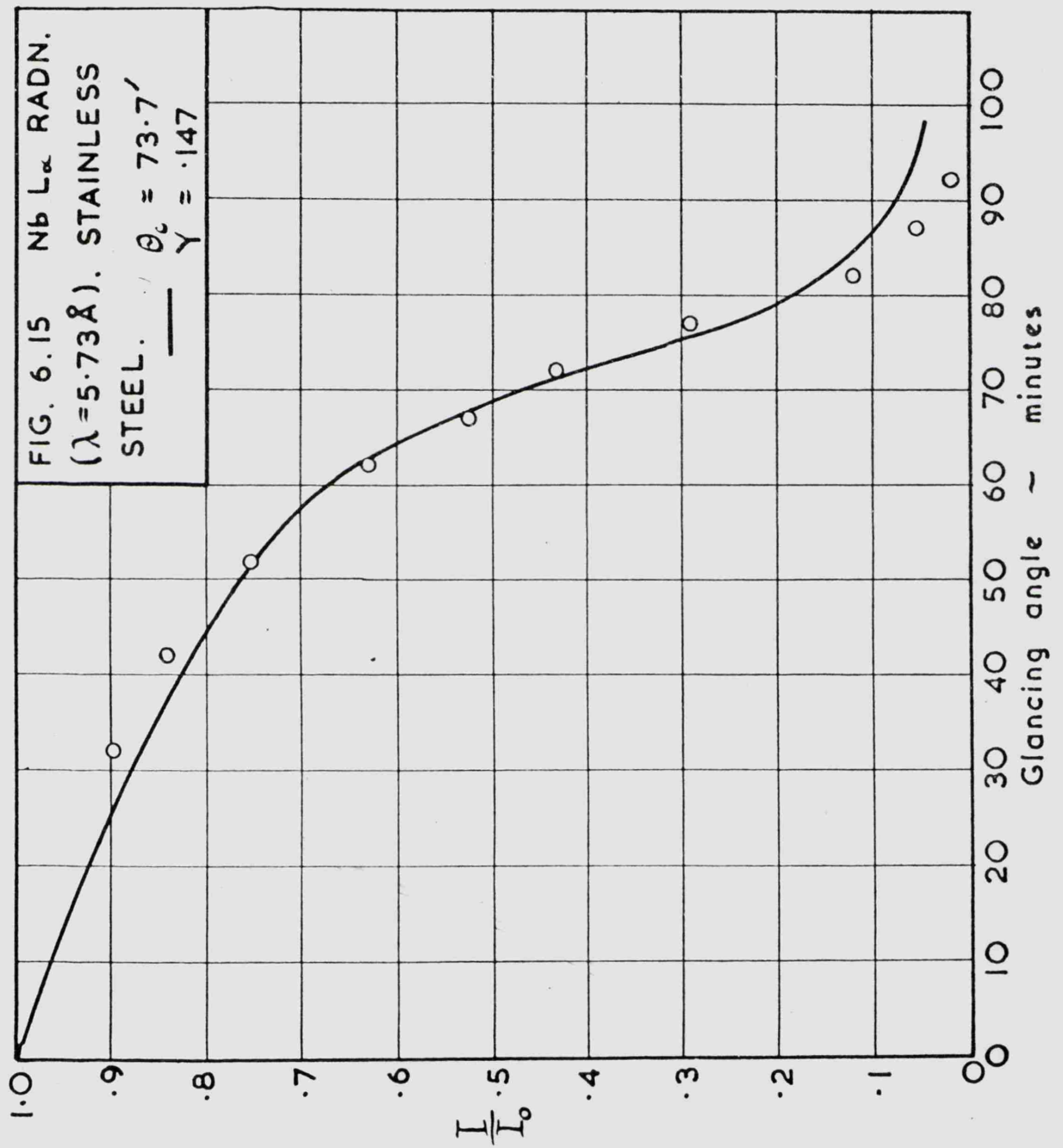
The experimental values of θ_c and S are compared with theory in Figure 6.24. The theoretical values were obtained from the Kallmann-Mark theory assuming the material was 100% iron. The abundance of

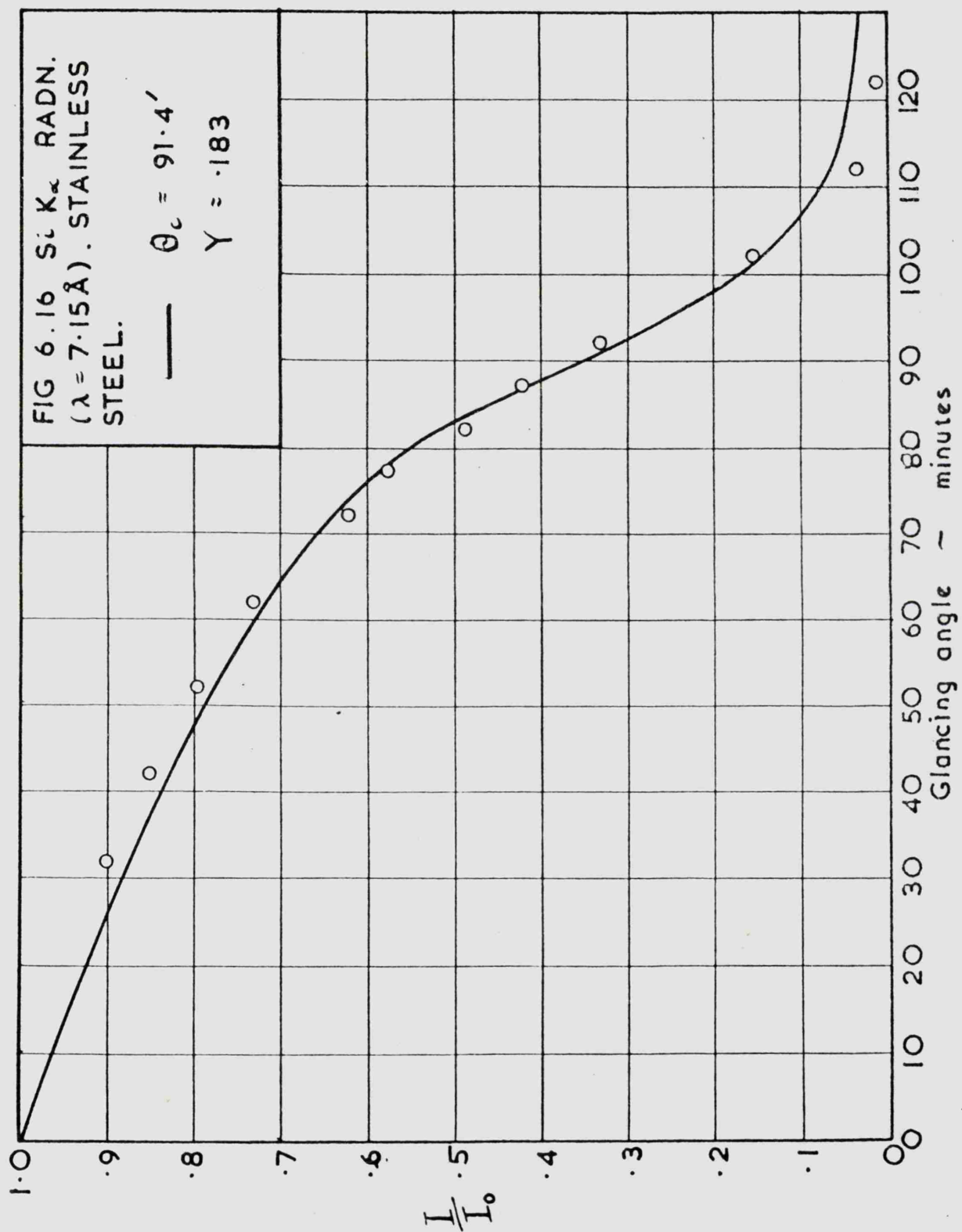
90.

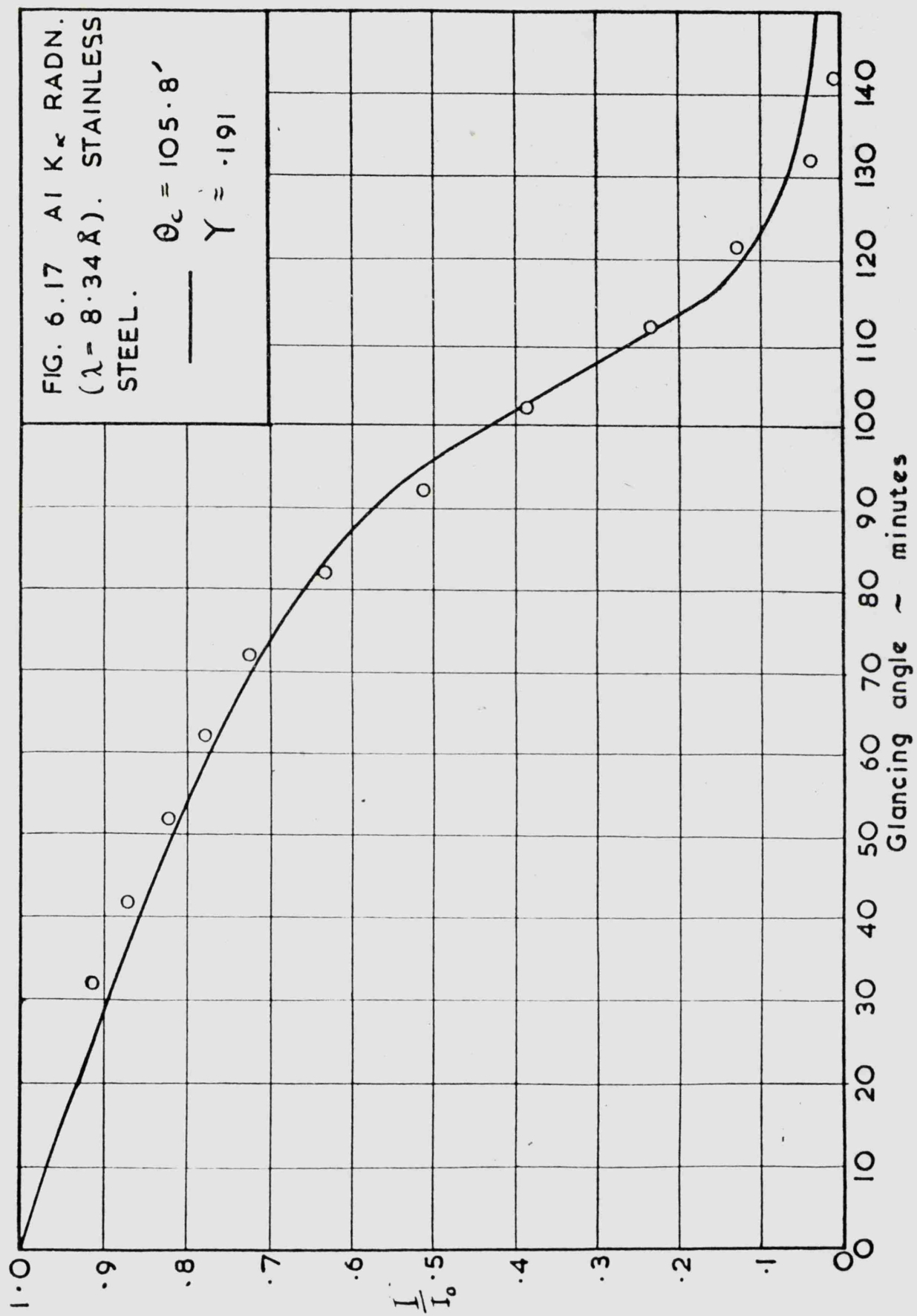
TABLE 6.2

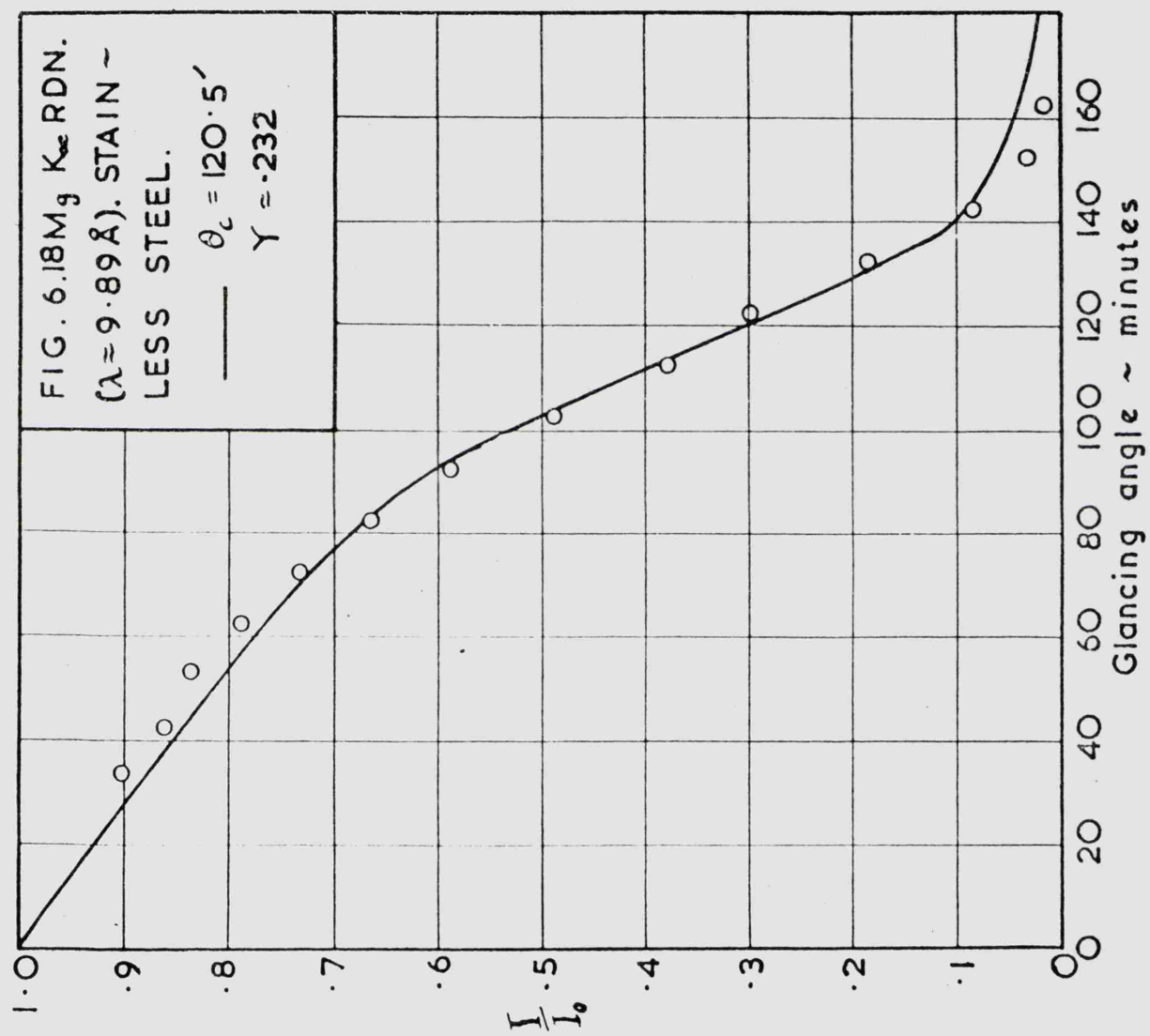
Reflection of various radiations by stainless steel.

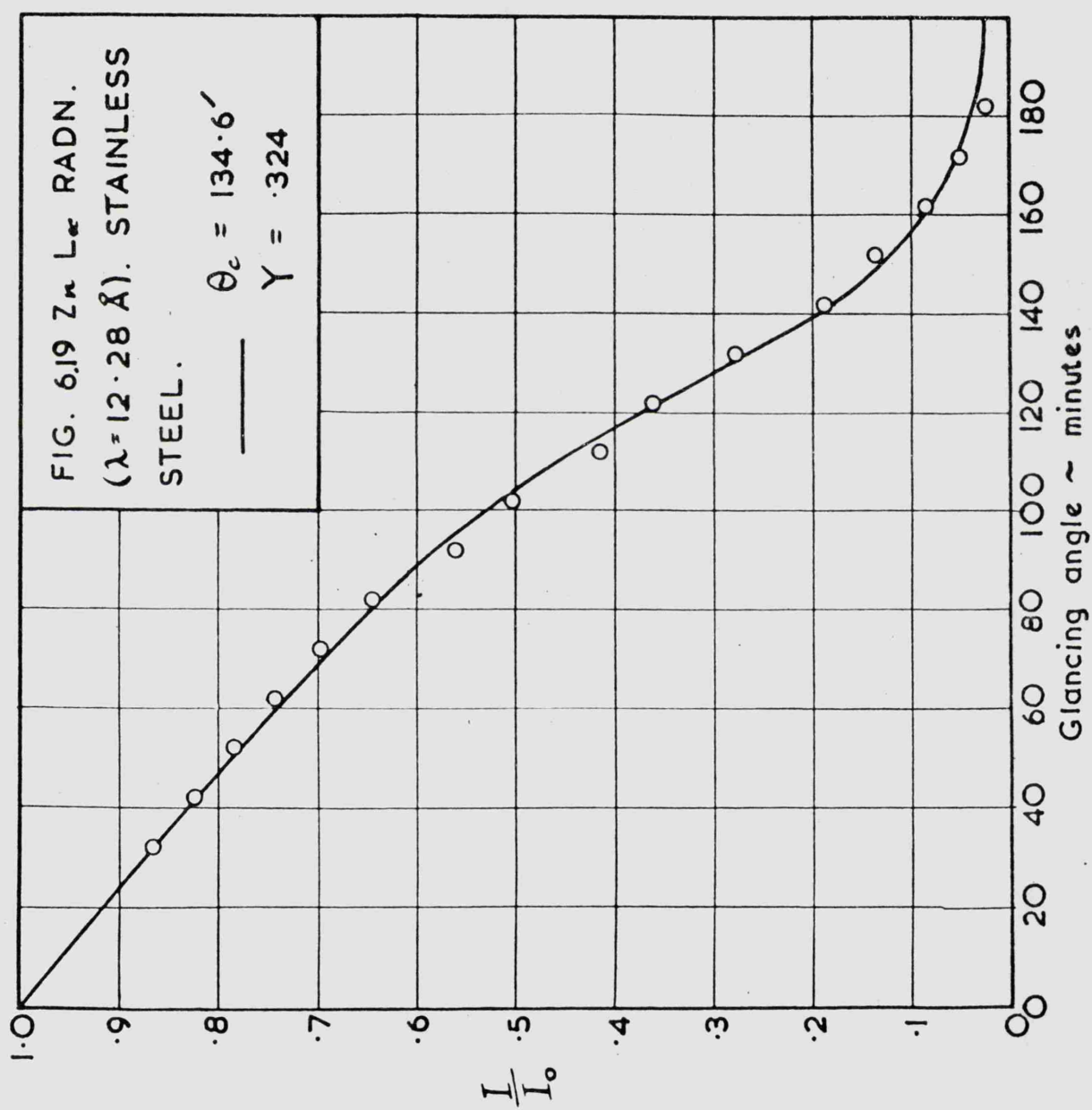
θ (min)	I/I_0							
	Nb L_α	Si K_α	Al K_α	Mg K_α	Zn L_α	Cu L_α	Ni L_α	Co L_α
32	.897	.902	.912	.904	.868	.862	.836	.782
42	.840	.853	.871	.860	.826	.818	.788	.767
52	.752	.798	.821	.836	.785	.778	.746	-
57	-	-	-	-	-	-	-	.704
62	.632	.733	.778	.786	.744	.745	.700	-
67	.526	-	-	-	-	-	-	-
72	.435	.624	.724	.732	.700	.667	.655	.644
77	.293	.577	-	-	-	-	-	-
82	.120	.488	.630	.662	.647	.638	.584	-
87	.051	.423	-	-	-	-	-	-
92	.016	.332	.511	.587	.563	.528	.529	-
102	-	.155	.385	.488	.504	.518	.448	.457
112	-	.036	.234	.375	.415	.427	.394	-
117	-	-	-	-	-	-	-	.361
122	-	.012	.128	.300	.363	.371	.334	-
132	-	-	.037	.184	.278	.295	.281	.319
142	-	-	.008	.081	.187	.212	.200	-
147	-	-	-	-	-	-	-	.220
152	-	-	-	.031	.137	.160	.159	-
162	-	-	-	.014	.085	.115	.117	.157
172	-	-	-	-	.050	.075	.075	-
177	-	-	-	-	-	-	-	.090
182	-	-	-	-	.025	.045	.047	-
192	-	-	-	-	-	.028	.030	.060

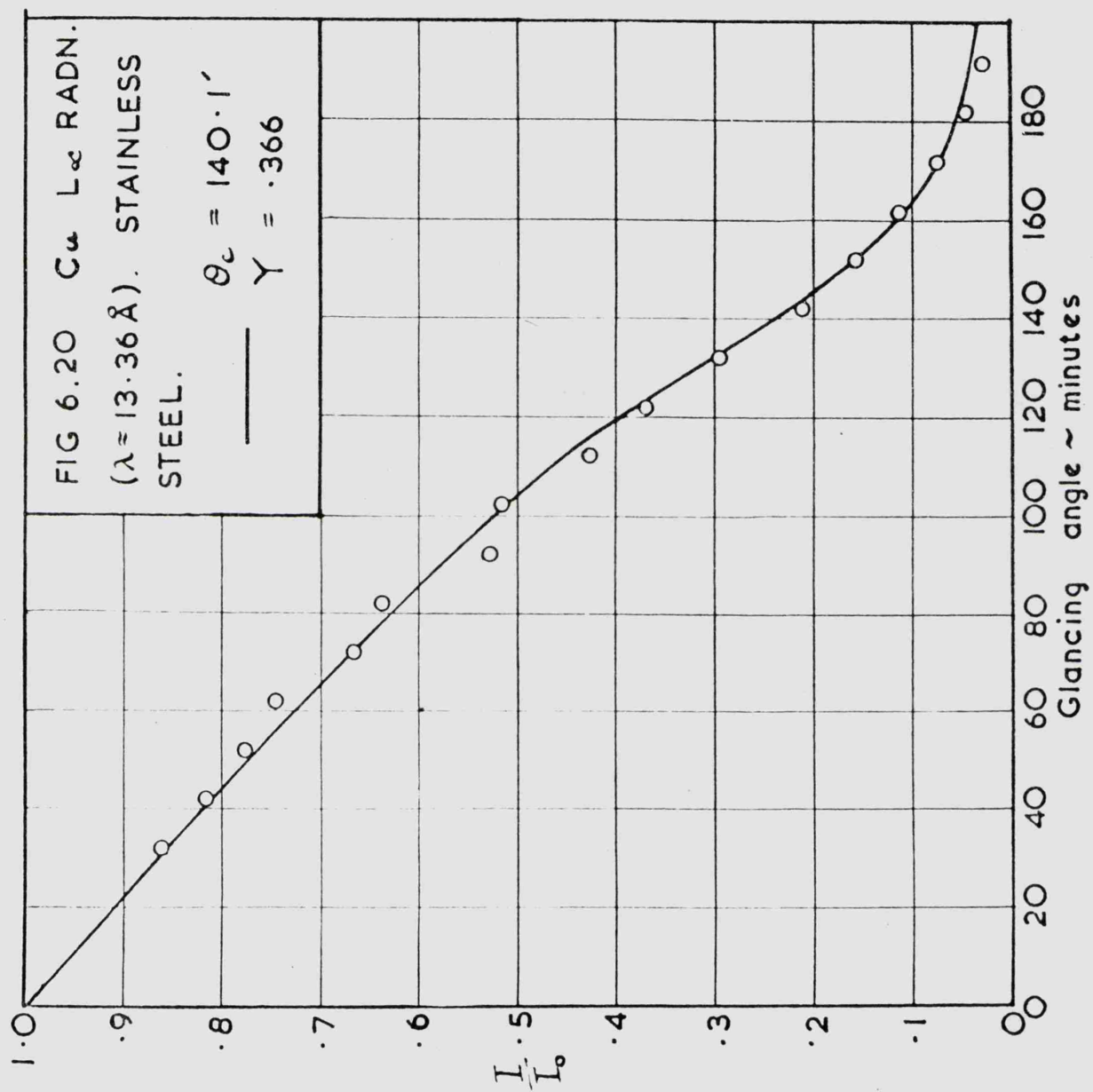


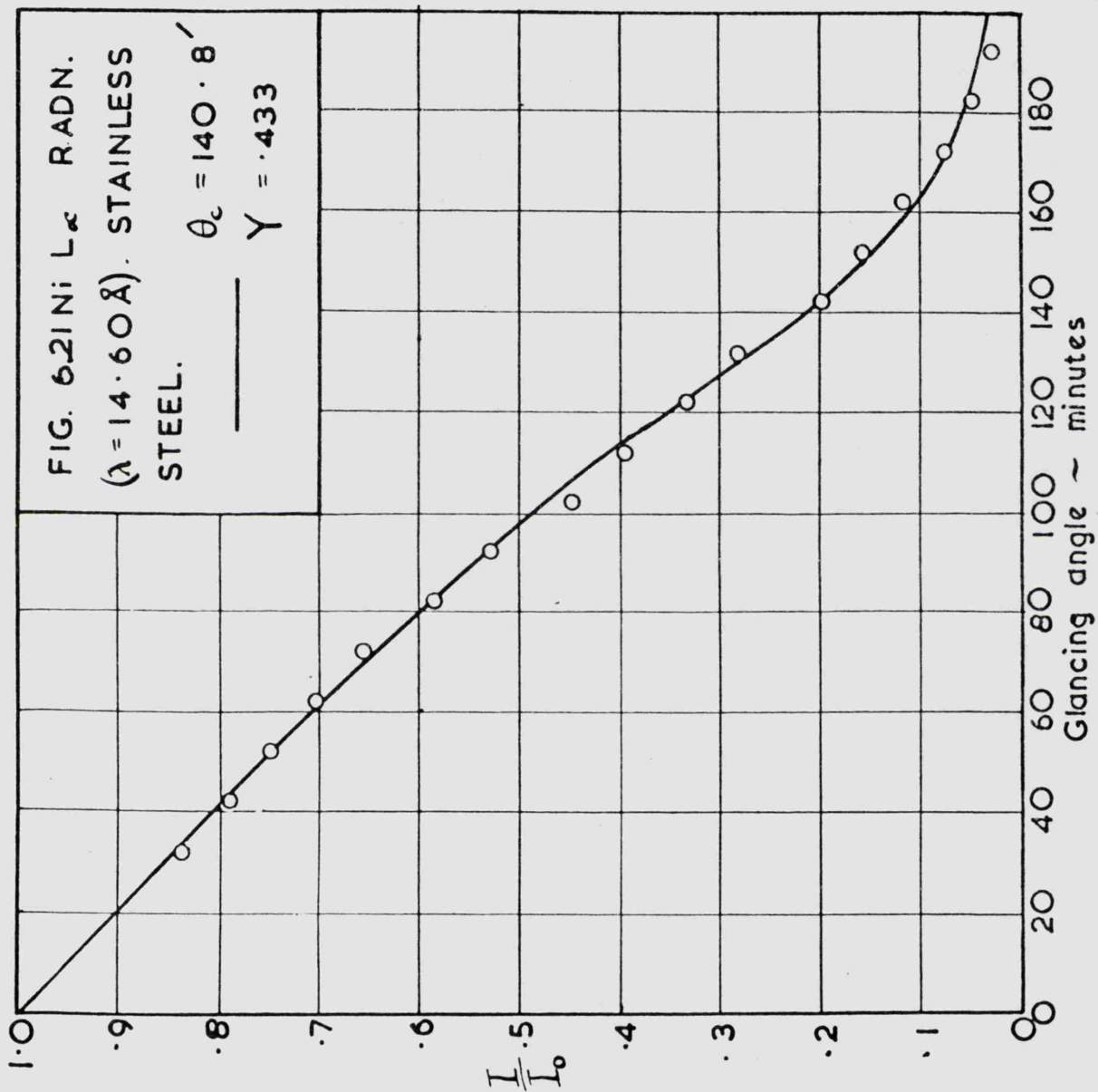


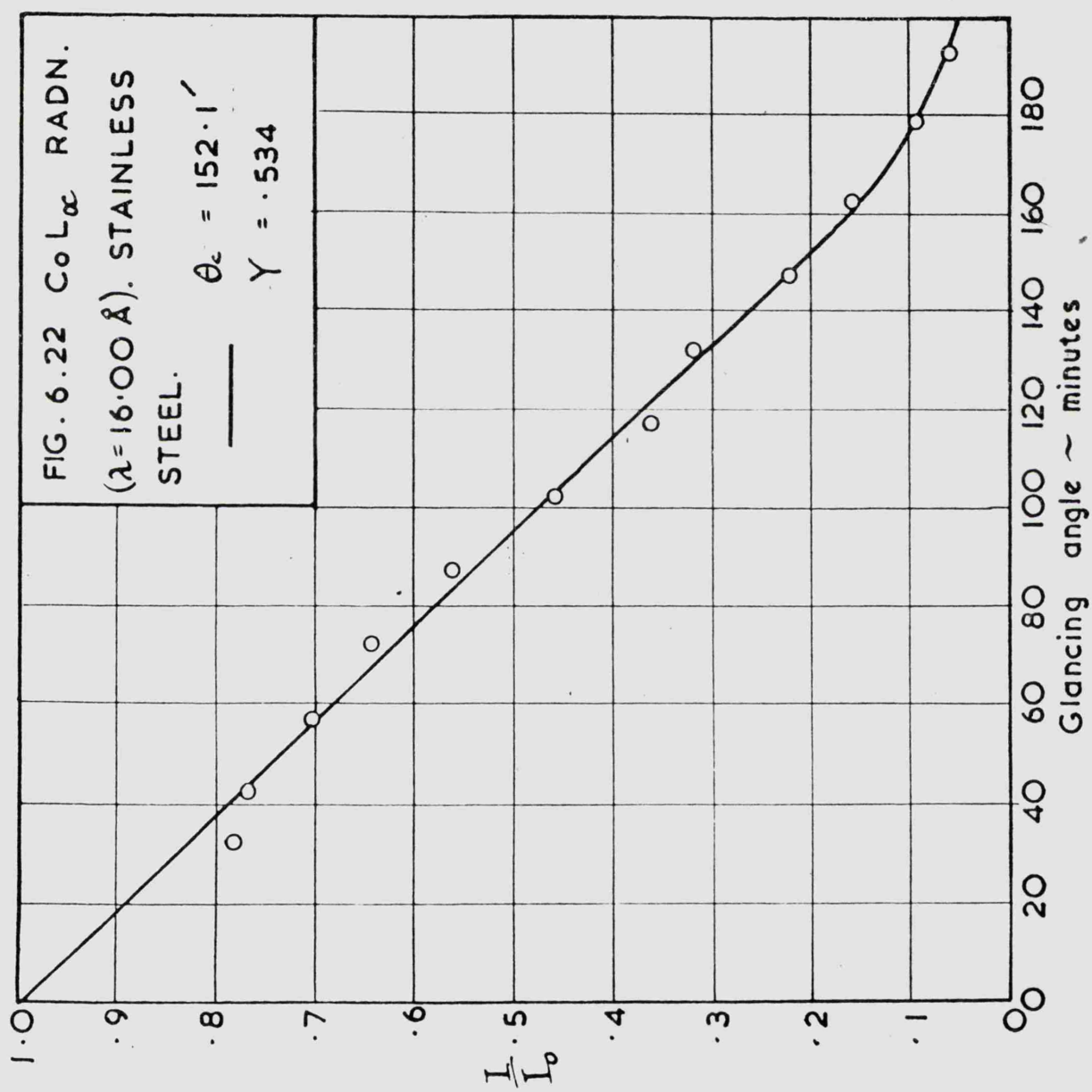


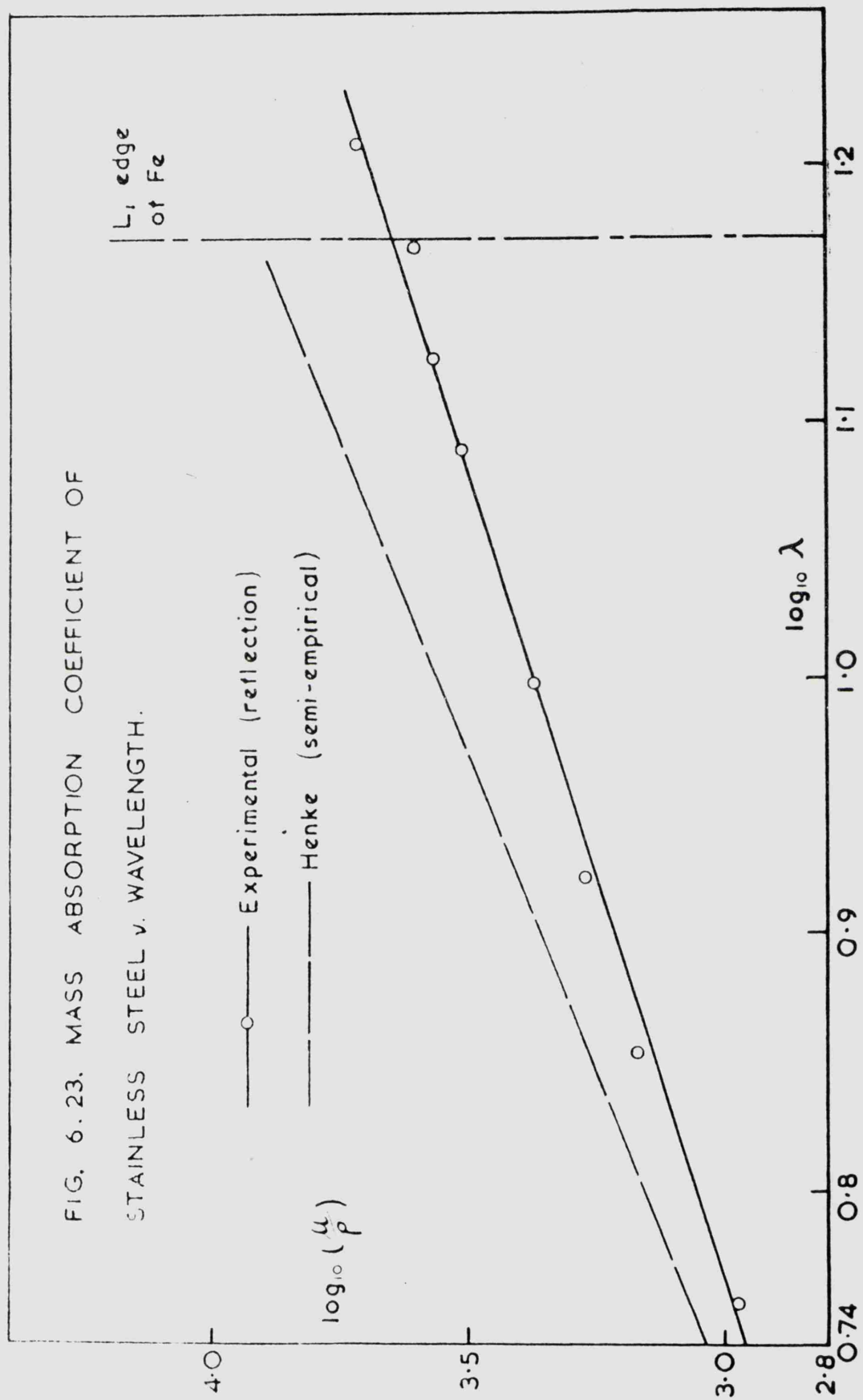


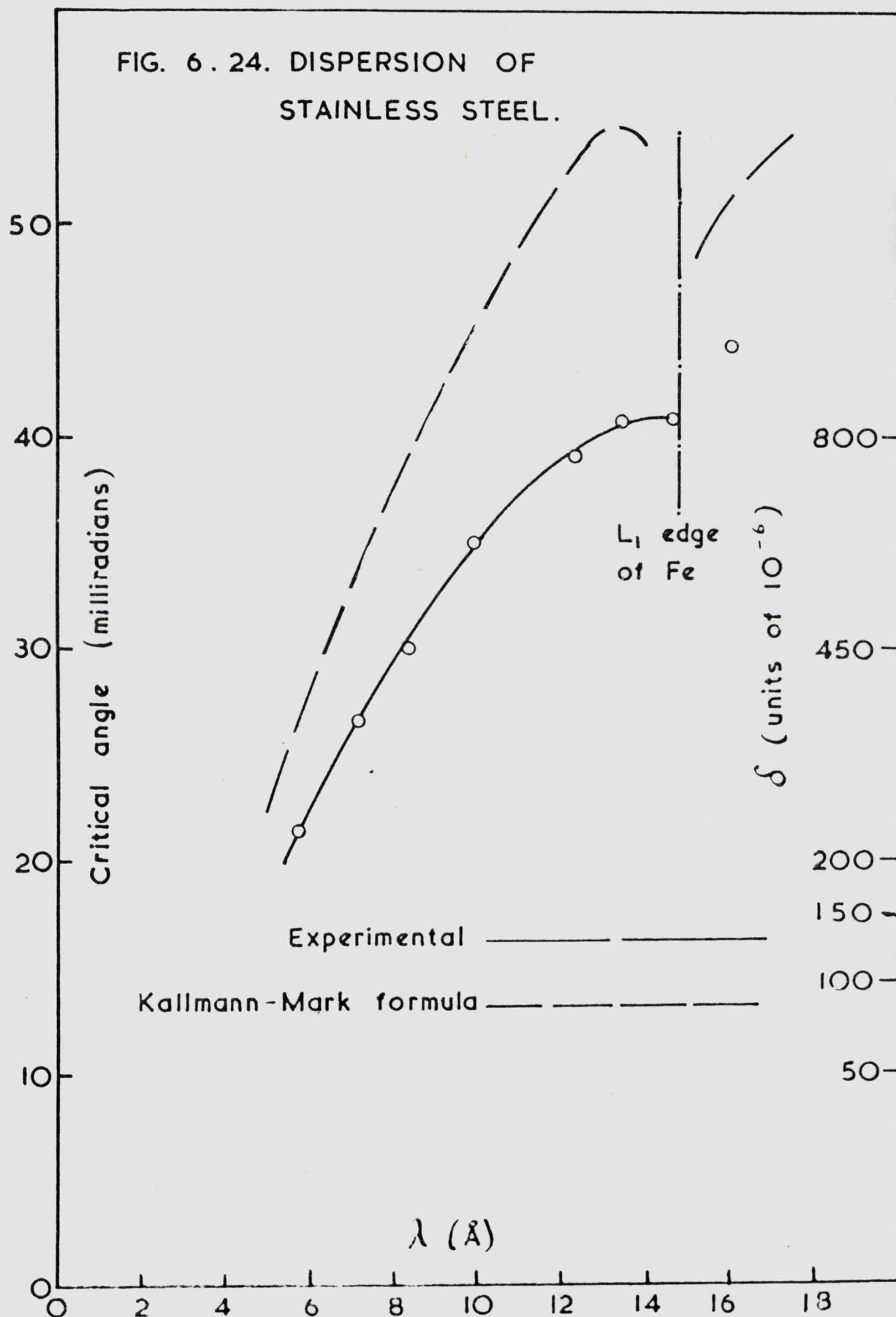












nickel and chromium absorption edges in this region makes the rigorous computation laborious, and the result of such a computation would differ little from that for pure iron, owing to the small quantities of these elements present and the proximity of their atomic number to that of iron.

As in the case of glass, the experimental values of S are considerably below those given by the theory, and the discrepancy once again increases with wavelength, so that the hypothesis of a reduced surface electron density which increases with depth seems preferable to that of a reflection trap.

Further confirmation of a considerably reduced surface density is given by the curves of $\frac{\mu}{\rho}$ versus λ . The experimental values are once again compared with those of Henke et. al. In this case, there is a large difference between the two sets of values and it seems unlikely that this is due to errors in the semi-empirical values, as the experimental values from which they are derived are not so much in error. It seems clear that a reduced electron density at the surface must be assumed, and that the density encountered by the radiation becomes smaller and smaller as the radiation becomes less and less penetrating, i.e. that the density is decreasing toward the extreme surface.

6 (v). Evaporated copper.

This specimen was made by evaporating a film of copper on the glass flat. This was done in a separate evaporation plant, at a pressure of about 0.1 micron Hg, the specimen then being transferred to the main

tank. The copper was evaporated from a tantalum boat and deposition took place in about 5 minutes. No attempt was made to measure the film thickness accurately, but from the amount of material in the boat, and the appearance of the film, it must have been over 1000 Å thick, so that a negligible amount of radiation penetrated to the substrate.

Reflection measurements were made on this specimen at one wavelength only, that of Al $K\alpha$. The curve of I/I_0 versus θ is given in Figure 6.25.

This surface was definitely a 'bad' one from the point of view of X-ray reflection. There is no evidence of a critical angle on the curve of Figure 6.25, and an impossibly high Y value of about 10 is indicated. The efficiency of reflection does not rise above 50%. The specimen was also examined by the photographic method, and the image of the reflected beam was extremely blurred. A rough estimate showed that at least 50% of the radiation was being reflected out of the main beam. As the surface appeared mirror smooth in visible light, it must be concluded that the elements of surface responsible for the blurring were very small.

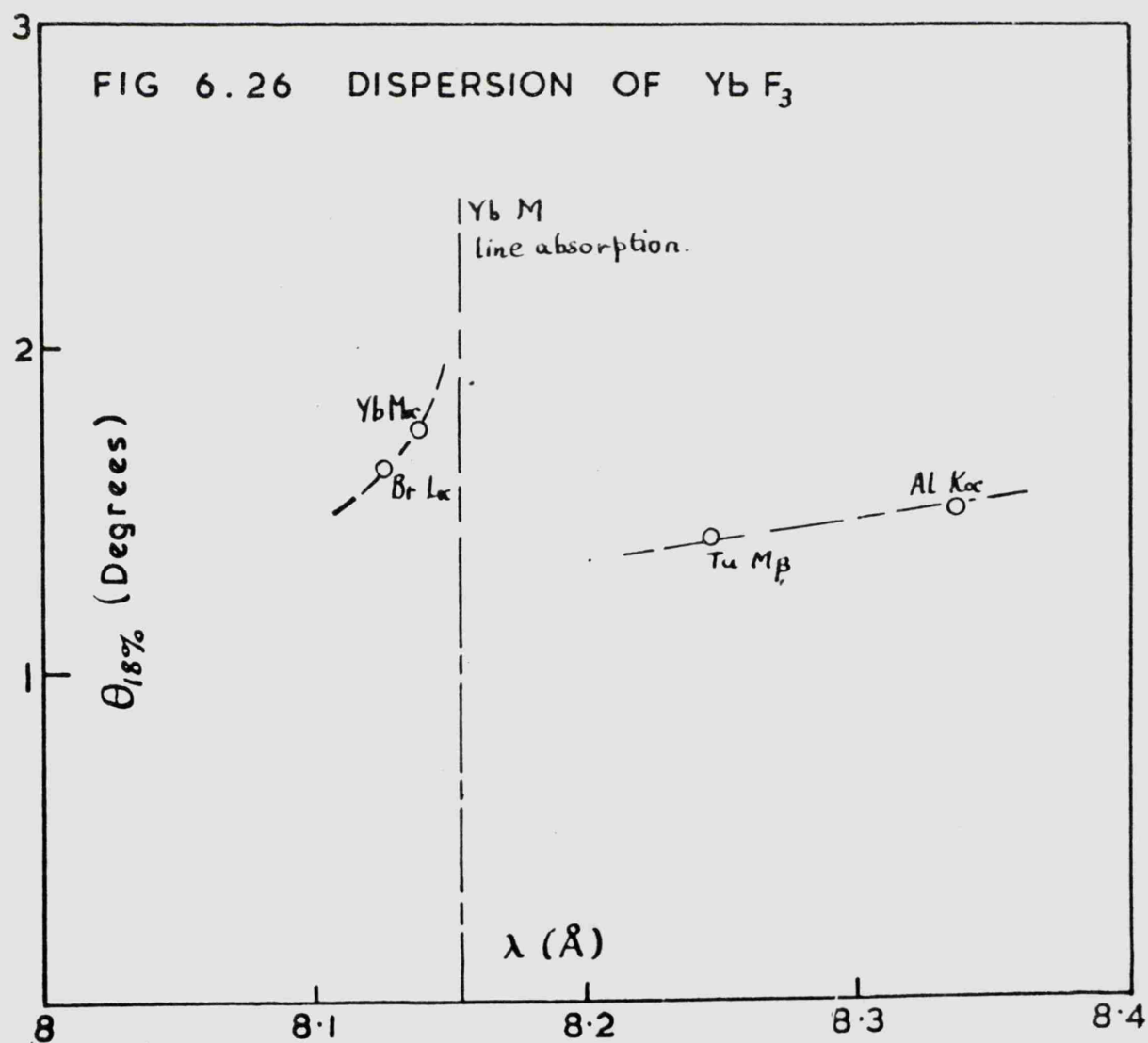
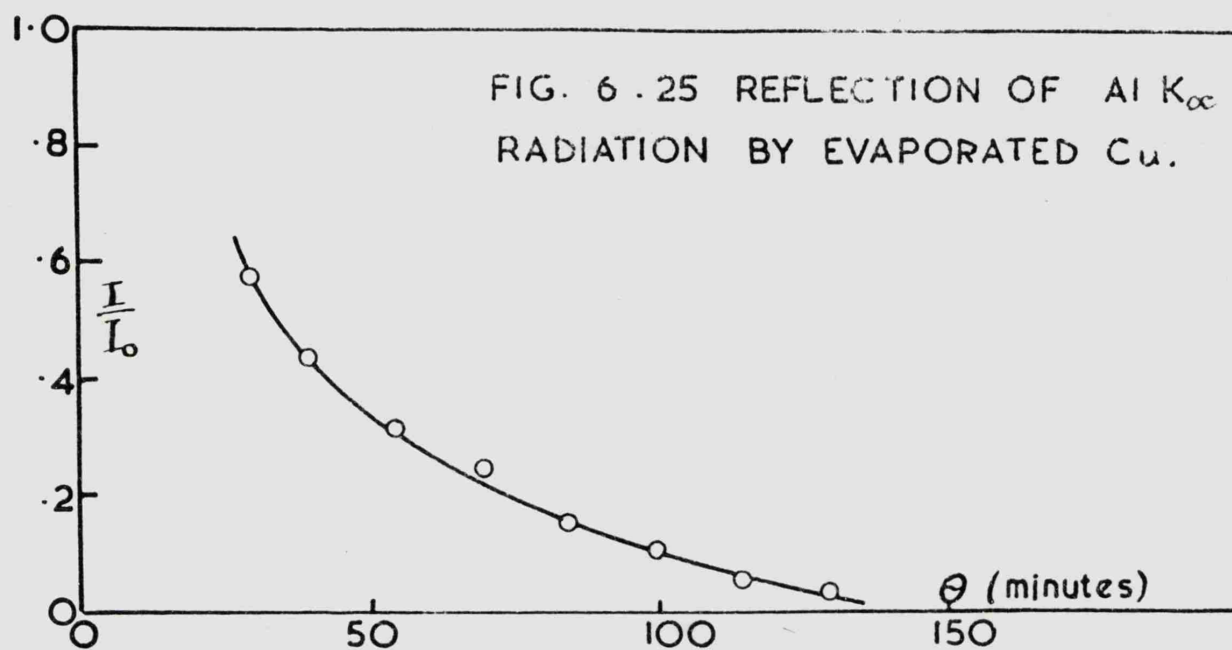
This experiment provided confirmation of the already well-known fact that evaporated surfaces are not, in general, suitable for X-ray imaging. However, this surface appeared to be worse than average as Hendrick has obtained quite reasonable reflection curves from evaporated specimens. It may be that the evaporation was too slow in the present case.

Work is continuing in this laboratory on the evaporation and reflecting power of surfaces produced by other methods such as electroplating and casting in epoxy resin. It is hoped that an alternative method to optical polishing will be found for making X-ray mirrors.

6 (vi). Ytterbium fluoride.

In Chapter 3 it was mentioned that some compounds of ytterbium show X-ray line absorption instead of the usual edge. One would expect, therefore, that the dispersion would be described by a formula more like the Drude-Lorentz equation (2.1) than the Kallmann-Mark. An investigation of an ytterbium fluoride film was made to test this hypothesis.

The specimen was a thin film of ytterbium fluoride evaporated on to a glass flat. The absorption line is at 8.154 \AA , so that the measurements were carried out at the wavelengths of $\text{Br } L_{\beta_1} (8.125 \text{ \AA})$, $\text{Yb } M_{\alpha_1} (8.138 \text{ \AA})$, $\text{Tu } M_{\beta} (8.246 \text{ \AA})$, and $\text{Al } K_{\alpha} (8.337 \text{ \AA})$. The curves of I/I_0 versus θ were not very reliable, as the evaporated layer gave reflection curves similar to that obtained for copper, but a rough value for θ_c could be obtained by finding the point on the curve where the reflection reached 18% (see Nähring, loc. cit.). Although, under the conditions of this experiment, this probably does not give a good value for θ_c , the 18% criterion does enable some sort of comparison to be made with radiation on each side of the



absorption line.

The value of ' $\theta_{18\%}$ ' is plotted as a function of wavelength in Figure 6.26. It can be seen that the value of this angle does rise on the short wavelength side of the edge so that it seems that the Drude-Lorentz theory predicts the right sort of variation. However, a calculation, neglecting damping, of the critical angle to be expected on this side of the edge gives a value which is five degrees greater than that for the long wavelength side. The measured difference is about 20 minutes. The discrepancy may be due to the fact that the Yb M_α line contained some satellite structure, unresolved by the monochromator, of intensity comparable with that of the main line, which tended to smooth out the observed variation. Or it may be that a more sophisticated dispersion treatment is required, based perhaps on the dispersion relations. Further work with apparatus of higher wavelength resolution could throw light on this problem.

6 (vii). Conclusions.

In this thesis, data has been given for the reflecting power of polished glass and stainless steel as a function of glancing angle and of wavelength in the range 5-16 Å. The results are more extensive than any published previously, and in particular the change of shape of the reflection curves with increasing absorption has been more carefully studied than before. It is believed that the results are superior to

any taken by photographic methods, owing to the unknown response of films in the soft X-ray region. The tabulated values of the reflection coefficient I/I_0 are accurate to within a few percent, which is sufficient for many practical applications of X-ray reflection.

The comparison of the reflection curves with theory shows that the Fresnel equations, when modified to take account of absorption, fit the data very well, except for a consistent discrepancy at angles beyond critical. This discrepancy, as well as the difference between the experimental and theoretical values of $\frac{H}{\rho}$ and δ , could be explained with the aid of a 'reflection trap' hypothesis, but a more likely model of the surface seems to be a mosaic structure combined with a reduced surface electron density. More work on the relation between the surface structure and the reflection of X-rays is obviously required, and it would seem desirable to combine the X-ray studies with other techniques for surface investigation, such as electron diffraction and electron microscopy, in order to obtain a more complete picture of the physics and chemistry of the surfaces, rather than to try to deduce a surface model from the X-ray data alone. Such an investigation would benefit from improved precision of the X-ray measurements. The perfection of a point-focus soft X-ray tube with a high and stable characteristic line emission would enable intensities to be measured more reliably, and the replacement of the vernier scale for glancing angle measurement by a tangent micrometer screw would lead to a gain in angular precision.

A kinematic reflector mount should be designed, to allow the easy interchange of specimens without upsetting the alignment, a feature missing from the present apparatus.

Any programme of surface structure studies should, of course, include evaporated films. The results of this investigation, and of others, have shown that they are unlikely to be of great use in X-ray optical systems.

The studies of dispersion described in this work give support to the Kallmann-Mark theory. The agreement between the experimental and theoretical values of \bar{S} is especially good around the Si K edge for Pyrex glass. However, until further information on the relation between surface structure and X-ray reflection is available, this method cannot be expected to yield reliable values for the refractive index.

The work on ytterbium fluoride showed that the Drude-Lorentz theory is qualitatively correct in the neighbourhood of an X-ray absorption line, but further work with apparatus of higher wavelength resolution is necessary. It may yet prove possible to utilise this anomalous effect in a high efficiency, narrow-band monochromator.

APPENDIX A.

'CURRENT MODE' OPERATION OF A PROPORTIONAL COUNTER.

In the usual mode of operation, a proportional counter is treated as the generator of a voltage pulse, which is fed into an amplifier of high input impedance. This arrangement is shown in Figure A.1.

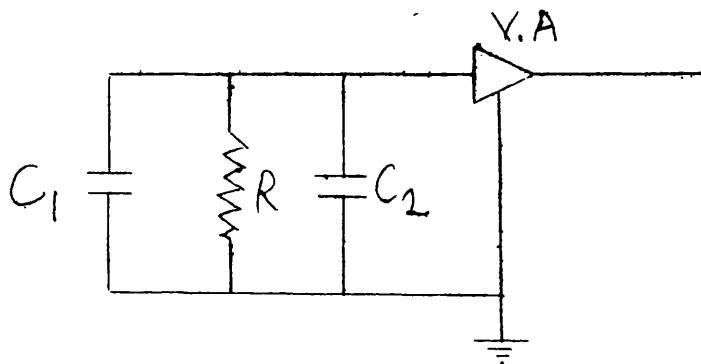


Figure A.1.

C_1 is the counter capacity, R is the resistance across which the voltage is developed, and C_2 is the amplifier input capacity, including strays due to lengths of cable, etc. The amplifier input impedance will be much greater than R , so that the input time constant \mathcal{T} is equal to $R(C_1 + C_2)$. The rise time of the voltage pulse is usually about $0.1 \mu\text{s}$, so that \mathcal{T} will normally be many times this. Under these conditions, the pulse amplitude as a function of time will be

$\frac{C_1}{C_1 + C_2} V(t)$. It can be seen that C_2 must be kept small ($\sim 5 \text{ pF}$) or

the pulse will be strongly attenuated. For this reason the cathode follower must be mounted close to the counter, to obviate the use of long cables.

Instead of observing the voltage pulse, we may treat the counter as the generator of a current pulse $i(t)$. This is related to the voltage pulse $V(t)$ from the counter by the equation:

$$i(t) = \frac{dQ(t)}{dt} = C \frac{dV(t)}{dt}.$$

The practical arrangement is shown in Figure A.2.

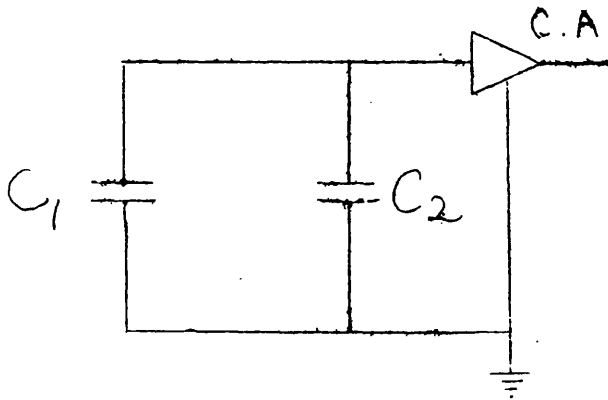


Figure A.2.

C.A. is a current amplifier of low input impedance r . The input time constant is $r(C_1 + C_2)$ and if this is smaller than the current pulse width (= voltage pulse rise time), then the input to the current amplifier is a faithful reproduction of the counter current pulse.

With transistor circuits, r can easily be made equal to about 1 - 10 ohms. The circuit of Figure 4.7 achieves a low input impedance

109.

by feedback through the resistor R_2 . The point X is a 'virtual earth'. It may be shown that this circuit has an input impedance approximately equal to $\frac{R_2}{A}$, where A is the voltage gain of the amplifier stage. For the actual circuit, this impedance was one or two kilohms. Although this is not as low as may be obtained with transistors, it is sufficiently low to enable quite a long input cable to be used.

APPENDIX B.

RESOLUTION OF PROPORTIONAL COUNTERS IN THE SOFT X-RAY REGION.

In 1949, Curran, Cockroft and Angus (52) showed experimentally that, if the gas gain of a proportional counter was sufficiently large, then the probability $P(x)$ of producing a pulse height x from an initial group of N electrons is given by the distribution function:

$$P(x) = x^{(Nm-1)} e^{-x} \quad . \quad . \quad . \quad (B.1)$$

where m is a parameter, found experimentally to be about $\frac{3}{2}$. The fractional standard deviation σ_N of this function is $(\frac{2}{3N})^{\frac{1}{2}}$. Curran et. al. showed also that the spread in pulse height due to fluctuations in the number of ion pairs produced by the initial ionizing effect is approximately equal to σ_N , so that the total fractional standard deviation of the pulse height distribution produced by monoenergetic particles becomes $(\frac{4}{3N})^{\frac{1}{2}}$. Using the fact that $N = \frac{E}{\bar{\omega}}$, where E is the energy of the ionizing particle and $\bar{\omega}$ = mean energy per ion pair (which we may take as 26 eV for a 90% argon, 10% methane mixture) we obtain the relation:

$$\sigma = 0.186 E^{-\frac{1}{2}} \quad . \quad . \quad . \quad . \quad . \quad (B.2)$$

111.

Byrne (53), using a new theory of the multiplication process which divides the electrons in the counter into two groups, according to whether their energy is above or below the ionisation energy, showed that equation (B.1) is of the correct form, and placed limits on the variation of the parameter m . He showed that m could not lie outside the range

$$1 \leq m \leq 1.64$$

so that the standard deviation of the function (B.1) lies between the limits

$$\left(\frac{1}{N}\right)^{\frac{1}{2}} \geq \sigma_N \geq \left(\frac{0.61}{N}\right)^{\frac{1}{2}}$$

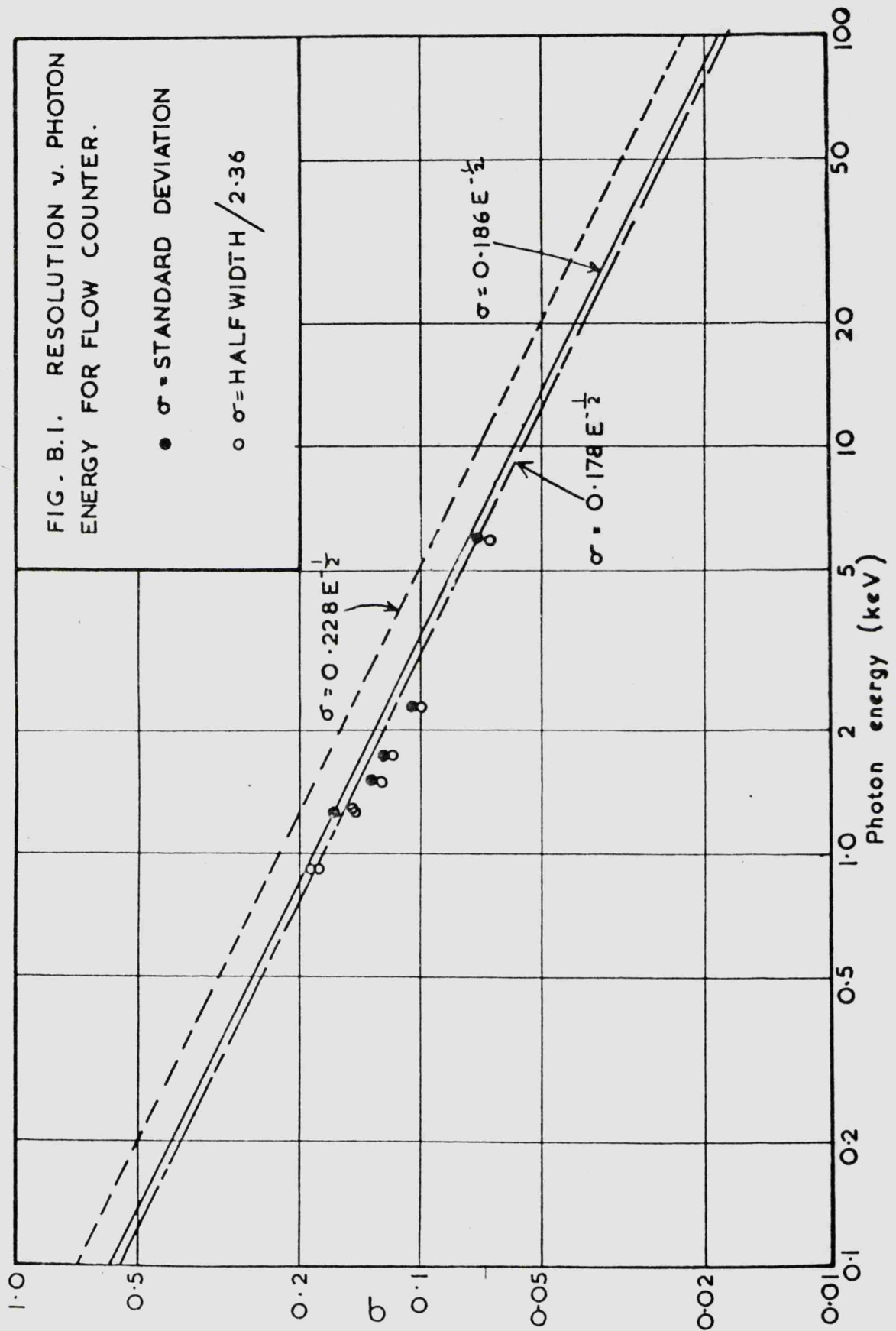
Making the assumptions, as before, that $W = 26$ eV and

$\sigma = 2\sigma_N$ we obtain the two limiting equations

$$\sigma = 0.228 E^{-\frac{1}{2}} \quad \dots \dots \dots (B.3)$$

$$\sigma = 0.178 E^{-\frac{1}{2}} \quad \dots \dots \dots (B.4)$$

In Figure B.1, the three curves (B.1) (B.2) (B.3) are plotted, together with experimental values of σ taken in the soft X-ray region. The pulse height distributions were recorded on an R1DL 400-channel pulse height analyser, using characteristic radiations picked out with the monochromator of the reflectometer, except for the measurement at 6kV, for which an Fe^{55} source was used. The standard deviation was calculated from these distributions by two methods: (a) the width of the peak at half maximum was measured and divided by 2.36 (open points),



(b) the standard deviation $\sqrt{\overline{x^2} - (\overline{x})^2}$ was computed (filled-in points). It can be seen from the figure that these two methods do not give quite the same result. This is to be expected, as the relation $\sigma = \frac{\text{half-width}}{2.36}$ is only valid for a normal distribution, to which an experimental pulse height distribution corresponds only approximately.

The experimental values of Q lie outside the limits set by equations B.3 and B.4, lying on a curve given by:

$$\sigma = (0.167 \pm 0.002) E^{-\frac{1}{2}}, \quad \dots \quad (B.5)$$

If we assume that Byrne's theory is correct, then we must examine the other assumptions leading to B.3 and B.4, in order to find a possible reason for the discrepancy.

Dealing first with the question of the mean energy per ion pair, we may calculate an 'experimental' value for ω from B.5, assuming that we are at the lower limit of the resolution given by the multiplication theory, i.e. that $m = 1.64$. The resulting value is 22-24 eV. This is considerably lower than the accepted value, and it is unlikely that the tabulated values are so much in error. It may be possible, however, that the flow gas used in these experiments (supplied by British Oxygen Co.) contained impurities which lowered the value of ω .

With regard to the second assumption, that the contribution to the pulse width from the initial ionizing event is equal to that from the multiplication process, this is stated by Curran et. al. to be only approximately true, and it seems possible that, under certain conditions, the contribution from the first process may be different from that from the second. Further work, both experimental and theoretical, seems desirable here.

REFERENCES

1. A. Köhler, Fortschritte auf dem Gebiet der Roentgenstrahlen 24,
236 (1916).
2. A. Einstein, Verh. d. Deut. Phys. Ges. 20, 80 (1918).
3. B. Walter, *ibid.* 21, 347 (1919).
4. W. Stenström, Dissertation, Lund (1919).
5. W. Duane and R.A. Patterson, Phys. Rev. 15, 526 (1920).
6. M. Siegbahn, Comptes Rendus 173, 1350 (1921).
7. C.G. Darwin, Phil. Mag. 27, 315 (1914).
8. A.H. Compton, *ibid.* 45, 1121 (1923).
9. M. Siegbahn, A. Larsson and I. Waller, Naturwiss. 12, 1212 (1924).
Phys. Rev. 25, 235 (1925).
10. R. Wuerker, Thesis, Stanford.
11. P. Drude, Theory of Optics.
12. A.H. Compton and S.K. Allison, X-rays in Theory and Experiment,
D. van Nostrand Co. Inc., New York, 1946.
13. H. Kallmann and H. Mark, Naturwiss. 14, 648 (1926).
Ann. der Phys. 82, 385 (1927).
14. A. Larsson, Dissertation, Uppsala, 1929.
15. R.W. Ditchburn, Light, 2nd edition (Blackie 1963).
16. R. de L. Krönig, J.O.S.A. 12, 547 (1926).
17. L.G. Parratt and C.F. Hempstead, Phys. Rev. 94, 1593 (1954).
18. H. Hönl, Z. Phys. 84, 1 (1933).

19. Y. Sugiura, J. de Physique 8, 113 (1928).
- 19a. R. de L. Krönig and H.A. Kramers, Z. Phys. 48, 174 (1928).
20. F. Holweck, Comptes Rendus 17C, 570 (1923).
21. R. Forster, Naturwiss. 19, 969 (1927).
22. T.H. Laby, R. Bingham and J. Shearer, Nature 122, 96 (1928).
T.H. Laby and R. Bingham, Proc. Roy. Soc 133, 274 (1931).
23. J. Thibaud, Comptes Rendus 187, 219 (1928).
24. J.A. Prins, Z. Phys. 47, 479 (1928).
25. H.E. Stauss, Phys. Rev. 34, 1021 (1929).
26. M. Schön, Z. Phys. 58, 165 (1929).
27. M.A. Valouch, Comptes Rendus 198, 283 (1929).
28. E. Dershem, Phys. Rev. 34, 1015 (1929).
29. E. Dershem and M. Schein, Phys. Rev. 37, 1246 (1931).
30. S.D. Gehman, Phys. Rev. 33, 141 (1929).
31. H.W. Edwards, Phys. Rev. 30, 91 (1927).
 ibid. 31, 172 (1928).
 ibid. 33, 463 (1929).
32. E. Nähring (a) Phys. Zeits. 31, 799 (1930).
 (b) ibid. 32, 179 (1931).
33. J.E. Henderson and E.R. Laird, Phys. Rev. 33, 291 (1929).
34. J.E. Henderson and E.B. Jordan, ibid. 36, 785 (1930).
35. C.B.O. Mohr, Proc. Roy. Soc. A133, 292 (1931).
36. H. Kiessig, Ann. Phys. 10, 715 (1931).

- 37. W. Ehrenberg. J.O.S.A. 39, 741 (1949).
 ibid. 39, 746 (1949).
- 38. R.W. Hendrick, ibid. 47, 165 (1957).
- 39. I.M. Rieser, ibid. 47, 987 (1957).
- 40. R. Groth, Ann. Phys. 2, 380 (1959).
- 41. B.A. Cooke, Thesis, Leicester (1963).
- 44. W. Ehrenberg and W.E. Spear, Proc. Phys. Soc. B63, 67 (1951).
- 45. J.B.S. Waugh, Nucleonics 18, 70 (1960).
- 46. H. Miwa and T. Tohyama, Proc. Conference on Nuclear Electronics,
 Vol. II, (International Atomic Energy Agency, 1962).
- 47. B. Nordfors, Dissertation, Uppsala 1961.
- 48. B.L. Henke, R. White and B. Lundberg, J. Appl. Phys. 28,
 98, (1957).
- 49. S.J.M. Allen, Unpublished. Appears in reference (12) Page 799.
- 50. B.L. Henke, Advances in X-ray Analysis. Vol. 4.
- 51. F.R. Hirsch, J.O.S.A. 25, 229 (1935).
 ibid. 28, 463 (1938).
- 52. S.C. Curran, A.L. Cockroft and J. Angus, Phil. Mag.
 40, 929 (1949).
- 53. J. Byrne, Proc. Roy. Soc. Edinburgh LXVI (A) 33 (1962).